EXPERIMENTAL AND MICROMECHANICAL ANALYSIS OF FLAX AND GLASS REINFORCED BIO-BASED COMPOSITES

A Dissertation
Submitted to the Graduate Faculty
of the
North Dakota State University
of Agriculture and Applied Science

By

Nassibeh Hosseini

In Partial Fulfillment of the Requirements
for the Degree of
DOCTOR OF PHILOSOPHY

Major Department:
Mechanical Engineering

April 2015

Fargo, North Dakota

North Dakota State University
Graduate School

Title

Experimental and Micromechanical Analysis of Flax and Glass Reinforced Bio-based Composites

By

Nassibeh Hosseini

The Supervisory Committee certifies that this ***disquisition*** complies with North Dakota State University's regulations and meets the accepted standards for the degree of

DOCTOR OF PHILOSOPHY

SUPERVISORY COMMITTEE:

Dr. Chad Ulven
Chair

Dr. Dean Webster

Dr. Long Jiang

Dr. Dilpreet Bajwa

Dr. Dennis Wiesenborn

Approved:

4/17/2015 — Date

Dr. Alan R. Kallmeyer — Department Chair

ABSTRACT

Two different novel high-functional bio-based resins from Methoxylated Sucrose Soyate Polyol (MSSP) and methacrylated epoxidized sucrose soyate (MAESS) were used as matrices for composites. Vinyl ester reinforced with flax fiber and E-glass fiber were also produced as the references to highlight the performance of bio-based composites. An appropriate processing conditions for MSSP and MAESS resins using compression molding was established to fabricate high fiber volume content composites. Mechanical properties of composites were assessed by tensile, flexural, interlaminar shear strength (ILSS), nano-indentation, and impact strength. Scanning Electron Microscopy (SEM) of fractured surfaces of flexural specimens were examined to investigate the fiber-matrix interface behavior. MSSP and MAESS resins reinforced with E-glass fiber performed similarly if not superior to previous bio-based and petroleum-based composites studied Tensile strength and modulus of E-glass reinforced MSSP were higher up to 40% and 75% respectively, compared to existing studies. For flexural strength and modulus 130% and 110% improvements were observed. The tensile strength and modules of MAESS and vinyl ester resins reinforced with E-glass fibers are 532 MPa, 36.79 GPa and 536 MPa, 36.40 GPa, respectively. The impact strength of the composites with MAESS resin reinforced with E-glass fibers was 237 kJ/m^2, whereas that of the vinyl ester resin reinforced with same E-glass fiber was 191 kJ/m^2. Results of SEM images along with flexural strength, interlaminar shear strength and impact tests revealed better wetting of fibers by matrix, stronger adhesion between fiber and matrix and greater interfacial bonding compared to corresponding E-glass/vinyl ester composites. The composites made from flax fiber with MSSP or MAESS resins achieve similar properties to E-glass/MSSP and E-glass/MAESS in terms of specific mechanical properties. Moreover, flax/MSSP and flax/MAESS composites perform similarly, if not superior to previous

bio-based and petroleum based composites studied. A micromechanical model and an analytical approach were also developed to predict the stress relaxation response of the flax/MSSP composite material consisting linear viscoelastic flax fiber and bio-based PU matrix. A good agreement between the micromechanical modeling data and experimental results was observed for the linear viscoelastic response of the bio-based composite.

ACKNOWLEDGEMENTS

A special thank you and acknowledgement first goes to Dr. Chad Ulven, my PhD advisor, for supporting me during these past four years. I have gained much over the years from my attendance of his classes, his guidance, his patience and our conversations which guided me on a journey to a new way of living life. Dr. Ulven is not only my advisor, he is a great role model and leader for me in my professional and personal life. I hope that I could be as lively, enthusiastic, and energetic as Dr. Ulven and to someday be able to command an audience as well as he can.

I thank my committee members, Dr. Dean Webster, Dr. Dilpreet Bajwa, Dr. Long Jiang and Dr. Dennis Wiesenborn, for their time, advice and contribution towards the improvement of my research.

I thank Prof. Ghodrat Karami and Dr. Samad Javid for supplying their Matlab code for the micromechanical model.

I would also like to thank Mercedes Alcock, of the Composites Innovation Centre in Winnipeg, MB, Canada for her help with the Dia-Stron measurements.

With immense gratitude, I also would like to thank my group members and friends for their collaborations and encouragement throughout of my research.

I thank the National Science Foundation and North Dakota Industrial Commission for funding support.

My deepest gratitude goes to my parents and my family for their unfailing love, support and advice. Thank you for learning all kind of new technology to be in touch with me and giving me your unconditional love throughout not only the course of my Ph.D. studies but my entire life.

Finally, I thank my best friend, my husband, Hesam. I cannot imagine what my life would be like if I weren't sharing it with you. Your unconditional love and unwavering support are a constant source of strength. Thank you for your patience and all your encouragement. I started this work just after I married you. This work was born on the wings of our love.

DEDICATION

This dissertation is dedicated to my husband, Hesam, and my parents, Mojtaba and Marzieh, for their constant encouragement, unwavering support, love, and pride.

TABLE OF CONTENTS

LIST OF TABLES

LIST OF FIGURES

CHAPTER 1. GENERAL INTRODUCTION

Polymer matrix composites continue to grow in importance globally in a wide variety of industrial sectors due to their design flexibility and low cost [2]. Polymer matrix composites consist of a synthetic polymer reinforced with synthetic fibers such as glass and carbon. However, there is a growing interest in manufacturing polymer composites based on renewable resources, such as natural fibers as reinforcements and vegetable oil-based polymers as matrices. Use of plant –based resources provides additional markets for farmers and reduces dependence on petroleum by offering a potential alternative to petrochemical based polymer resins and synthetic fibers. Moreover, the USA is the world leader in producing several main types of oilseed feedstock. Particularly, North Dakota is the 9th leading U.S. state in soybean production by producing 5.46 million metric tonnes in 2014. The first natural-fiber-based polymer composites emerged in the early 1900s [3], when natural materials appeared as possible materials for use in automotive applications. However, the environmental driving force for using natural fibers has never been as important as it is in today's composite market [4]. Moreover, the use of vegetable oil-based resins provides improved materials from renewable resources and it maintains not only chemical sustainability with low environmental impact, but also, it offers a high mechanical and impact strength. Plant oil-based biocomposites are mainly referred to as bio-based resins with synthetic or natural fibers. The performance of composite depends on the fiber volume fraction, type of fiber reinforcement and on interfacial properties. The interfacial interactions are mainly influenced by the degree of dispersion of fiber in resin and physical/chemical interactions between fiber and matrix. The potential for new products and new applications from natural fiber reinforced plant oil-based composites is far from being exhausted due their availability, low cost, high corrosion resistance, ease of processing, high specific mechanical strength, and their

environmentally friendly nature. Some real examples of using epoxidized soybean oil-based matrix and natural fibers are in floors, walls and roofs of houses.

In last decade, there has been an extensive research conducted by many authors in different research institutes and companies on plant oil-based bioresins in terms of applications, synthesis, and characterization of biocomposite [2, 5-20]. These studies include different plant oil-based resins such as soybean, canola and linseed oils.

The main disadvantage of these bio-based resins are their low glass transition temperature (T_g), and low mechanical properties such as modulus and hardness due to flexibility in fatty acid chains. In order to obtain a rigid polymer from plant oils with high modulus, strength, durability, and resistance towards thermal stress and chemical attacks for structural and engineering applications, introducing reactive sites such as epoxy, acrylate or methacrylate functions are necessary. However, the development of bio-based resins for structural applications is still a challenge for the polymer and composite industries. Procter & Gamble (P&G) Chemicals suggested substituting the sucrose with fatty acid to obtain sucrose esters of soybean oil. Sucrose esters of soybean oil provides molecules with even higher hydroxyl functionality due to the presence of eight fatty acid chains per molecule versus the three for the soybean oil [21].

Therefore, the main goal for this research is to investigate the development and processing of new generation bio-based resins which were prepared by ring-opening Epoxidized Sucrose Soyate (ESS) with acids or alcohols in detail [21, 22] [23] in bio-based composites to solve the problem of flexibility of fatty acid chains. Two novel bio-based thermoset polymers reinforced with flax fiber and improves the knowledge-based of biocomposite to meet the needs of a growing composite market.

1.1. Research Objectives

The need to replace fossil-based materials has led to an increased interest in natural fibers and bio-based polymers. This research seeks to advance this technology by investigating different types of novel functionalized sucrose soyate resins from renewable origins as matrix materials with flax fiber and E-glass fibers as reinforcements.

When it comes to using new resins to produce composites, it is important to investigate the effect of process variables on the quality of composites fabricated for high mechanical performance. Part of this study will also investigate the mechanical and thermo-mechanical properties of the novel bio-based resins, MSSP and MAESS resins reinforced with E-glass fibers and comparison of mechanical properties of the composites with the existing bio-based resins and petroleum-based resins reinforced with E-glass fibers.

Due to the high cost of synthetic fibers, natural fibers have attracted the attention of the composites industries as a potential reinforcement. These fibers are based on cellulose and offer advantages of chemical sustainability, low density, nonabrasive nature, and low cost. Therefore, this study will also investigate using flax fiber in the two novel bio-based thermoset matrices-MSSP and MAESS, and vinyl ester resin as reference. The specific mechanical properties of the flax fiber reinforced bio-based resins will also be compared with E-glass/bio-based resins in order to see the potential replacement of the corresponding fiberglass composites with flax fiber composites.

To fully understand the adhesion performance of bio-based resins with flax and E-glass fibers, the interactions at the microscopic and nano-scale will be assessed by analyzing the fracture surface using scanning electron microscope (SEM) and nano-indentation tests. These analyses are helpful to gather qualitative data to support the results of the interfacial bonding in

interface and interphase regions. Finally, it is important to develop a numerical method to predict the mechanical properties for flax/MSSP composite considering viscoelastic properties of both MSSP resin and flax fiber to have more accurate prediction. Therefore the following eight objectives were established for this study:

1. Establish the appropriate processing conditions for MSSP and MAESS resins using compression molding to fabricate high quality fiber volume content composites.
2. Substantiate the composites made from MSSP resin perform similarly if not superior to previous bio-based and petroleum-based composites studied.
3. Confirm improved mechanical properties of E-glass/MAESS over those of E-glass/vinyl ester composites or previous bio-based composites.
4. Prove the composites made from flax fiber with MSSP or MAESS resins achieve similar properties to E-glass/MSSP and E-glass/MAESS in terms of specific mechanical properties. Moreover, to prove flax/MSSP and flax/MAESS composites perform similarly, if not superior to previous bio-based and petroleum based composites studied.
5. Substantiate the increased interfacial properties in the bio-composites by analyzing failure surface and interphase properties by SEM and nano-indentation.
6. Develop an analytical and numerical method to predict and define the viscoelastic behavior of flax/MSSP composite materials in three axial directions, which are often complicated to measure experimentally.
7. Employ a numerical method to examine the effect of the fiber/matrix volume ratios, the local stress/strain distributions, and volume-averaged stresses and strains for flax/MSSP composite.

8. Perform an experimental study to validate the numerical modeling results for the linear viscoelastic response of flax/MSSP composite material.

1.2. Outline of Dissertation

The dissertation is divided into 8 Chapters. After this first Chapter, an overview of relevant literature for this study will be presented (Chapter 2), including recent research on the synthesis of new bio-based polymeric units, using natural fiber reinforcements in composite applications, and theoretical and numerical methods for predicting composite properties. Chapter 3 provides the required information to fabricate the studied composites, including, composite Fabrication, constituent materials used in this study and manufacture of composite. Effect of processing conditions of compression molding in mechanical properties is also discussed. Finally, different characterization and analysis techniques on novel resins and their composites are discussed.

Chapter 4 and Chapter 5 report the investigation of mechanical and thermo-mechanical properties of novel Methoxylated Sucrose Soyate Polyols (MSSP) and Methacrylated Epoxidized Sucrose Soyate (MAESS)-based resins, respectively, which were reinforced with unidirectional E-glass fiber (50% fiber volume fraction).

Mechanical properties of new resins and the resulting composites were assessed by tensile, flexural, interlaminar shear strength (ILSS), nano-indentation, and impact strength testing. Scanning Electron Microscopy (SEM) of fractured surfaces of specimens were examined to investigate the fiber-matrix interface behavior. Finally, to highlight the performance of bio-based resins in composites, the results of bio-based composites were compared with previous studies of similar bio-based and petroleum-based composites.

The main goal in Chapter 5 was to manufacture composites based on the new high functionalized sucrose soyate resins from renewable origins (MSSP and MAESS) as matrix materials with flax fibers as reinforcements. For certain applications, especially in automotive and building product applications, using natural/biofiber composites are emerging as a viable alternative to glass fiber reinforced composites. Natural fibers have an advantage over glass fibers in that they are less expensive and abundantly available from renewable resources and have a high specific strength. Therefore, the motivation in Chapter 6 was drawn from investigating the compatibility of these novel resins with flax fibers and comparing the mechanical and thermo-mechanical properties of these new resins reinforced with flax fiber with those reinforced with glass fibers.

Chapter 7 involves a micromechanics procedure to predict the mechanical properties of composites in three major directions, which are often complicated to measure experimentally. Local stress/strain fields will be also be monitored within the components of composite materials in a micromechanics analysis. In this study, random fiber distribution with identical fibers (RND) model was examined. Finite element micromechanical analyses were performed on the selected model representing Repeating Unit Cells (RUCs) of Unidirectional (UD) composite. The stiffness values from micromechanical analysis of RND model for glass fiber-reinforced with bio-based thermoset composite were compared to experimental data to confirm theoretical data gained from the model.

Chapter 8 presents the general conclusion of this study and revisits the eight specific objectives stated for this dissertation. Finally, the limitations of this study and possible avenues for future research will be presented.

CHAPTER 2. PLANT OIL-BASED BIOCOMPOSITE: LITERATURE REVIEW

This Chapter provides relevant information about the current state of bio-based composite materials, processing, and associated literature. Background on oil-based resins is also discussed including structure, and why it is of interest to investigate as a new generation of resin material in bio-based composites. Also, the relevant literature for the bio-based resins and fiber materials, and composite processing is discussed here. Finally, a proper numerical modelling approaches is discussed here in order to predict and define the viscoelastic behavior of the flax/MSSP composite.

2.1. Materials

2.1.1. Reinforcements for Biocomposite

Reinforcing agents are used to improve the performance of neat polymers. The fibers have high aspect ratios in order to provide better wetting and physicochemical interactions with matrix. Mechanical properties of composites depends on some elements of matrix and fiber such as, the type, orientation, distribution, shape, and the void content. There are different types of reinforcing materials which are used with oil-based resins including (1) synthetic fibers such as glass carbon, and aramid fibers, (2) natural fibers such as jute, flax, and hemp, and (3) combination of natural and synthetic fibers. Figure 2-1 shows percentage values of synthetic fiber and resins in the fiber composite market [24]. Natural fibers are widely used in composite applications due to their high specific strength, good thermal properties, low cost, renewability and high toughness [4, 25].

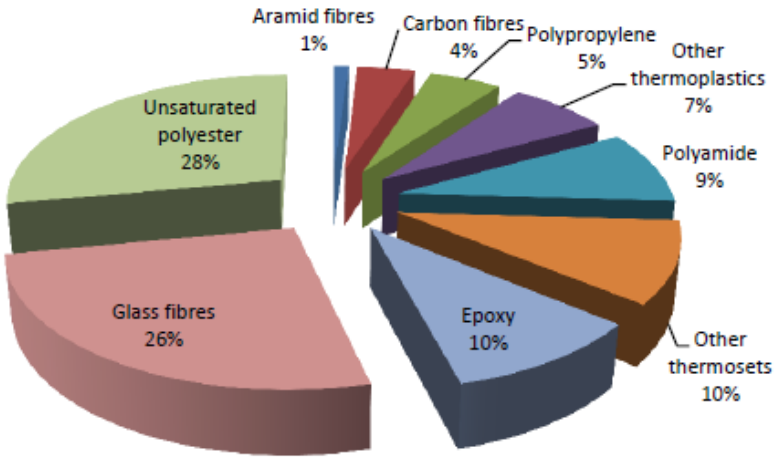

Figure 2-1.Percentage values of synthetic fiber and resins in the fiber reinforced composite market [24].

2.1.1.1. Glass fiber

Glass fibers are the most widely used reinforcements in the current fiber composite industry due to their low price and their easy manufacture. However, glass fibers have low elastic modulus compared to carbon and aramid fibers and there is also some health risk regarding to skin irritation. The price for E-glass, S-glass fiber are approximately $2 to $4 per kilogram and $24 to $40 per kg, respectively.

E-glass fiber is the most common glass fiber which are used in the preparation of composite materials. E-glass fiber were widely used for different types of synthetic/plant oil-based polymer composite applications due to their low cost, availability, chemical resistance and high strength. In particular, use of glass fiber reinforced polymer is justified where high performance materials for high temperature applications are needed. However, in situations where specimens are exposed to lower stresses and temperatures, alternative materials with significantly lower cost such as natural fibers are more reasonable. In addition to financial constraints, the use of glass fibers in some sectors such as automotive industry is not preferred because of its high density (2.5 g/cm^3) which increases the specific weight of composites, which

limits its applications in many advanced applications where low weight is preference. Moreover, the glass fiber wastes remaining from the recycling and disposal of GRP, is a crucial issue of the aforementioned composites.

2.1.1.2. Carbon fiber

Carbon fiber show a very high strength and modulus up to 2000 °C and it has lower specific gravity than E-glass fiber. Therefore, the use of this fiber with synthetic or bio-based resins has many advanced applications. However, fiber availability, high expense (up to $30 to $80 per kg) and resin incompatibility are some disadvantages to the use of carbon fiber in composite industries. Imbedding high strength and high modulus carbon fibers in a composite improves strength and rigidity of neat polymers tremendously.

2.1.1.3. Sisal

Sisal fiber is a leaf fiber which has found a lot of increasing interest as a promising reinforcement in new applications due to its high specific strength and modulus durability, renewability, availability and its cost. This fiber is renewable and does not have any health risks. This fiber can be fire resistant by treating with borax [26].

2.1.1.4. Flax

Flax is one of the oldest fiber crops in the world. This fiber extracted from the bast of the flax plant. The fiber is soft and flexible and its best grades are used for linen fabrics. As early as in 1908, the first commercial natural-fiber-based polymer composites, with cellulose fiber in phenolics was used in the automobile industry [3].

Table 2-1 shows the physical properties of some of the most common natural and synthetic fibers for composite applications. Synthetic fibers such as carbon, aramid, and glass fibers can be synthesized with a specific range of mechanical properties, whereas, natural fibers

show a broad range of characteristic properties. This is attributed to the natural variability in plant, variation in fiber cross section area along its longitudinal axis, the growing condition and test methods even for the same kind of fiber [27-29]. Tensile strength and modulus, density, electrical resistance and other characteristic properties of plant-based fibers also depend on the age of the plant, their locations, the origin of the fiber (i.e. plant stem, leaf, shell), length and diameter of individual filaments. The processing methods which are used to extract the fibers and damage sustained through processing can also affect the quality and quantity of extracted fibers which in turn affects the mechanical performance of composites. Fibers are mainly extracted mechanically. For instance, first processing stage of fiber extraction is retting and then some mechanical processing including scutching and hackling. Because of these physical issues described along with collection, grading, and sourcing of natural fibers, there are some challenges for the commercialization of natural fiber composites.

The major constituents in natural fibers are cellulose, hemicellulose, lignin, pectin, and waxes. The celluloses and hemicelluloses are the main structural parts of natural fibers. Because of hydrophilic nature of these components, they have very poor interface and poor resistance to moisture absorption when they are used to reinforce hydrophobic matrices [27]. Since the low interfacial properties between fiber and polymer matrix often reduces their potential as reinforcement, chemical modifications are considered to improve the interface of fibers. Chemical treatments improve the adhesion between natural fibers and matrix by activating hydroxyl groups or introducing new chemical functionalities on the fiber surface. Some other disadvantages of natural fibers included lack of thermal stability, strength degradation, and poor impact properties [6, 30]. All natural fibers contain natural sugars which start to caramelize in

the 150 °C to 200 °C range, so they cannot be utilized with high temperature plastics such as nylon.

Table 2-1. Physical Properties of Flax Fiber and E-Glass Fiber Material [31-33].

Fiber	Density (g/cm^3)	Young's Modulus (GPa)	Tensile Strength (MPa)	Specific Young's Modulus $GPa/(g/cm^3)$	Specific Tensile strength $GPa/(g/cm^3)$	Elongation at Failure (%)
Sisal	1.45	9-22	530-630	6-15	365-434	3.7-5.2
Flax	1.4-1.55	12-85	500-2000	8.6-60.7	360-1430	1-4
Jute	1.3-1.45	13-27	400-800	9-20	275-615	1.5-1.8
E-glass	2.50	70-73	2000-3400	27-28	769-1346	2.5-3
Carbon	1.7	230-240	4000	135-140	2350	1.4-1.8

2.1.2. Thermoset Resins for Biocomposite

Thermosetting polymers, vinyl ester, polyester, polyurethane, epoxy resin, etc., have been used in composite industries with natural fibers due to their high modulus, strength, durability, and resistance towards thermal stress and chemical attacks. Thermosetting materials are cured using heat or heat and pressure and/or light irradiation [34]. Table 2-2 shows the physical properties of some of the most common synthetic resins for composite applications. The following paragraphs will focus on the vinyl ester, epoxy, and polyurethane thermosetting polymers and discuss their chemistry, properties, and resulting applications in biocomposites.

Table 2-2. Properties of Common Synthetic Polymers Used in Composites [35, 36].

Property	Polyurethane	Vinyl ester	Epoxy
Density (g/cm3)	1.1–1.2	1.2–1.4	1.1–1.4
Tensile modulus (GPa)	2.1-2.3	3.1–3.8	3–6
Tensile strength (MPa)	40-62	69–83	35–100
Tensile elongation to break (%)	7-9	4-7	1-6
Cure shrinkage (%)	N/A	N/A	1–2
Izod impact strength (J/m)	78-170	2.5	0.3

2.1.2.1. Polyurethanes

Polyurethanes are an important class of thermoplastics and thermosets depending on the nature of the polyol and isocyanate components used. Polyols and isocyanates are the main components of polyurethane. The mechanical, thermal, and chemical properties of polyurethanes depend on the chemical structures of polyols and isocyanates. The chemical structure of Methylene Diphenyl Diisocyanate (MDI) which is an aromatic diisocyanate is shown in Figure 2-2. Different types of isocyanates are di-or polyfunctional isocyanates contain two or more than two –NCO groups per molecule. Their chemical structure could be aliphatic, cycloaliphatic, polycyclic or aromatic. PU resulting from aromatic isocyannates have lower oxidative and ultraviolet stabilities; but they are more rigid [37]. The synthesis of polyurethane (PU) can be carried out by the reaction simplified in of an aromatic isocyanate with a polyol (Figure 2-3).

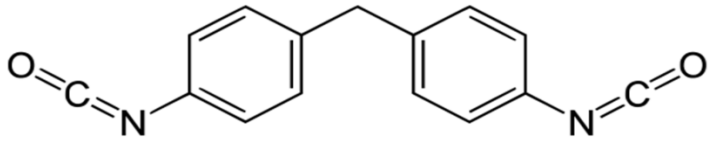

Figure 2-2. Chemical structure of an aromatic diisocyanate.

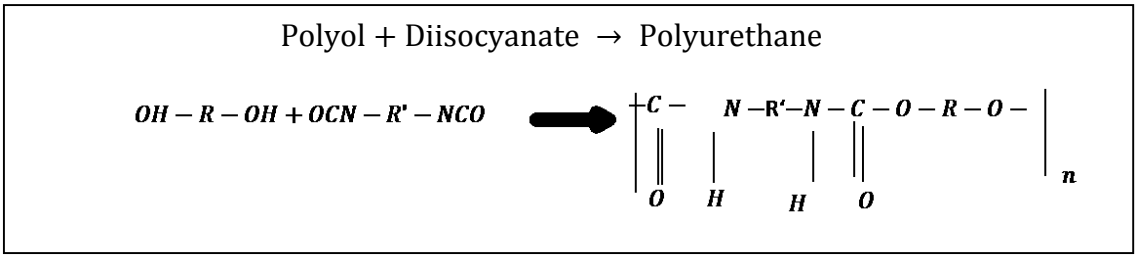

Figure 2-3. Polyurethane synthesis.

Wherein the urethane groups — NH-(C=O)-O- link the molecular units, R and R' are aliphatic and aromatic nature respectively. Polyurethanes are important materials used in many

commonly used products such as foams, both rigid (used as insulation in building construction and in application) as well as flexible such as those used in furniture. In addition, thermoplastic polyurethanes have many applications such as in footwear, car interior, medical devices, adhesive, and coatings. Polyurethanes in general show better abrasion resistance, toughness, chemical resistance, and mechanical strength compared to other polymers such as polyesters and polyesteramides.

2.1.2.2. Vinyl ester

Vinyl ester (VE) resins are oligomers with unsaturated terminal sites which are formed by the reaction between bisphenol-A and unsaturated carboxylic acid such as acrylic or methacrylic acid. Figure 2-4 shows the most common vinyl ester system which is the product of reaction between a bisphenol-A with methacrylic acid. These reactive groups can form a crosslinked network by the free-radical copolymerization with or without the addition of a reactive monomer such as styrene, which is less expensive than epoxy base. VE resins are comprised of approximately 30-50% styrene of the final volume of the resin system in many industrial VE resins. Use of lower styrene in VE resins results in higher viscosity which may cause some difficulties in composite processing such as lower wettability between the resin and fiber. VE displays similar shrinkage behavior to UP systems. Styrene and the end acrylic or methacrylic groups of VE resin can crosslink to form a network. The cure reaction conditions such as initiators, catalysts, concentration of the monomers, and temperature determine the mechanical properties of the final product. VE combine the best chemical and mechanical properties of unsaturated polyesters (UP) and epoxies. VE offers better moisture and chemical resistance than polyesters, as fewer ester groups in the VE structure. Different combinations of accelerators, promotors, initiators and inhibitors are used in the curing of VE systems. The

kinetics of curing reaction of vinyl ester has been investigated via different techniques, DSC curing behavior, DMA and FTIR.

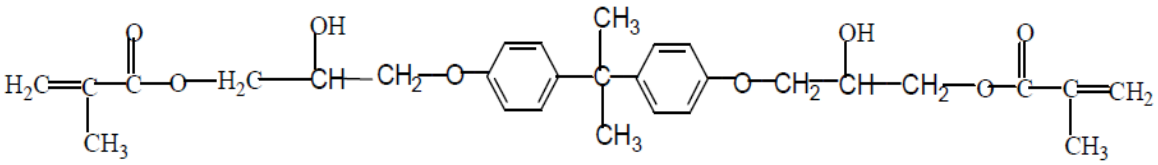

Figure 2-4. Bisphenol-A epoxy based vinyl ester resins [38].

2.1.2.3. Epoxy resin

Epoxy resin is a broad class of high performance oligomers for which cross-linking occurs through the reaction of a highly reactive epoxy group. The term "epoxy" is defined as a molecule consisting of oxirane rings. There are several different ways for curing of epoxies such as, through homopolymerisation, thiols and alcohols. Epoxies are mainly cured through reacting with amines and anhydrides type hardener. The capability of the oxirane group to undergo a large variety of addition and polymerization reactions has been used for the production of many different epoxy thermosetting materials.

Figure 2-5 shows the chemical structure of diglycidyl ether of bisphenol A (DGEBA) which is the most common type of epoxy. Epoxies show high mechanical properties, good resistance to chemical attacks, high temperature resistance, and offer excellent fiber-matrix adhesion properties necessary for durability and structural performance. The epoxy resins are used mainly in coatings, casting materials binders, aerospace and marine applications.

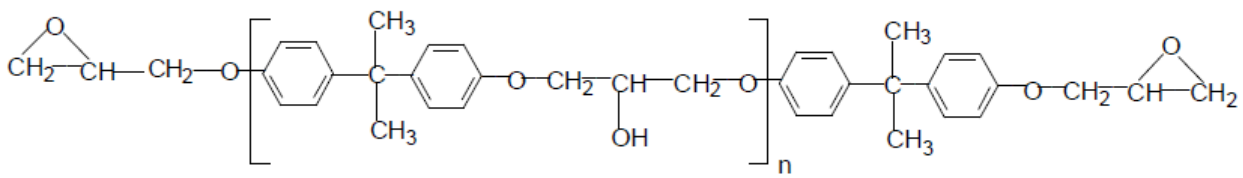

Figure 2-5. Chemical structure of diglycidyl ether of bisphenol A (DGEBA) epoxy [38].

2.1.3. Renewable Oil- Based Polymer for Biocomposites

Use of natural fiber with synthetic plastic is not sufficiently environmentally friendly because of the petroleum-based source and the non-renewability nature of the polymer matrix. However, using vegetable oils, fatty acids and their derivatives as raw materials in creating various types of polymers has gained focused attention in various composite industries [39]. Over the last decade, a broad range of chemical routes to utilize natural triglyceride oils for synthesizing monomers as the basis for coatings, inks, plasticizers, lubricants, polymers and composite materials has been developed. Although most of the focus on bio-based polymers has been on the development of bio-based thermoplastics, recent studies have been focused on the development of bio-based thermosetting polymers [40]. In addition, a broad range of properties have been obtained from the use of glass fiber to reinforce bio-based resins using different modifications routes and polymerization processes with the resins [9, 10, 41-43]. Agricultural products typically cannot be used as they appear in nature. They need to be converted into functional polymers, fermentated, and modified. Research efforts need to focus on interdisciplinary approaches that integrate plant science, material science and engineering to develop new, improved materials from renewable resources that could be biodegradable and enhance global sustainability. The main elements of vegetable oils are triglycerides which have the structure shown in Figure 2-6. The presence of triglycerides in the chemical structure of the bio-based polymers, such as vegetable oil polymers, incorporates desirable flexibility and toughness into the resins [44]. A primary variable that differentiates one vegetable oil from another is the number of double bonds in the fatty acid. However, additional functional groups can be presented such as hydroxyl groups in castor oil. The number of double bonds for most common oils vary from 0 to 3 per fatty acid chain. In order to synthesize new monomers and

rigid composite resins from plant triglycerides, functionalizing the triglyceride molecule thereby introducing reactive sites is necessary [45]. Some modifications to the plant oil triglycerides to functionalize the molecules include epoxidation, maleinization, amidation, hydroxylation, acrylation and glycerolysis reactions. Since the epoxy functions are highly reactive, epoxidation is one of the most important and useful modifications to functionalize triglycerides using the double bonds of unsaturated fatty compounds.

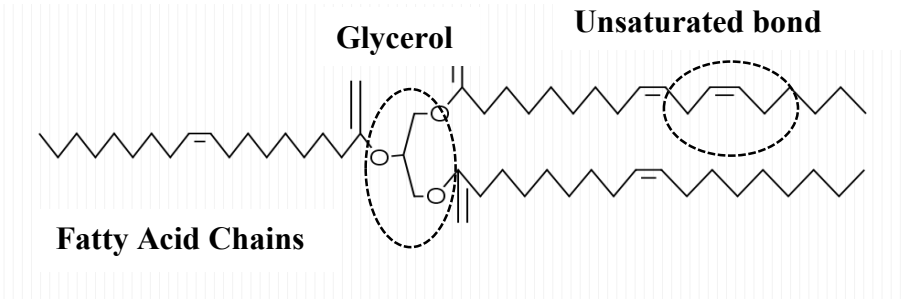

Figure 2-6. Triacylglycerol with double bond in fatty acid chains.

Afterwards, in order to use the functionalized triglyceride molecules in the synthesis of cross-linked thermosetting polymers, such as vinyl ester, polyester, polyurethane, epoxy resin, various techniques of polymerization should be implemented [21]. Besides, the modification of double bonds can add some functionalities like epoxy, hydroxyl and maleates [10, 46-48] which could further be cross-linked for being used in syntheses of different varieties of vegetable oil-based polymer composites such as, epoxies, polyurethanes, and polyesters. The following subsections will review some recent literature on bio-based renewable material for composite applications.

2.1.3.1. Bio-based Epoxy Composite

Biocomposite materials have been manufactured using plant oil-based epoxy resins with natural or synthetic reinforcements, in order to explore the possibility of producing strong and durable epoxidised plant oil-based polymer composite. Khot et al. [10] used an acrylated

epoxidized soybean oil (AESO) to make composite materials. As result of the reaction of acrylic acid with epoxidized triglycerides, acrylated epoxidized soybean oil was synthesized. They used resin transfer molding method to produce 35 wt% to 50 wt% glass fiber-reinforced composites from acrylated epoxidized soybean oil. These composites exhibited a tensile modulus of 5.2 to 24.8 GPa and a tensile strength of 129 to 302.6 MPa, depending on the range of fiber content [10]. Dweib *et. al.* [12] and O'Donnell *et. al* [17] manufactured biocomposites using vacuum assisted resin transfer molding with recycled paper, hemp, flax, cellulose, pulp fibers and chicken feathers as natural fibers and AESO resin as plant oil-based resin. Depending of the type of fiber, flexural modulus were reported 1.5-6 GPa for 10-55 wt% fiber reinforcement.

2.1.3.2. Bio-based Polyurethane Composite

Plant oil-based polyurethane resins are extensively used in the field of biocomposite due to their compatibilities with bast fibers such as flax and jute fibers. Different chemical modification on the surface of fibers may improve this compatibility and cause improvement in fiber-matrix interlocking at the interphase. Husic *et. al.* [41] used both soybean-based polyurethane and petrochemical-based polyurethane in glass fiber composites, which were referred to as Soy and Jeffol polyurethane respectively. All the results of mechanical properties showed that soy polyurethane has comparable mechanical performance to Jeffol polyurethane, in glass fiber composites as is reported in Table 2-3.

Desroches *et al.* [49] presented a comprehensive review on three different synthetic approaches to obtain polyols from vegetable oils. Also, they provided a useful list of commercial bio-based polyols and their corresponding industrial synthetic routes for the production of polyurethanes. Several studies have investigated the synthesis of Castor Oil-based Polyol (COPO) by alcoholyzed castor oil for the production of polyurethane through poly-condensation

reactions with different isocyanate components [47, 50]. The polyurethane made from castor oil is relatively soft since the number of hydroxy groups per molecule is only 2.7. Sucrose esters of soybean oil-sucrose soyates-, provides molecules with high hydroxyl functionality due to the presence of eight fatty acid chains per molecule versus the three for the soybean oil [21].

2.1.3.3. Bio-based Polyester Composite

Methacrylic anhydride modified soybean oil (MMSO) was used as the resin and reinforced with flax fiber with the fiber to resin ratio of 60:40, by a compression molding as described in ref. [51] [5]. The mechanical performance of the resultant composites were highly improved. When the MMSO was used with woven flax fabric, the impact strength 26 kJ/m^2. The flexural strength and modulus were about 98 MPa and 6 GPa, respectively. Tensile strength and The effect of the natural fibers and Young's modulus of the composites increased from 2.7-7.4 MPa and 0.29-1.39 GPa, respectively. Mechanical properties of some the biocomposite which were already discussed are also summarized in Table 2-3.

Table 2-3. Mechanical Properties of Some Plant Oil-based Polymer Composites in Literature.

Composite (fiber fraction wt%)	Tensile Modulus (GPa)	Tensile Strength (MPa)	Flexural Modulus (GPa)	Flexural Strength (MPa)	Glass Transition Temperature (°C)	Ref.
Glass/AESO (35)	5.2	129	9	206	80	[10]
Hemp/AESO (20)	4.4	35	2.6	35.7	--	[10]
Flax/AESO (34)	3.6	30	4.2	65	--	[10]
E-glass/soy (70)	17.07	259	18.86	418	140	[41]
E-glass/Jeffol (70)	18.65	276	27.07	444	150	[41]
Flax/MMSO (55)	--	--	6	98		[5]

2.1.4. Progress in Renewable Oil- Based Polymer for Biocomposites

This work focuses on the two novel MSSP and MAESS bio resins that have been found to be promising candidates for use in the advanced composites and engineering polymer fields.

The replacement of petroleum-based polymers with bio-based counterparts is a recent innovation in the field of "green composites". Green composites are consist of natural fibers and a bio-based matrix [3, 52]. Some economic advantages of using bio-based polymers include global accessibility and relative low cost. For example, the US northern plains are rich with renewable resources, so producing valuable polymers from such low cost and renewable resources provides unique opportunities for rural economic development [39]. Additionally, bio-based polymers have potential benefits for the green composite industry due to the ease of natural oil polymer preparation, the low cost and abundant supply of natural oils [48]. Several studies have investigated the synthesis of Castor Oil-based Polyol (COPO) by alcoholyzed castor oil for the production of polyurethanes through poly-condensation reactions with different isocyanate components [47, 50]. The polyurethane made from castor oil is relatively soft since the number of hydroxy groups per molecule is only 2.7.

However, in order to obtain a rigid polymer with high modulus, strength, durability, and resistance towards thermal stress and chemical attacks, higher functionalities of polyol are needed. While, epoxidized soybean oil-based polyols provide higher functionalities, they still offer relatively, low mechanical properties such as modulus and hardness due to the flexibility in their fatty acid chains. Sucrose esters of soybean oil provides molecules with even higher hydroxyl functionality due to the presence of eight fatty acid chains per molecule versus the three for the soybean oil [21]. Pan et al. reported the synthesis of even higher functionality polyols which were prepared by ring-opening Epoxidized Sucrose Soyate (ESS) with acids or alcohols in detail [21, 22].

Throughout this study, two novel resins from epoxidized sucrose soyate (ESS) have been utilized. The epoxidation of these sucrose esters (ESS) has recently been reported by Pan et al. as

shown in Figure 2-7 [23]. When the ring-opening of ESS is reacted by methanol, the resultant polyol is referred to as MSSP and when it is reacted by methacrylated acid it is referred to as MAESS [1, 22]. The chemical structure of MSSP and MAESS are shown in Figure 2-8.

Nelson et al [22] and Yan et al [1, 22] reported a detailed description of the synthesis of Methoxylated Sucrose Soyate Polyol (MSSP) and methacrylated epoxidized sucrose soyate (MAESS) resins. Polyols derived from sucrose esters have a unique structure which can offer a high hydroxyl functionality of about 10 epoxy groups per molecule while retaining a very high bio-based content. This high functionality polyol contained 300 g MSSP per OH equivalent (300g / OH eq.). The MSSP had a high viscosity (113,000 mPa.s) which was attributable to a significantly higher degree of hydrogen bonding in the polyol resins [22]. The high functionality MAESS contains 245 g MAESS per epoxy equivalent (245 g/epoxy eq [1]. The MAESS resin was too viscous to be used for thermoset formulations. Therefore, styrene was introduced as a reactive diluent to reduce the viscosity, as well as a co-monomer to increase the rigidity of the resulting thermoset. On the other hand, it reduced the renewable content of the material. 30 wt% styrene was used which is the optimum formulation reported by Yan et al.[1]. The research concluded these novel high functional bio-based resins provide higher ranges of cross-linked density and hardness when creating resins in coating applications [21, 22]. In this study, the potential applications of these novel polymers as matrices and flax fibers as reinforcements in composites have been explored for the first time.

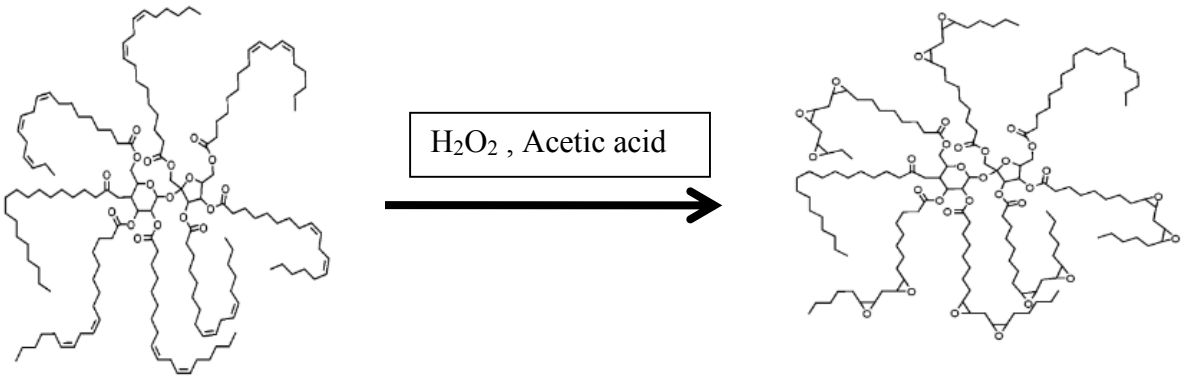

Figure 2-7. Synthesis of ESS from Sucrose Esters of Soybean [23].

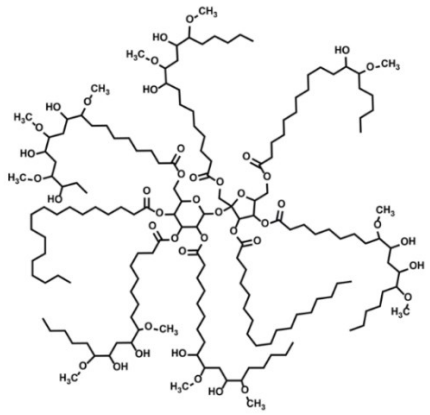

MSSP

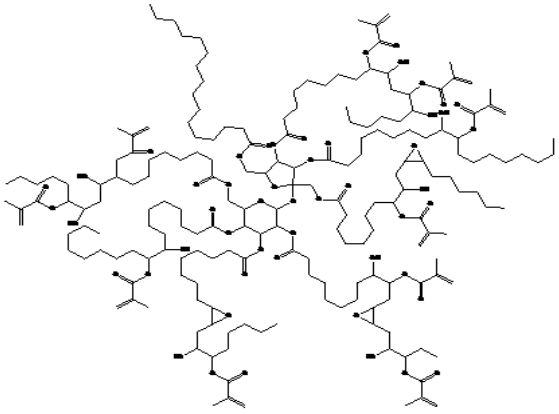

MAESS [1]

Figure 2-8. A schematic of chemical structures of the biobased thermosetting resins used in the composite preparation.

2.1.5. Composite Processing Technique

In recent years the processing and production technologies for biocomposites have also advanced. To date, injection molding, extrusion, compression molding, sheet molding and resin transfer molding are the major manufacturing processes for natural fiber- reinforced composites.

2.1.5.1. Pultrusion

The pultrusion process has been utilized to manufacture polymer composite parts for decades. Polymer resins used in this process have traditionally included polyester, vinyl ester, epoxy or other petroleum-based resins. Pultrusion technology which was developed in 1950s, is a process of pulling reinforcing fibers through a bath, where they are soaked with formulated resin, and then pulled through a heated die creating a continuous composite profile. The pultrusion process has been successfully applied in fabricating traditional composites using fiber reinforcement like glass fibers and carbon fibers [53]. There are a several advantages for pultrusion over other composite forming processes. Higher composite strength can be achieved via pultrusion due to the alignment and the tension that fibers experience during the process. Pultrusion is also a highly automated process with very little manual interface, so it enables high volume production of constant cross-section parts with consistent quality and excellent structure. Furthermore, pultrusion is a relatively cost effective process which has the potential of making composites with higher fiber content. Based on its distinct advantages, pultrusion is considered as a good choice for manufacturing natural fiber composites by improving the consistency of composite quality and the overall properties by means of better impregnation, distribution, and alignment of the reinforcing fibers [54, 55]. Chandrashekhara et al. used a mixture of epoxidized soy oil based resin with a commercial epoxy-amine system formulated for use in pultrusion [9]. Pultruded glass fiber composites (63 wt.%) were prepared with this resin. It was observed that

although the tensile and flexural properties were not strongly affected by the replacement of the synthetic epoxy by the bio-based resin, there was a clear improvement in the resistance of the composite to impact damage. Since the epoxy groups in the fatty acid chains are not terminal, the resulting molecular structure contains a large concentration of dangling chains that have a plasticizing effect, leading to more flexible material than the synthetic counterparts. In addition, the use of synthetic resins in composite decreases the force needed to pultrude the composite bars (almost 30% reduction for the formulation made with a 30% replacement of the epoxy resin by the bio-based one). This benefit was explained by the lubricity properties contributed by the oil.

2.1.5.2. Compression Molding

Compression molding is one of the most common processing used to manufacture high fiber content composite parts. Thermoset compression molding uses mats made of natural fibers. The mats are sprayed with resin and compressed into their final contour in a hot tool (Figure 2-9); due to the air-permeability the parts can be covered easily in a vacuum covering process [56].

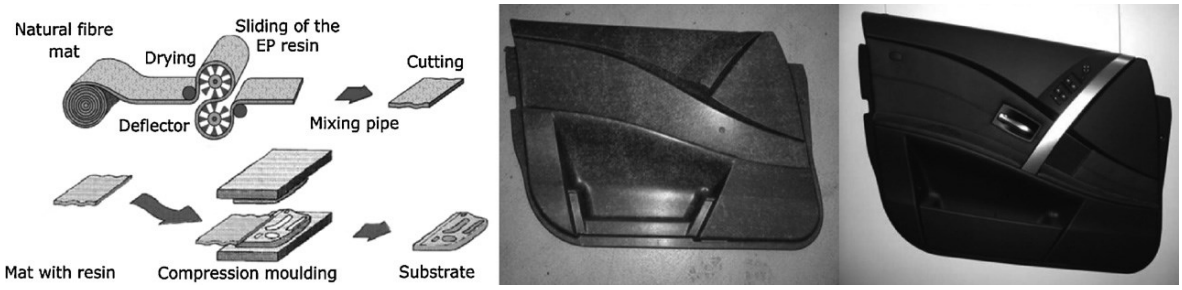

Figure 2-9. Thermoset mat compression process and ready component part; raw and covered by all functional and decorative details. Adopted from [56].

Idicula, M., et al. studied the dynamic and static mechanical properties of the short abaca/sisal hybrid fiber reinforced polyester composite produced by using the thermoset

compression molding process [57]. They also investigated dynamic properties, such as the storage modulus, damping behavior and static mechanical properties (i.e., tensile, flexural and impact properties) as a function of the total fiber volume fraction and the relative volume fraction of the two fibers. They showed the storage modulus was increased with fiber volume fraction above T_g of the matrix. A maximum storage modulus value was maximum at a volume fraction of 0.40. The tensile modulus and flexural strength were also had the highest value at volume fraction of 0.40, which shows effective stress transfer between the fiber and the matrix.

In another study, Idicula, M., et al. investigated the thermal conductivity, diffusivity and specific heat of thermoset compression molded polyester/natural fiber (abaca/sisal) composites for several fiber surface treatments as functions of the filler concentration [58]. Thermo-physical behavior of hybrid Pineapple Leaf Fiber (PALF) and glass fiber reinforced polyester composites were also evaluated with constant total fiber loading equal to 0.40 volume fraction by varying the ratio of PALF and glass. The results showed that the chemical treatment of the fibers reduces the composite thermal contact resistance. Hybridization of natural fibers with glass allows a significantly better heat transport ability of the composite. Thermal conductivity, which is measured in the direction transverse to the plane of composite plate, could be well represented by a series prediction model [58].

2.2. Application of Biocomposites

Petroleum-based composites have a lot of applications in construction and building, automobile panels, transportation, aerospace, agricultural equipment, and so on. Use of renewable and sustainable materials require low cost of raw materials. The use of biocomposites from plant oil-based polymers and natural fibers have found tremendous potential applications in next generation of materials. There are various structures have been made of plant oil-based

composites such as, car door paneling, sandwich plates, tubes, packaging, adhesive, resins, electronics, aerospace, sport equipment, housing and transportation, and so on [59]. Biocomposite of epoxidized soybean oil and flax fiber composites showed sufficient mechanical properties for being use in a variety of applications such as automotive, construction industries, civil engineering and agricultural equipment [60]. Combinations of synthetic and natural fibers have also been successfully used for structural beams and mechanically tested with good results [12].

2.3. Micromechanical Modeling of Composite

While, there have been numerous studies on prediction of the mechanical properties of natural fibers, including elastic stiffness or strength [33, 61], their viscoelastic behavior has rarely been addressed. Analysis of Hashin (1966) showed that the viscoelastic effect in a unidirectional fiber composite is significant for axial shear, transverse shear and transverse uniaxial stress, for which the influence of matrix is dominant [62]. Viscoelastic contribution of these natural fibers to the overall rate-dependent behavior requires studying the viscoelastic behavior of both matrix and fiber.

The main objective of Chapter 6 is to examine the viscoelastic behavior of flax fiber and bio-based MSSP matrix in order to predict the mechanical properties using the characteristics of its constituents, i.e., micromechanical analysis. Two micromechanical analyses, including the finite element analysis (FEA) and analytical equations were analyzed to predict the relaxation behavior of composite material. To rely on micromechanical analysis, the particular approach must be validated through comparison to experimental data. Hence, experimental tests were performed to verify the numerical and algebraic equations. To this end, instantaneous elastic modulus and stress relaxation parameters of the constituents were determined using experimental

tests for both flax fiber and bio-based PU. The mechanical properties of the composite in the micromechanical analysis strongly depends on the accuracy of stress relaxation parameters. Therefore, in order to achieve reliable results, measurements were taken using Dia-Stron miniature tensile tester to measure stress relaxation parameters for the flax fiber. Dia-Stron miniature tensile tester has recently been used to study tensile testing, dimensional properties, failure analysis and bending moment for different kinds of fibers, but never, to the author's knowledge, on stress relaxation of flax fibers. The stress relaxation parameters from this test were used as the input for micromechanical analysis in finite element analysis in ABAQUS.

2.3.1. Micromechanical Model for the Composite Material by FEA

The micromechanical methods are the most common approach to determine the viscoelastic behavior of composite materials. Most micromechanical methods use periodic homogenization, which approximates the composite by periodic phase arrangements. A repeating unit cell (RUC) composed of fiber and matrix with a pre-determined packing of fiber is assumed as representative of the composite as a whole. Figure 2-10 shows SEM image of the cross section of flax/MSSP composite with three different fiber arrangement. As it is shown in this picture, it is assumed that the cross section area of fiber is circular and fiber distribution is random.

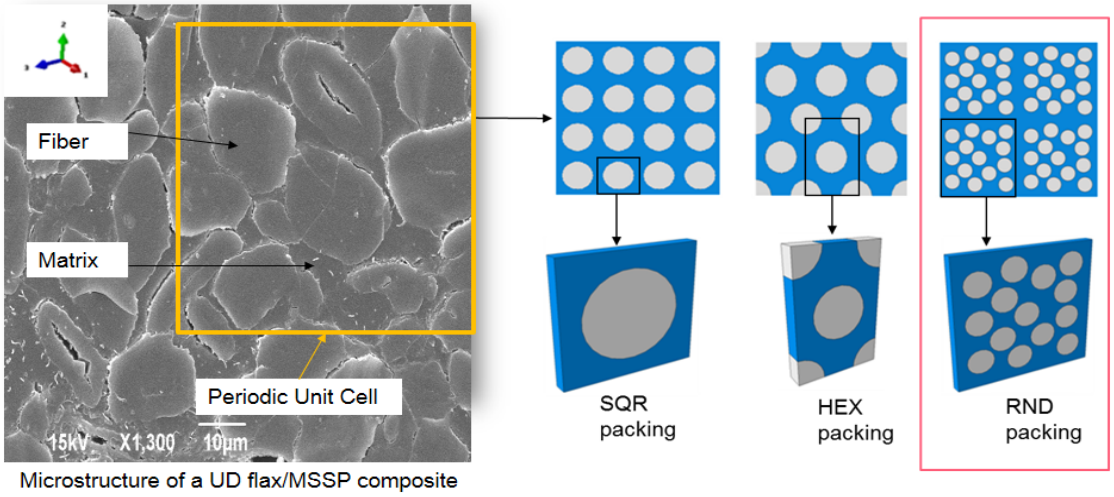

Figure 2-10. SEM image of the cross section of flax/MSSP composite with three different fiber arrangement.

Figure 2-11 shows the meshed unit cell of random packing of fiber representing periodic microstructure of a unidirectional composite. The fibers with the same diameter are distributed randomly in the matrix domain. The unit cell section consists of eight cylindrical fibers. Depending on fiber volume fraction, different diameter values were used for cross section of fibers. Javid et al. [63] showed that due to the assumption of perfect fiber and matrix bounding, the only parameter could affect the averaged stress values is fiber volume fraction. Therefore the shape of fibers cross-section might not have any effects on numerical results of modeling.

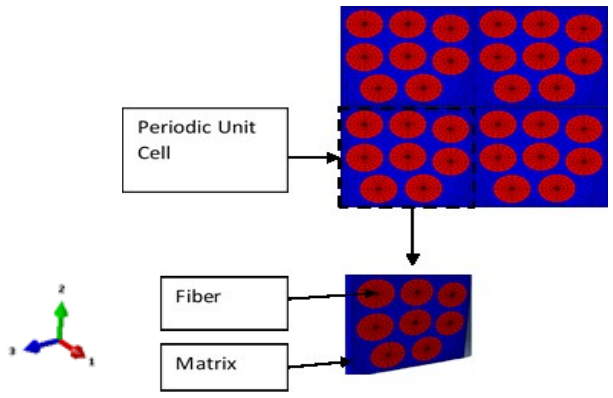

Figure 2-11. A rectangular repeating unit cell representing UD composites in random packing of flax fibers. The fibers are aligned in direction 1.

The response of the unit cell under specified loading conditions and appropriate boundary conditions is then analyzed to measure the composite's viscoelastic properties [64-66]. Several micromechanical approaches have been developed for prediction of aligned fiber composite viscoelastic response using synthetic fiber and matrix properties [66-71]. They have showed that time-dependent or viscoelastic properties (as demonstrated by creep and stress-relaxation tests) of polymeric resins affect mechanical properties prediction of the bio-based composite. To the author's best knowledge, previous studies have not accurately addressed the viscoelastic behavior of flax fiber in these composites. This study, therefore, assessed material and viscoelastic properties of both flax fiber and bio-based polyurethane resin to obtain more accurate prediction of mechanical properties of the composite.

2.3.2. Linear Viscoelastic Material

Mechanical properties of fiber and matrix play an important role in predicting the response of the composite. A wide range of constitutive relations from linear elastic to nonlinear-viscoelastic [72-77] have been assumed for the material properties of matrix and fiber in composite materials. In this work, the basic finite element models employed in the simulation of the composite deformation are described by the linear viscoelastic model for the matrix and flax fiber. Under small deformation assumption, a linear relationship between the strains and stresses is assumed, which can be expressed by the following Voigt vector form:

$$\begin{Bmatrix} \varepsilon_{11}(t) \\ \varepsilon_{22}(t) \\ \varepsilon_{33}(t) \\ \varepsilon_{12}(t) \\ \varepsilon_{13}(t) \\ \varepsilon_{23}(t) \end{Bmatrix} = \int_0^t \begin{bmatrix} S_{1111} & S_{1122} & S_{1133} & S_{1112} & S_{1113} & S_{1123} \\ S_{2211} & S_{2222} & S_{2233} & S_{2212} & S_{2213} & S_{2223} \\ S_{3311} & S_{3322} & S_{3333} & S_{3312} & S_{3313} & S_{3323} \\ S_{1211} & S_{1222} & S_{1233} & S_{1212} & S_{1213} & S_{1223} \\ S_{1311} & S_{1322} & S_{1333} & S_{1312} & S_{1313} & S_{1323} \\ S_{2311} & S_{2322} & S_{2333} & S_{2312} & S_{2313} & S_{2323} \end{bmatrix} \begin{Bmatrix} d\sigma_{11}(\tau)/dt \\ d\sigma_{22}(\tau)/dt \\ d\sigma_{33}(\tau)/dt \\ d\sigma_{12}(\tau)/dt \\ d\sigma_{13}(\tau)/dt \\ d\sigma_{23}(\tau)/dt \end{Bmatrix} d\tau \quad i,j,k,l = 1,2,3 \text{ (2-1)}$$

The 6×6 matrix of compliance coefficients is a function of time, i.e., $S_{ijkl} = S_{ijkl}(t)$ at any particular time t, and strains can be related to stresses by equation $\varepsilon_{ij} = S_{ijkl}(t)\sigma_{kl}$. Therefore,

the compliance coefficients and the related engineering constants should be characterized at each individual time step. Different crystal systems can be characterized exclusively by their symmetries. For instance, in highly anisotropic materials, any component of stress can cause strain in all six components and in an isotropic case, the elastic constants are reduced to two constants.

For the inverse analysis, each RUC is exposed to six independent load cases (three axial and three shear loads). Load case 1, 2, and 3 are axial forces in direction 1, 2, and 3, which are associated with σ_{11}, σ_{22}, and σ_{33} respectively. Load case 4, and 5 are 6 are shear loads which are associated with τ_{12}, τ_{13}, and τ_{23} respectively. The six sets of analyses provide six distinct sets of time history stress–strain data for a typical transversely isotropic material and thirty-six sets of data for a heterogeneous material. For every load case, the localized stress and strains can then be volume-averaged over RUC volume for the homogenization characterization procedure at each time step to obtain time-dependent averages:

$$\begin{cases} \sigma_{ij}(t) = \frac{1}{V}\int_v \sigma_{ij}(t)dv \\ \varepsilon_{ij}(t) = \frac{1}{V}\int_v \varepsilon_{ij}(t)dv \end{cases} \tag{2-2}$$

where v is the volume of the RUC. The reason behind these volume averaging is the assumption that the RUC is presenting a point within the continuum domain, and therefore has a homogenized material properties.

2.3.3. Stress Relaxation Loading and Periodic Boundary Conditions

In the current study, the six load cases were in the form of ramped constant strain (displacement) to the unit cell. In order to observe the stress relaxation behavior, the displacement was kept constant throughout the time domain. The periodic boundary conditions require opposite faces of the unit cell undergo identical deformation. Thus, constraint relations

between the nodes on the parallel faces were used to enforce periodicity constraints on the RUC. For detailed implementation of periodicity constraints as well as the rigid body conditions on a RUC one can refer to Garnich and Karami [11] and Naik et al. [12] and Javid et al. [63].

CHAPTER 3. SYNTHESIS AND THERMO-MECHANICAL CHARACTERISATION OF MSSP AND MAESS BASED BIORESINS AND BIOCOMPOSITES

The experimental approach for this study is divided into the following sub-sections: (1): Composite Fabrication; Constituent materials used in this study including E-glass fabric, flax fabric, bio-based resins and VE resin and manufacture of composite are discussed, (2): Effect Of Processing Conditions of Compression Molding in Mechanical Properties; Effects of different parameters in compression molding process on the quality of composite parts, including compression pressure, preheated mold temperature and cure temperature are investigated here, and (3): Characterization and Analysis Techniques; Advanced mechanical and thermo-mechanical testing of the new thermoset resins and the resulting composites are discussed. Also, the relevant stress relaxation test for MSSP bio-based resin reinforced with flax fiber materials is explained here in order to verify numerical methods.

3.1. Composite Fabrication

The following paragraphs describe the bio resins and fiber reinforcements, as well as composite processing used in this study.

3.1.1. Fiber Reinforcement

Two types of fiber reinforcement were used in this study. The unidirectional E-Glass fabric (237 g/m^2, 0.96 wide, 0.2 mm thick) with proprietary silane sizings was supplied by Fiber Glast Development Corp. This fabric had an 80×18 plain weave style, which was developed with 95% of the fibers in the principal direction and only 5% in the off-axis direction. The flax fiber was Biotex Flax 275g/m^2 unidirectional fabric. The unidirectional flax fiber with 1.44 specific gravity was provided by Composites Evolution Ltd., Chesterfield, UK. E-glass and flax fibers were used as-received without any further treatments. Tensile tests were conducted using the

standard method for single fiber for measuring tensile strength (ASTM D 3379-75) with 1.5 mm/min crosshead speed by Dia-Stron on 15 fibers. The tensile strength and modulus of the flax fiber were measured 658.78 ±99.45 MPa and 39.72 ± 5.85 GPa, respectively.

3.1.2. Resin

Two novel plant oil-based resins including, MSSP and MAESS, and vinyl ester resin as a reference were used in this study. MSSP and MAESS were prepared as described in section 2.1.4, and according to the procedure in the literature [1, 22]. ESS has relatively low viscosities at high percent solids (2600 mPa.s) while, the polyol versions of these molecules had a higher viscosity which was attributed to a significantly higher degree of hydrogen bonding in the polyol resins [22]. Table 3-1 shows the properties of MSSP and MAESS.

The isocyanates were obtained from Bayer Material Science based on a modified diphenylmethane diisocyanate (MDI) isocyanates with an NCO content of 31.5% [Baydur PUL 2500]. Polyurethane resin was prepared by mixing bio-based high functional MSSP polyol with isocyanate crosslinker, with NCO:OH ratios of 1.0:1.0, which is the optimum formulation reported by Nelson et al. [22].

Styrene, Luperox P (t-butyl peroxybenzoate) and cobalt naphthenate (6% cobalt content) were purchased from Sigma-Aldrich. Cumyl Peroxide, commercially available as Trigonox 239A, containing 45% cumene hydroperoxide, was generously provided by Akzo Nobel. Styrene was used as the reactive diluent for the curing of MAESS, at 30% of total weight, which is the optimum formulation reported by Yan *et. al.* [1]. The resin was cured using a mixture of Luperox P as a high temperature initiator, trigonox 239A as a room temperature initiator, and cobalt naphthenate (CoNap) as a promoter. The mixing ratio of luperox P, trigonox 239A and CoNap were 2, 3, and 1 wt%, respectively.

The vinyl ester (VE) system Hydropel® R037-YDF-40, provided by AOC resins. The hardener was a 2-butanone peroxide (Luperox® DDM-9) solution, which was obtained from Sigma-Aldrich Co. The mixing ration of VE to hardener is 100 to 1 weight parts.

Table 3-1. Properties of MSSP and MAESS Resins [1, 22].

Resin	Viscosity (Pa.s) [a]	Equivalent weight
MSSP	113.00	300 g / OH eq.
MAESS	95.01	245 g /.epoxy eq
Measured by rheometry at 25 °C, the viscosity was taken at a frequency of 100 Hz.		

3.2. Composite Processing

The composites examined in this study were processed using a compression molding process to achieve a 50% fiber volume fraction. E-glass fibers and flax fibers were dried at 100 °C overnight to prevent void formation during molding. Before running the experiment, resins and hardener were homogenously mixed. A scheme of the composite preparation and a schematic of resin flow in the closed compression molding is shown in Figure 3-1 and Figure 3-2. Resin flowed from center to the corners in the hand lay-up technique, with the middle of each layer of fiber fabric being pre-soaked by matrix and then stack over the other layers of fabric to ensure the resin was uniformly distributed throughout fibers.

Figure 3-1. Scheme of the preparation of composite: (a) Mold prior to resin mixing, (b) Press machine, (c) Flax/MSSP and E-glass/MSSP composites.

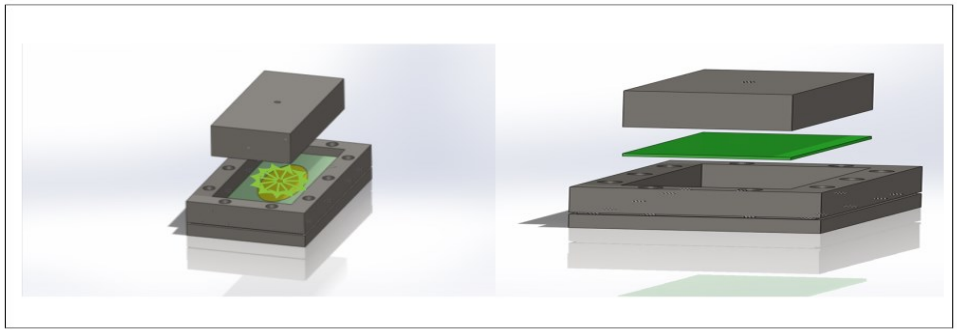

Figure 3-2. Schematic of resin flow during compression molding process.

The fiber reinforced composites used in this study include:

1. MSSP reinforced with E-glass fiber, which is referred to as E-glass/MSSP and the results of mechanical properties will be presented in Chapter 4 and Chapter 6.
2. MAESS reinforced with E-glass fiber, which is referred to as E-glass/MAESS and the results of mechanical properties will be presented in Chapter 5.
3. MSSP reinforced with flax fiber, which is referred to as Flax/MSSP and the results of mechanical properties will be presented in Chapter 6.
4. MAESS reinforced with flax fiber, which is referred to as Flax/MAESS and the results of mechanical properties will be presented in Chapter 6.
5. VE reinforced with E-glass fiber, which is referred to as E-glass/VE and the results of mechanical properties will be presented in Chapter 6.
6. VE reinforced with flax fiber, which is referred to as Flax/VE and the results of mechanical properties will be presented in Chapter 6.

The curing condition for E-glass/MSSP, which will be discussed in Chapter 4 is at 150 °C for the first hour under the pressure of 50 kN. However, the E-glass/MSSP and Flax/MSSP composites which will be discussed in Chapter 6, were cured under the pressure of 100 kN at

room temperature for 12 hours, followed by post-curing at 150 ºC for 1 hour to be comparable with the rest of composites. The E-glass/MAESS and Flax/MAESS, E-glass/VE and Flax/VE composites were cured at room temperature for 12 hours, followed by post-curing at 150 ºC for 1 hour, 175 ºC for one hour, and 200 ºC for 4 hours.

3.3. Effect of Processing Conditions of Compression Molding in Mechanical Properties

The mechanical properties of the composite products depend on different fabrication variables. The mechanical strength of the composites is related to the fiber volume content and fiber alignment. In the present study, the fiber volume fraction of finished parts were either the same or normalized with respect to 50 vol % in order to be compared. In this study, first, the effects of three parameters, including compression pressure, pre-heated mold temperature, and cure temperature, on the composite quality were investigated. In order to correctly estimate the influence of chosen variables on the part quality in this part of study, all specimens are tested with MSSP resin with E-glass and flax fibers. The ultimate strength and modulus measured by tensile testing served as an indicator of the quality of fiber reinforced composites.

The effect and the optimization of process variables on this composite processing approach was determined by employing trial and error analysis in the lab. At room temperature, when the pressure of press was low, 50 vol% of fiber was not achieved, and therefore the desired strength was not achieved. On the other hand, by increasing the pressure, most of the resin flashed out and the fiber volume fraction increased, but the fiber was not soaked enough and the mechanical strength decreased. The optimum pressure in this case was determined as 110 kN. However, when the composite fabrication was conducted at high temperature, the viscosity of resin decreased and therefore, 110 kN was too high for this case. The optimum pressure to achieve desirable properties with 50 vol% of fiber was found to be 50 kN. When the mold was

preheated, after soaking the fibers with resin most of the resin flashed out, therefore room temperature was found to be the optimum temperature for molding (i.e. preheating the mold resulted in high fiber volume fraction, even under the low pressure). Finally, the most important parameter was curing temperature. Two different curing methods were conducted to determine the optimum curing condition. In the first method the composite plate was cured at 150 °C for one hour and then it was held at room temperature for 12 hours. In the second method, the composite plate was cured at room temperature for 12 hours, and then it was post cured at 150 °C for one hour. Curing at room temperature results in higher strength and modulus. As mentioned before, the mechanical properties for both curing methods are reported in this study for composites made from MSSP. The mechanical properties under the first condition is reported in Chapter 4 and the curing condition under the second condition is reported in Chapter 6. However for the composite made from MAESS resin, a curing condition similar to second method was applied (i.e. cured at room temperature for 12 hours to obtain partial curing of the resin, followed by post-curing at 150 ºC for one hour, 175 ºC for one hour, and 200 ºC for 4 hours). The fiber/resin ratio was about 50:50 by volume. Five specimens of each series were prepared. The samples were conditioned at room temperature and tested.

In general, in the compression molding process, the compression pressure and cure temperature have major effects on the quality of the composite product. Experimental results showed that optimum compression pressure, control of resin viscosity by temperature of the mold and curing temperature are significant parameters for improvements in the mechanical properties of the composite. After determining the optimum conditions and predicting the response under these conditions, the composite samples were fabricated with optimum parameter settings.

3.4. Characterization and Analysis Techniques

All mechanical tests were conducted at ambient temperature. Five specimens were tested for each of the mechanical tests and three specimens were tested for thermal analysis.

3.4.1. Thermal Analysis

Completion of the curing reaction was determined by Differential Scanning Calorimeter (DSC). Modulated differential scanning calorimetry (MDSC) Q1000 from TA Instruments is an advanced high performing version of traditional DSC. Besides providing information about the heat flow of DSC, MDSC provides required information about the non-reversing and reversing features of thermal functions. MDSC was used to ensure that the composite samples were fully cured and measured glass transition temperature. In materials such as high crystalline thermoplastics in which the reduction of amorphous content occurs, variation of properties upon glass transition will usually decrease [78]. The smaller signal changes decrease the sensitivity of the DSC technique to the glass transition, though MDSC technique has value in measuring the T_g by separating non-reversing transitions such as volume relaxation and curing from the glass transition which is impossible by traditional DSC. To simulate curing reaction. aluminum pans containing 10-15 mg of samples were heated from 0 °C up to 250 °C at a ramping rate of 3 °C/min using an amplitude of modulation of ± 0.3 °C and a period of 40 s under nitrogen flow of 50 ml/mins The enthalpy of reaction (ΔH_{rxn}) was determined by analyzing an uncured sample (t = 0). Samples cured at 150 °C for different time periods of 15 min and 60 min were also analyzed to determine the residual enthalpy of reaction (ΔH_{res}).

Dynamic mechanical analysis (DMA) was conducted using a Q800 TA Instrument Dynamic Mechanical Analyzer in dual cantilever mode and three point bending mode to measure glass transition temperature and HDT, respectively. Glass transition temperature and Heat

Distortion Temperature (HDT) or softening temperature of the composite were measured by running the DMA according to ASTM D7028 and ASTM D648, respectively. To measure glass transition temperature dual cantilever fixture was used with a fixed frequency of 1 Hz with a strain rate of 0.01% and a heating rate of 5 °C/min from 30 to 180 °C. The sample dimensions used were 60 mm × 12.5 mm × 3 mm. Heat Distortion Temperature usually denotes the highest temperature to which a polymer may be used as a rigid material in application and the material is able to support load for some considerable period of time. To measure HDT a three-point bending fixture was used in DMA samples were heated from 25 °C to 300 °C at the rate of 3 °C/min at which a material deflects by 0.25mm under the application of a load (1.82 MPa).

3.4.2. Mechanical Testing

Physical properties of the composites were measured according to ASTM D2734. Density of composite plates was calculated by a Mettler Toledo 33360 density determination kit at room temperature. Weight fraction of fiber in the E-glass reinforced composite plates, (W_f), was measured by resin burn-off method (ASTM D2584). The composite samples were burnt in a furnace at 600 °C until only fibers remained. Void contents in the composite were measured according to ASTM D2734. Voids are formed by carbon dioxide, which is a by-product of the isocyanate reaction with air moisture [21].

Tensile, flexural, and interlaminar shear strength were determined using Instron 5567 machine test. The tensile strength and modulus were evaluated in accordance with ASTM D3039. Three-point bending test was used to determine flexural strength and modulus according ASTM D790. Interfacial properties of the composites were also measured using a three-point bending method according to ASTM D2344. Izod impact strength of notched and un-notched specimens were evaluated using Tinius Olsen impact testing instrument in accordance with

ASTM D256. Impact strength is calculated by dividing absorbed energy by the specimen (J) during impact by the notched area.

Nanoindentation test were carried out using T1900 TriboIndenter instrument manufactured by Hysitron Inc equipped with a Berkovich pyramidal tip to characterize the interphase region of the composite. Elastic modulus and hardness were measured from load-displacement data. To perform tests, the 50 nm depth was picked to allow accurate measurements with the most localized indent. Also, it prevents interference of indents. On the other hand, having a smaller size indent allows to have more measurements over interfacial region. Fracture surfaces of flexural specimens were examined using JEOL JSM-6490LV scanning electron microscope (SEM). To prevent the samples from becoming electrically charged, samples were prepared through a coating of gold-palladium (Model SCD030, Balzers, Liechtenstein).

3.4.3. Stress Relaxation Test

Goal of stress relaxation test is to characterize time-dependent behavior of the MSSP resin and flax fiber under tensile force. Crosshead speed had a sharp ramp in order to avoid a primary fluctuation in results before they become stable. Once the desired strain was reached, strain was held constant, and the decay in stress was recorded as a function of time for a specific time span until the material was fully relaxed. Prony series is one of the appropriate models used to model the viscoelastic behaviors of materials in stress relaxation tests. For the linear viscoelastic material, the time-dependent shear modulus, i.e. G(t) is expressed by the following Prony series as:

$$G(t) = G_0 \left(1 - \sum_{i=1}^{n} g_i \left(1 - e^{\frac{-t}{\tau_i}}\right)\right) \quad (3\text{-}1)$$

where G_0 is instantaneous shear modulus and g_i, and τ_i are material-dependent coefficients. Stress relaxation behavior of polyurethane matrix was measured using standard method for measuring tensile strength (ASTM D 3039) with 2 mm/min crosshead speed until the strain reached 1%. The mechanical properties of flax fiber strongly depends on the on cross section area measurement accuracy. Using approximate value in cross sectional area calculation can significantly underestimate the value of tensile and stress relaxation. Therefore, in order to have accurate results for stress relaxation values, an accurate cross section area measurement is required. To fulfill this aim, Dia-Stron miniature tensile tester (Ltd. Andover, UK) was used at room temperature. One key to Dia-Stron's accuracy is a laser scanner right into the analyzer package and a sample rotation feature which facilitates measurement of the elliptical fiber cross section all along fiber length. Stress relaxation tests were performed on 25 single fibers using Dia-stron with 0.4 mm/sec crosshead speed until the strain reached 1 %. The load was applied under computer control and, for each single fiber, the load against extension was recorded. Using measured fiber diameters and a fixed gauge length of 4 mm; this data was converted to stress against strain.

3.4.4. Experimental and Analytical Approach

To verify the analytical expression as well as the finite element analysis, the experimental test of the stress relaxation under 0.2 % deformation in fiber direction was performed on five samples. Instron Universal Testing machine was employed to measure stress relaxation in uniaxial tension at 25 ºC. Test specimens were pulled to the strain level of 0.2% using crosshead speed of 5 mm/min according to ASTM D2991. Stress relaxation tests are becoming more important when viscoelastic materials such as resins or natural fibers are incorporated in composites. Goal of these tests are to characterize nonlinear and time-dependent behavior of

resin, flax and glass fiber reinforced polyurethane composites under tensile force. Relaxation test is, in simple words, analysis of the material properties when a constant strain is applied. It will lead to a stress decrease over time. Instron Universal Testing machine was employed to measure stress relaxation in uniaxial tension at 25 ºC. Specimens with dimensions 150 mm×15mm×3mm (l, w, t) were used. Test specimens were pulled to the strain level of 0.4% using crosshead speed of 5 mm/min according to ASTM D2991. Crosshead speed had a sharp ramp in order to avoid a primary fluctuation in results before they become stable. Once the desired strain was reached, strain was held constant, and the decay in stress was recorded as a function of time for a time span. The stress decay was calculated as σ_t/σ_0, where σ_0 is initial stress at zero time (t=0) and σ_t is stress at subsequent times. Also, stress value was converted to corresponding modulus E(t) by dividing stress σ_t by corresponding strain (ε_0). Stress decay was recorded right after predetermined strain.

CHAPTER 4. UTILIZATION OF METHOXYLATED SUCROSE SOYATE POLYOLS AS A NOVEL BIO-BASED RESIN IN COMPOSITE APPLICATION

A novel bio-based high-functionality polyol, Methoxylated Sucrose Soyate Polyol (MSSP), was used as matrix in a composite to investigate mechanical and thermo-mechanical properties of MSSP-based PU resin reinforced with unidirectional E-glass fiber (50% fiber volume fraction). Mechanical properties of the new MSSP-based PU thermoset and the resulting composite were assessed by tensile, flexural, interlaminar shear strength (ILSS), nano-indentation, and impact strength testing. Scanning Electron Microscopy (SEM) of fractured surfaces of flexural specimens were examined to investigate the fiber-matrix interface behavior. Finally, to highlight the performance of bio-based PU resin in composites, the results of E-glass/MSSP-based PU composite were compared with previous studies of similar bio-based and petroleum-based composites.

4.1. Curing Analysis of Neat Resin

In order to determine the completion of the curing reaction before conducting any tests, degree of cure is determined by DSC. Bio resin MSSP has been cured at 150 °C for two different periods of time of 15 and 60 min. Figure 4-1 shows non-isothermal DSC scans of cured and uncured samples with ramping at the rate of 10 °C/min. Total heat of reaction determined by calculating the integrated area of the exothermic peak in the curve of uncured MSSP resin in Figure 4-1 and is found to be 130 J/g. The glass transition temperature (T_g) are noted by the sudden decrease in the heat flow of cured sample at around 100 °C as was shown in dashed line in Figure 4-1. The hump observed in dashed line between temperatures of 160 °C and 240 °C is due to residual heat of reaction (ΔH_{res}). This heat is found by calculating the area of small bump in the curve. Residual heat of reaction for MSSP PU samples are not substantial after sample

cured at 150 °C for 60 min. This result indicates that the polyurethane resin is fully cured or its conversion is high. Table 4-1 reports heat of reaction and degree of cure for MSSP resin samples.

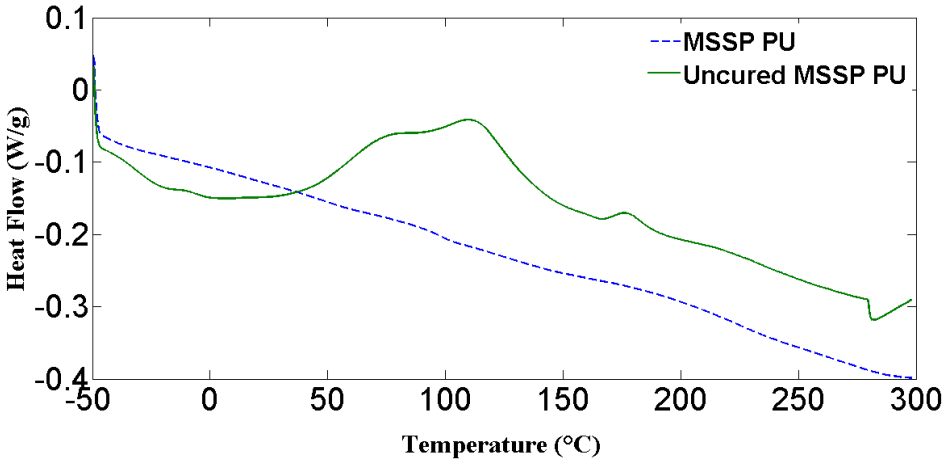

Figure 4-1. DSC curves for uncured MSSP PU and MSSP PU cured at 150 °C (t=0 and t=60 min).

Table 4-1. Heat of Reaction and Degree of Cure for MSSP Resin.

Sample	ΔH (J/g)	Degree of Cure (%)
Uncured MSSP (t = 0)	130.0	0.0
Cured MSSP (t = 15 min)	10.50	91.89
Cured MSSP (t = 60 min)	3.58	97.23

4.2. Physical Properties

Density of composite plates was calculated by a Mettler Toledo 33360 density determination kit at room temperature. Weight fraction of fiber in the E-glass reinforced composite plates,(W_f), was measured by resin burn-off method [D2584]. The composite samples were burnt in a furnace at 600 °C until only fibers remained. The physical properties of the composite plates are reported in Table 4-2. Void contents in the composite were measured according to ASTM D2734. Voids are formed by carbon dioxide, which is a by-product of the isocyanate reaction with air moisture [41].

Table 4-2. Physical Properties of E-glass Reinforced Composites.

Composite	Density (g/cm^3)	Fiber Volume Fraction (%)	Fiber Weight Fraction (%)	Void content (%)
E-glass/MSSP	1.74	50	73.62	0.7

4.3. Tensile and Flexural Test

Tensile and flexural strength and modulus were measured for MSSP based neat resin and E-glass fiber reinforced MSSP-based composite plates. The results of these tests are shown in Table 4-3. Measured mechanical properties of neat resin and E-glass/MSSP are compared in Figure 4-2. As expected E-glass/MSSP tensile and flexural strength and moduli show substantial increase compared to neat resin. Compared to neat resin 893% and 1240% higher tensile strength and flexural strength was measured respectively. In existing studies [79-82], E-glass reinforced composites using bio-based and petroleum based polyurethane matrices have been characterized by means of tensile and flexural tests. All of these composites have the same fiber type in a unidirectional orientation. The fiber volume fraction were either the same or normalized with respect to 50 vol % in order to be compared. Composite samples using MSSP as matrix have comparable properties with E-glass/ petrochemical-based PU of mentioned studies. E-glass/MSSP shows superior tensile and flexural strength and modulus compared to E-glass bio-based composites. On average mentioned properties were measured 80% or higher than existing studies [79-81] . Compared to [82] 130% and 110% greater flexural strength and modulus was measured respectively and 40% and 73% higher tensile strength and modulus respectively. Higher mechanical properties of E-glass/MSSP in this study are attributed to high functionality and rigid compact chemical structure of MSSP oligomers in polyol resin.

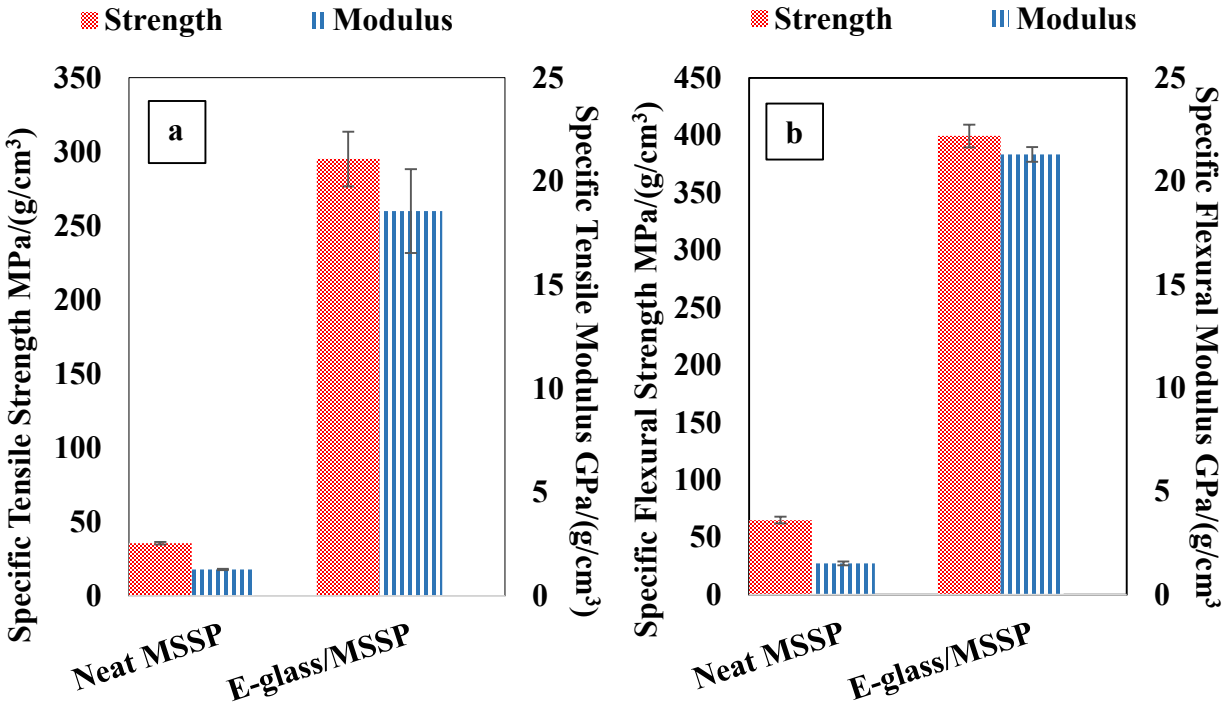

Figure 4-2. Specific tensile strength and modulus (a), specific flexural strength and modulus (b) of MSSP and 50 vol. % E-glass/MSSP composites.

4.4. Interfacial Properties

As adhesion between fiber and matrix plays a key role in transferring the stress from the matrix to the reinforcement, better interlaminar shear properties will enhance the overall performance of the composite [3, 83]. Results of short beam shear test of E-glass/MSSP composites are presented in Table 4-3. Observing SEM images taken from fracture surface of flexural samples shown in Figure 4-4. There are fractions of matrix sticking to the broken fibers, confirming strong adhesion between fiber and matrix. Existing studies [41, 82] have characterized interlaminar shear strength of E-glass fiber bonding with bio-based and petroleum based PU resin. Comparing results presented in Table 4-3 with those presented in [41], 48% and 54% higher values of ILSS have been reached using MSSP compared to bio-based and

petroleum based PU, respectively. Compared to results of [82], E-glass/MSSP showed 100% better results of ILSS.

4.5. Fiber-Matrix Interaction

Mechanical properties of composites are strongly affected by distribution of fibers in the matrix, adhesion between fiber and matrix and wetting fibers by matrix [81]. SEM images were taken from cross section and fracture surface of the composite samples in order to investigate mentioned factors. Figure 4-3 shows images of E-glass/MSSP composites cross section. As seen, E-glass fibers have been well distributed throughout the cross section area. Well dispersion of fibers into matrix will result in enhancement of mechanical properties such as modulus and strength. SEM images of fractured surface are shown in Figure 4-4. There are several fiber bundles which have been pulled out together from the other half of the sample but there are fractions of resin stuck on the surface of fibers. This can be result of good wetting of the fiber as well as better adhesion between the fiber and the matrix.

E-glass fiber may also participate in the curing process by physical and or chemical interaction of the E-glass fiber surface with the resin due to presence of commercial sizings on the surface of E-glass fibers. The likelihood of physical and or chemical interaction of the E-glass fiber surface with the resin, along with high functionality of hydroxyl groups of MSSP based PU, leads to a good wetting of fibers and strong adhesion between fibers and matrix. This will result in a high ILSS of current composite compared to existing studies [84]. Therefore higher ILSS of current composite compared to existing studies comes from better wetting of fibers and stronger adhesion between fibers and matrix.

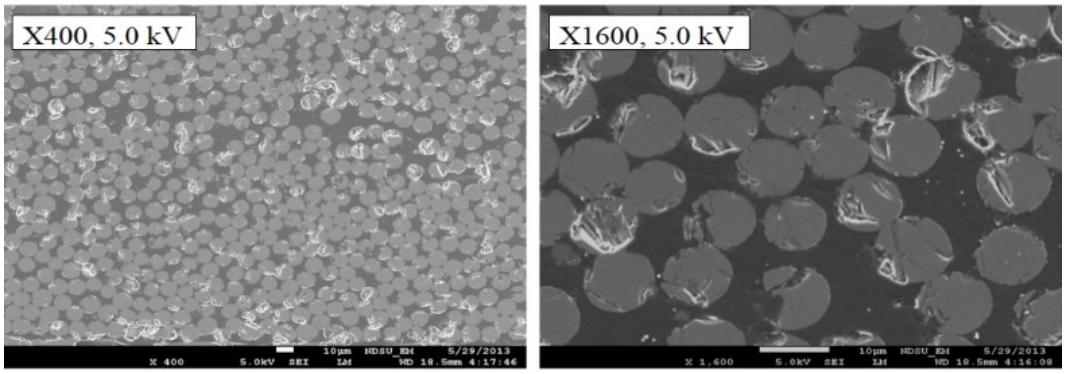

Figure 4-3. Cross section of E-glass/MSSP composite.

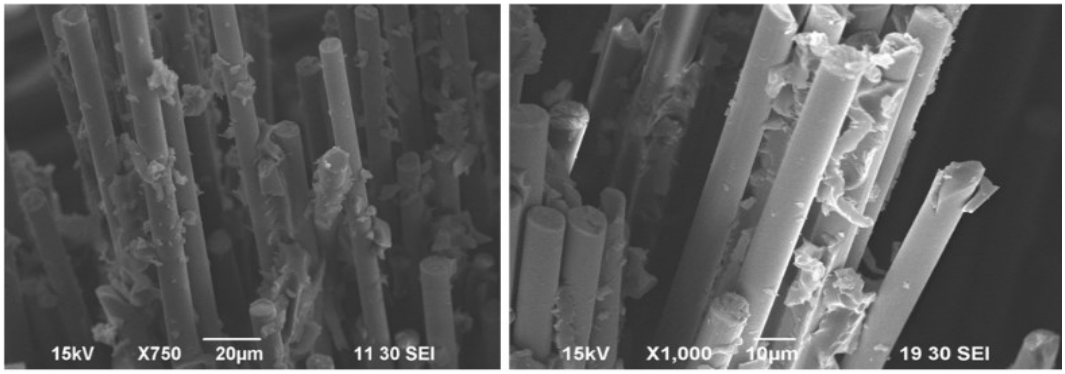

Figure 4-4. Fracture surface of E-glass/MSSP sample.

4.6. Izod Impact Test

Table 4-3 presents the Izod impact strength (absorbed energy/cross-sectional area) results of the biobased composites. The original notched Izod impact strength of 13.55 kJ/m^2 of MSSP increased to 240.54 kJ/m^2 when E-glass fibers are inserted as reinforcement. Increased impact strength during the Izod impact test may be explained by considering the crack propagation. During impact cracks initiate and propagate freely in the neat resin, but in composites crack initiates and then peeling along the fibers leads to fiber breakage or fiber pull out. All will increase absorbed energy during impact [81]. Dwan'isa *et al.* [81] found a linear relation between increase wt% of E-glass fibers as reinforcement and increase of impact strength of E-

glass/soy-based PU. Comparing impact strength of E-glass/soy-based with 70 wt% extrapolated results) of Dwan'isa *et al.* [81], 230% higher impact strength is observed.

It is expected that increase in flexural and tensile modulus results in decrease of impact properties [85]. But as seen, current E-glass/MSSP has superior flexural and tensile modulus as well as greater impact properties compared to existing E-glass/MSSP composites. Higher cross linking density of the cured resin along with higher concentration of chain dangling in the molecular structure have improved modulus as well as impact properties of current E-glass/MSSP composite [86]. Also, as mentioned most of the impact energy is dissipated by debonding, fiber and/or matrix fracture, and fiber pullout, therefore the impact response of the fiber composites is vastly affected by the interfacial bond strength and the matrix and fiber properties [5]. As discussed earlier, current E-glass/MSSP has exhibited greater interfacial bonding compared to other bi-based composites. This is also another reason for greater impact properties of the composite.

Table 4-3. Mechanical Properties of Neat PU and 50 Vol. % E-glass/MSSP Composites.

Sample	Tensile Properties[a]		Flexural Properties[a]		ILSS[a]	Impact Strength[a]	
	Strength (MPa)	Modulus (GPa)	Strength (MPa)	Modulus (GPa)	(MPa)	Unnotched (kJ/m^2)	Notched (kJ/m^2)
Neat PU	39.19 (0.90)	1.41 (0.01)	71.58 (3.28)	1.67 (0.11)	---	21.33 (0.03)	13.55 (2.21)
E-Glass/MSSP	525.31 (32.81)	33.05 (3.59)	710.98 (17.44)	37.92 (0.63)	40.64 (2.14)	270.19 (32.31)	257.01 (16.79)

[a] Values in parentheses are standard deviations

4.7. Nanoindentation Test

In this study, a Berkovich indenter produces a line of nano indents of 50 nm deep along a random path starting from the matrix and ending on the fiber. The SEM photographs of

indentation made on polished cross section of specimen are shown in Figure 4-5. The interphase zone between matrix and fiber is shown by 2-3 indents in the graph of Figure 4-5 which is equivalent of 1 to 1.5 μm. The initial gradient of the unloading curve is used to calculate the stiffness of the sample at that point. The thickness and stiffness of interphase are the main focus of this test, as they are influential factors affecting mechanical performance of the composite. Table 4-4 shows measured hardness, H, and reduced elastic modulus, E_r based on nanoindentation test. The thickness of interphase has also significant impact on mechanical properties especially on interlaminar shear strength and un-notched impact toughness. Previous studies [87, 88] have shown that softness of interphase will reduce the shear stress concentration and thus improving the adhesion between fiber and matrix. In another study Kim *et al.* [89] showed that the thickness of interphase significant affects the fracture behavior and mechanical performance of the composite under interlaminar shear loading. Comparing the results presented in Table 4-4 it is observed that the average thickness of interphase region and hardness of current composite is almost higher or in the range of existing studies [90]. Presence of chain dangling in the molecular structure of MSSP has resulted in softer and relatively thicker interphase.

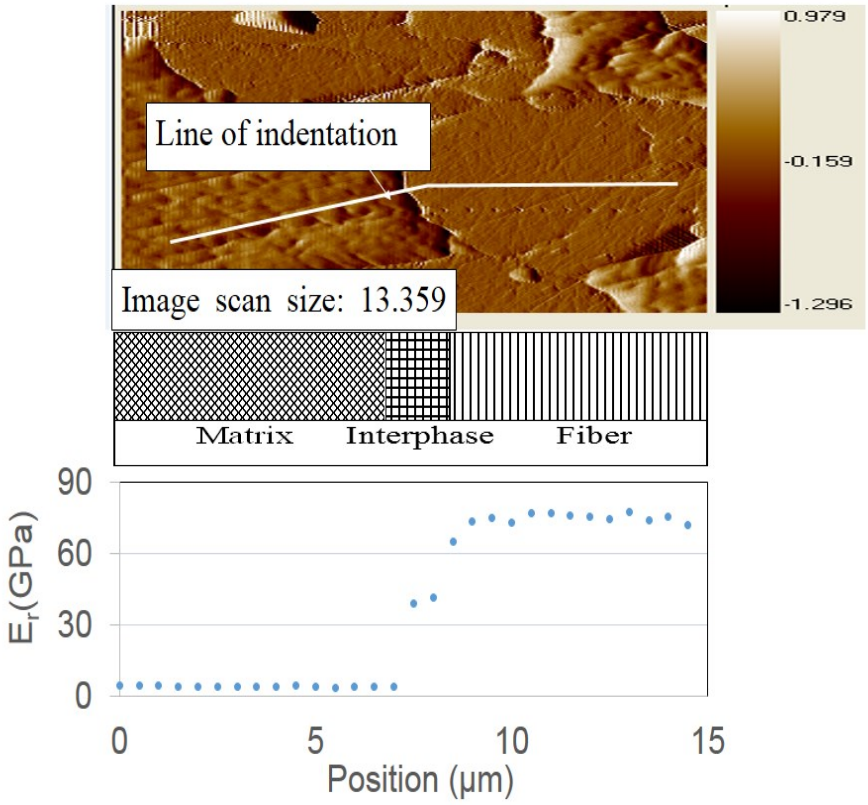

Figure 4-5. Measured reduced modulus (E_r) of E-glass fiber reinforced MSSP.

Table 4-4. Hardness and Reduced Modulus, E_r, For E-glass/MSSP Measured by Nanoindentation.

		Hardness (GPa)	E_r (GPa)
E-glass/MSSP	Matrix	0.23 (0.01)	4.51 (0.22)
	Interphase	3.61 (0.32)	48.64 (4.37)
	Fiber	6.25 (0.28)	74.45 (4.47)

[a] Values in parentheses are standard deviations

4.8. Thermo-mechanical Properties

Glass transition temperature (T_g) can be measured by monitoring the response of either storage modulus (E'), loss modulus (E''), or loss tangent (tan δ) as a function of temperature [91, 92]. Tan δ is the ratio of the loss modulus to the storage modulus E''/E', which combines the viscous and elastic components into a single term. T_g can either be defined as the inflexion point

at which a significant drop of the storage modulus occurs (onset point) or the temperature where the maximum tan δ and loss modulus are observed [91]. In general, glass transition temperature measurement based on onset (onset of storage modulus reduction) is very sensitive to the point where tangent lines are selected to be drawn. Based on the position of the points, it can vary few degrees. Because of mentioned reason, tan δ method was applied to measure T_g of MSSP and its subsequent composite. Log storage modulus, E', and tan δ of the neat MSSP and composite were recorded over shown temperature range at the heating rate of 3 °C/min in Figure 4-6a and Figure 4-6b. The storage modulus was recorded in order to observe resin and composite thermal behavior over the temperature range.

As seen in Figure 4-6a, at up to 100 °C neat resin and E-glass/MSSP composite behaved the same. This is due to the fact that at low temperatures fibers do not have much contribution to imparting stiffness of the material. At higher temperatures any water molecules adhering on to the fibers evaporates and as result fibers will be stiffer. This ultimately contributes to improved modulus of the composite at high temperatures. Presence of a region where changes of storage modulus vs. temperature is less noticeable which indicates that a stable cross-linked network exists. On the other hand, higher modulus of composite can be attributed to the mechanical restraint introduced by fibers, which reduces the mobility and deformability of the matrix. A strong interaction between fiber and matrix will restrict the mobility of the polymer chains in the interface region. Other authors have also reported similar observations [93]. Over the studied temperature range, E' is remarkably increased in the composite. This substantial increase in E' in composite is attributed to fiber insertion and increase of the overall material stiffness. Comparison between E' values measured at 40 °C reveals significant improvement compared to neat resin. E' was measured 20 GPa for E-glass reinforced with MSSP based polyurethane, while

this value is only 2 GPa for neat resin. Stiffness at high temperatures is determined by the amorphous regions, which are soft above the relaxation transition.

Variations of tan δ of the resin and the subsequent E-glass reinforced composite as a function of temperature is shown in Figure 4-6b. Tan δ value is higher for the neat resin compared to E-glass/MSSP composite. Based on Dwan'isa *et al.* [94] this is due to higher net volume of resin and also less mobility of chains in the composite. The glass transition temperature is determined by the peak of the tan δ curves. The measured values are presented in Table 4-5. Observation of one peak for both neat resin and E-glass reinforced campsite is the indication of one T_g and in other words single phase system. Upon fiber insertion no significant change in T_g was observed. As mentioned before, E-glass fiber may also participate in the curing process by physical and or chemical interaction of the E-glass fiber surface with the resin, which in turn decreases chain mobility and therefore it will increase Tg of the composite. On the other hand, possible dangling chains in chemical structure of resin might decrease the interphase modulus and in turn reduce the glass transition temperature. These two phenomenon have resulted in only slight increase of T_g. Shape of tan δ curve is slightly broader for composite, which is due more heterogeneity of the materials compared to neat resin. Compared to existing studies [94, 95] higher values of T_g was measured both for neat resin as well as ensuing composite. This is attributed to great structural rigidity and high functionality of the sucrose molecule which is the core of sucrose soyate.

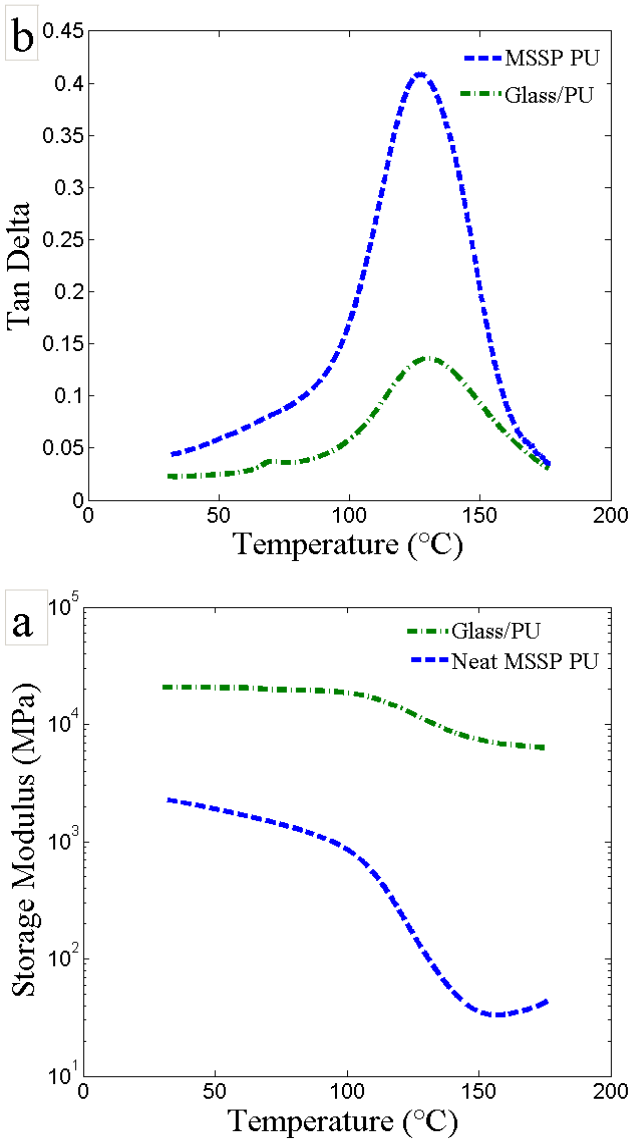

Figure 4-6. Storage modulus (E') (a) and glass transition temperature (T_g) (b) of MSSP neat polyurethane and E-glass reinforced polyurethane composite.

The HDT or softening point of polymer-based materials is another thermal properties for designing industrial products. Table 4-5 shows HDT for neat PU, and E-glass/MSSP composite. It should be mentioned that a significant increase in the HDT by inserting fibers is due to high modulus of E-glass fibers as well as the high interfacial adhesion and crystallinity of the MSSP. Even resin alone has relatively high softening temperature. The HDT value of MSSP is 57 ºC.

Table 4-5. Thermal Properties for Neat PU and 50 Vol. % E-glass/MSSP Composite.

Sample	T_g °C (tan δ)	HDT (ºC)
Neat PU	128.09 (2.85)	57 (2.4)
E-glass/ MSSP	132.22 (1.91)	302.35 (5.9)

[a] Values in parentheses are standard deviations

In conclusion, the objective number 2 of this dissertation was met as observing the improved mechanical properties of E-glass reinforced MSSP composites. For tensile strength and modulus up to 40% and 75% improvements and for flexural strength and modulus 130% and 110% improvements were observed, compared to existing studies. Also, the results of SEM images of failed samples revealed better wetting of fibers by matrix, stronger adhesion between fiber and matrix and greater interfacial bonding compared to other bio-based composites. This resin is a great alternative to current bio-based and petroleum-based resins. Superior mechanical properties along with better thermal properties make this novel resin suitable for variety of applications both in low and high temperatures.

CHAPTER 5. MECHANICAL AND THERMAL PROPERTIES OF GLASS REINFORCED METHACRYLATED EPOXIDIZED SUCROSE SOYATE (MAESS) COMPOSITE

A novel high-functional bio-based resin from methacrylated epoxidized sucrose soyate (MAESS) were used as a matrix, and E-glass fibers were used as reinforcements. The prepared bio-based composites were characterized by tensile, flexural, and impact strength testing. Scanning electron microscopy and interlaminar shear strength (ILSS) were examined to study the fiber‑matrix interface behavior. To highlight the performance of bio-based MAESS resin in composites, the results of E-glass/MAESS composite were compared against E-glass/VE as a control.

5.1. Curing Analysis of E-Glass/MAESS Composite

Figure 5-1 shows an MDSC scan for (a) the E-glass/VE and (b) E-glass/MAESS composites. Samples were machined from different parts of a cured composite panel. The T_g was determined from the reverse heat flow runs (green lines). The total heat flow from conventional DSC method (blue line) does not show any inflection points to indicate glass transition temperature (T_g) of composite samples. As mentioned earlier, in MDSC method, the signal of the heat flow is converted into a reversing and a non-reversing signal through Fourier transformation deconvolution. Briefly, the reversing signals are those which are heat capacity events such as the glass transition and melting. The non-reversing components of heat flow signals refer to kinetic reactions such as decomposition, crystal reorganization and perfection, and cure [96]. As indicated at Figure 5-1, the non-reversing curves (red line) do not show any endothermic peak which indicate the VE and MAESS resins are fully cured or its conversion is high. On the other hand, the reversing curve (green line) shows heat capacity events such as the glass transition

temperature (T_g) sensitive to heating rate the resulting T_g, is distinguishable at reversing curve which is sensitive to heating rate. The glass transition temperature (T_g) are noted by the sudden decrease in the heat flow of cured samples at around 109 °C and 126 °C in MAESS/E-glass and E-glass/VE composites respectively as was shown in reversing curve (green line) in Figure 5-1.

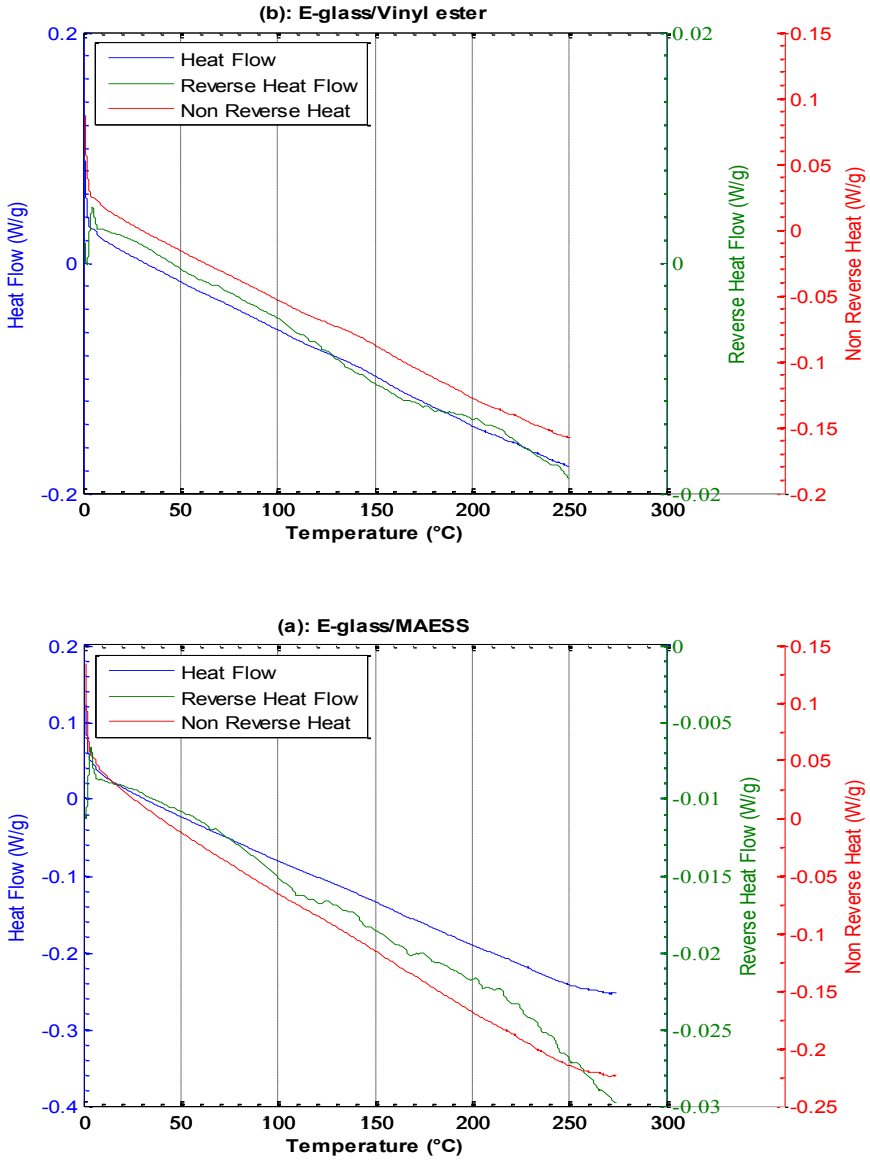

Figure 5-1. MDSC scans of (a) cured E-glass/MAESS and (b) cured E-glass/VE composites.

5.2. Tensile and Flexural Test

The physical properties of the composite plates are reported in Table 5-1. Tensile and flexural strength and modulus of MAESS based neat resin and E-glass fiber reinforced MAESS and VE composite plates were measured and the results are shown in Table 5-2. As seen, E-glass/MAESS tensile and flexural strength and moduli have significant higher values compared to neat resin. Measured mechanical properties of E-glass/VE and E-glass/MAESS are compared in Figure 5-2. Composite samples using MAESS thermoset as matrix have comparable properties with corresponding E-glass/VE composites. E-glass/MAESS showed only comparable tensile strength and only 10% decrease in tensile modulus, when the results were compared with E-glass/VE. The comparison results between E-glass/MAESS and E-glass/VE reveals that when E-glass/MAESS is under tensile deformation, they showed a comparable modulus and strength, since the E-glass fiber are able to support the majority of the load, while, when they are under the flexural deformation which has both tensile and compression deformation, the polymer support the majority of the load. Therefore, this decrease in flexural modulus can be attributed to the lower compression modulus of MAESS resin than VE. In existing studies [10, 25, 43] fiberglass reinforced composites using bio-based and petroleum based VE matrices have been characterized by means of tensile and flexural tests. E-glass/MAESS shows superior tensile and flexural strength and modulus compared to E-glass/epoxy or VE bio-based composites. On average mentioned properties were measured 20% or higher than existing studies [25, 43] . Compared to [25], 20% and 95% greater flexural strength and modulus was measured respectively and 115% and 270% higher tensile strength and modulus respectively. Higher mechanical properties of E-glass/MAESS in this study are attributed to high functionality and rigid compact chemical structure of the oligomers in MAESS thermoset resin.

Table 5-1. Physical Properties of E-Glass Reinforced Composites.

Composite	Density (g/cm^3)	Fiber Volume Fraction (%)	Fiber Weight Fraction (%)	Void content (%)
E-glass/VE	1.74	50	71.72	4.11
E-glass/MAESS	1.76	50	71.10	2.69

5.3. Interfacial Properties

As adhesion between fiber and matrix plays a key role in transferring the stress from the matrix to the reinforcement, better interlaminar shear properties will enhance the overall performance of the composite [3, 83]. Results of short beam shear test of E-glass/MAESS and E-glass/VE composites are presented in Figure 5-2 and Table 5-2. Existing studies [97] have characterized interlaminar shear strength of E-glass/VE/ fiber after coating the fibers with carbon nano-tube to improve ILSS. Comparing results presented in Table 5-2 with those presented in [97], comparable values of ILSS have been reached using MAESS before any treatments on fiber. Furthermore, SEM images were taken from fracture surface of the composite samples in order to investigate the adhesion between fiber and matrix.

SEM images of fractured surface for E-glass/VE and E-glass/MAESS are compared in Figure 5-3. As seen, there are several fiber bundles which have been pulled out together from the other half of the sample at both E-glass/VE and E-glass/MAESS composites. Observing SEM images taken from fracture surface of E-glass/MAESS composites shown in Figure 5-3a, there are remnants of matrix sticking to the surface of fibers, which also confirms strong adhesion between fiber and matrix in bio-based composite. This can be result of good wetting of the fiber as well as better adhesion between the fiber and the matrix in E-glass/MAESS composites. As mentioned before, likelihood of hydrogen bonds formation in the interphase region of fiber is high in E-glass/MAESS composites [84], due to high functionality of hydroxyl groups of MAESS thermoset resin. Therefore higher ILSS of E-glass/MAESS composite compared to E-

glass/VE and also existing studies comes from better wetting of fibers and stronger adhesion between E-glass fibers and MAESS thermoset resin.

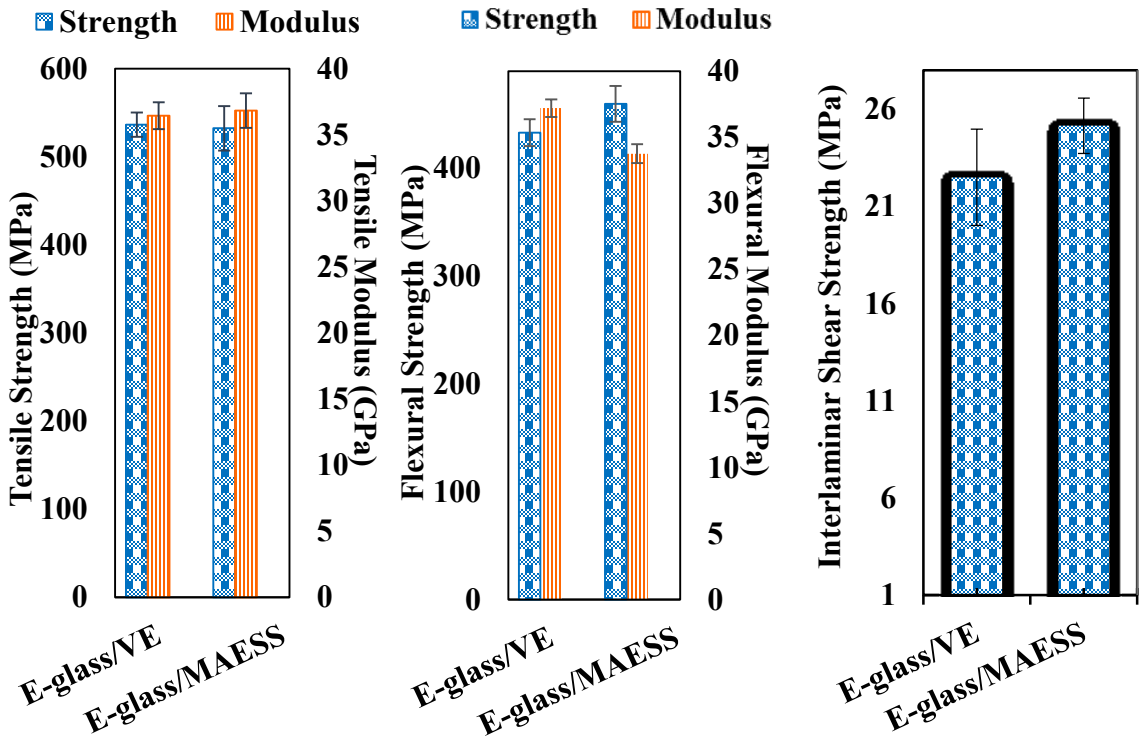

Figure 5-2. Tensile strength and modulus, Flexural strength and modulus, interlaminar shear strength of 50 vol. % E-glass/MAESS and E-glass/VE composites.

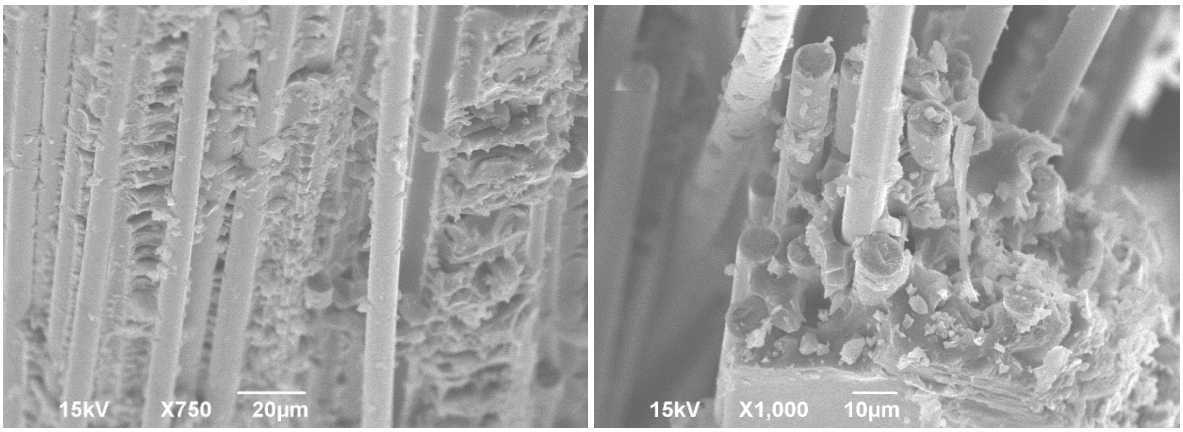

(a)

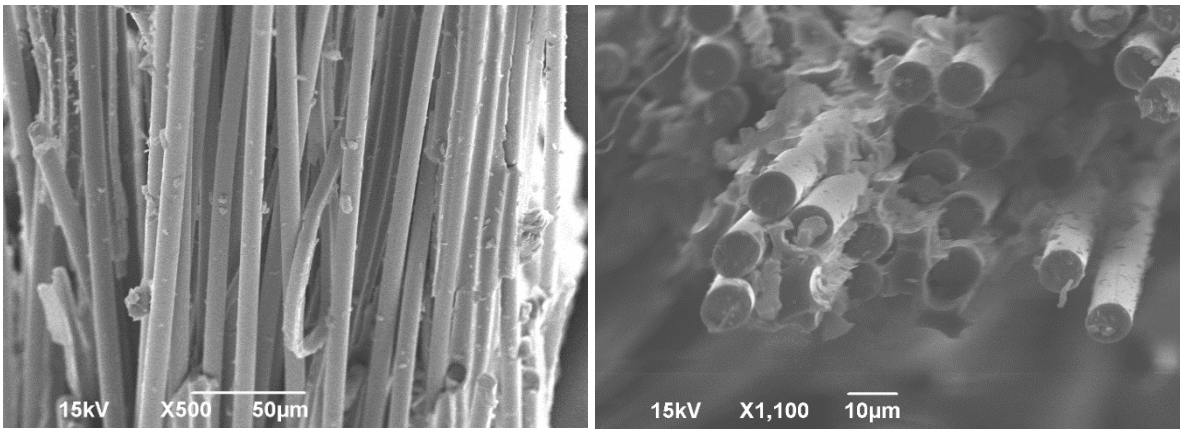

(b)

Figure 5-3. SEM photograph of (a): E-glass/MAESS and (b): E-glass/VE.

5.4. Izod Impact Test

The Izod impact tests show a high impact strength for the E-glass/MAESS composite, and lower impact resistance for the E-glass/VE composites, as reported in Table 5-2. The notched Izod impact strength of MAESS thermoset resin increased from 14.54 kJ/m^2 to 236.84 kJ/m^2 when E-glass fibers are inserted as reinforcement. In composites crack initiates and then peeling along the fibers leads to fiber breakage or fiber pull out depending on the adhesion between fiber and matrix, but in resin cracks initiate and propagate freely in the neat resin. Comparing impact strength of E-glass/MAESS with E-glass/VE composite 25% higher impact

strength is observed in bio-based composite. The impact strength of notched specimen was found to be higher for MAESS based composite samples in comparison with that of VE based composite samples. It is expected that replacing petroleum based VE resin with MAESS results in increase of impact properties [85]. This increase is due to the long aliphatic chains originally from the soybean oil, which contributes to the toughness of the composite. Similar trend was observed for other similar resin system also [98]. Higher cross linking density of the cured bio-based resin along with higher concentration of chain dangling in the molecular structure have improved modulus as well as impact properties of current E-glass/MAESS composite [86]. Also, as mentioned most of the impact energy is dissipated by debonding, fiber and/or matrix fracture, and fiber pullout, therefore the impact response of the fiber composites is vastly affected by the interfacial bond strength and the matrix and fiber properties [5]. As discussed earlier, current E-glass/MAESS has exhibited greater interfacial bonding compared to E-glass/VE composites. This is also another reason for greater impact properties of the bio-based composite.

Table 5-2. Mechanical Properties of Neat MAESS, 50 vol. % E-glass/MAESS/, and 50 vol. % E-glass/VE Composites.

Sample	Tensile Properties [a]		Flexural Properties [a]		ILSS [a]	Impact Strength[a]
	Strength (MPa)	Modulus (GPa)	Strength (MPa)	Modulus (GPa)	(MPa)	Notched (kJ/m^2)
Neat MAESS	32.01 (0.10)	1.45 (0.02)	55.96 (3.47)	1.50 (0.14)	--	14.54 (1.82)
E-glass/VE	536.07 (13.86)	36.40 (1.02)	432.68 (12.38)	37.18 (0.66)	22.47 (2.47)	191.04 (18.14)
E-glass/MAESS	531.81 (25.10)	36.79 (2.31)	459.25 (4.76)	33.73 (1.68)	25.12 (0.96)	236.84 (7.95)

[a] Values in parentheses are standard deviations

5.5. Thermal Properties

Log storage modulus, E', and tan δ of the composites were recorded over shown temperature range at the heating rate of 3 °C/min in Figure 5-4. As seen in Figure 5-4a, at up to 78 °C E-glass/MAESS and E-glass/VE composite behaved the same. Broader transition from the glassy to the rubbery region for the E-glass/MAESS composite is characteristic for a wider distribution of crosslinking density and lower homogeneity of these networks [99]. However, at higher temperature, MAESS composites show higher storage modulus, which might attributed to reinforcing action due to improvement of wetting or surface energy that occurs at the interface region between E-glass fiber and MAESS resin. This ultimately contributes to improved modulus of the composite at high temperatures.

Variations of tan δ of the resin and the subsequent composite as a function of temperature is shown in Figure 5-4b and Table 5-3. Tan δ value is higher for the neat resin compared to E-glass/MAESS composite. Based on Dwan'isa *et al.* [94] this is due to higher net volume of resin and also less mobility of chains in the composite. The glass transition temperature is determined by the peak of the tan δ curves. The measured values are presented in Table 5-3. Observation of one peak for both neat resin and fiberglass reinforced campsites is the indication of one T_g and in other words single phase system. Upon fiber insertion no significant change in T_g was observed. Take into account that E-glass fibers may also participate in the curing process by reaction of some possible reaction of E-glass fiber sizings with the styrene at lower temperature before all epoxy groups react at high temperature curing, and in turn alter the MAESS matrix network structure. This resulted in slight decrease of T_g. Shape of tan δ curve is slightly broader for E-glass/MAESS composite. This suggests that bio-based composite has broadened glass transition region because of more heterogeneity of the materials compared to E-glass/VE composites.

Since vegetable oils have usually a broad molecular weight distribution that generally results in broad peak of tan δ curve than that of the petroleum-based composite [99, 100]. Compared to existing studies [43] higher values of T_g was measured both for neat resin (40 °C increase) as well as ensuing composite (25 °C increase). This is attributed to great structural rigidity and high functionality of the sucrose molecule which is the core of sucrose soyate. Rigidity of sucrose molecule has been shown to give more rigid thermosets in previous studies [22, 101]. The crosslink density (ν_e) was evaluated as follow, an expression derived from the rubber elasticity's theory:

$$E' = 3\nu_e RT \tag{5-1}$$

where E' is the storage modulus in the rubbery plateau above T_g. The rubbery plateau region was peaked 40 °C above glass transition temperature at 153°C, 169 °C, and 150 °C for neat MAESS, E-glass/VE/, and E-glass/MAESS composites respectively. R is the gas constant (8.314 $J\ K^{-1}/mol^{-1}$), and T is the temperature in Kelvin. Using Eqn. (1), v_e is calculated and reported at Table 5-3.

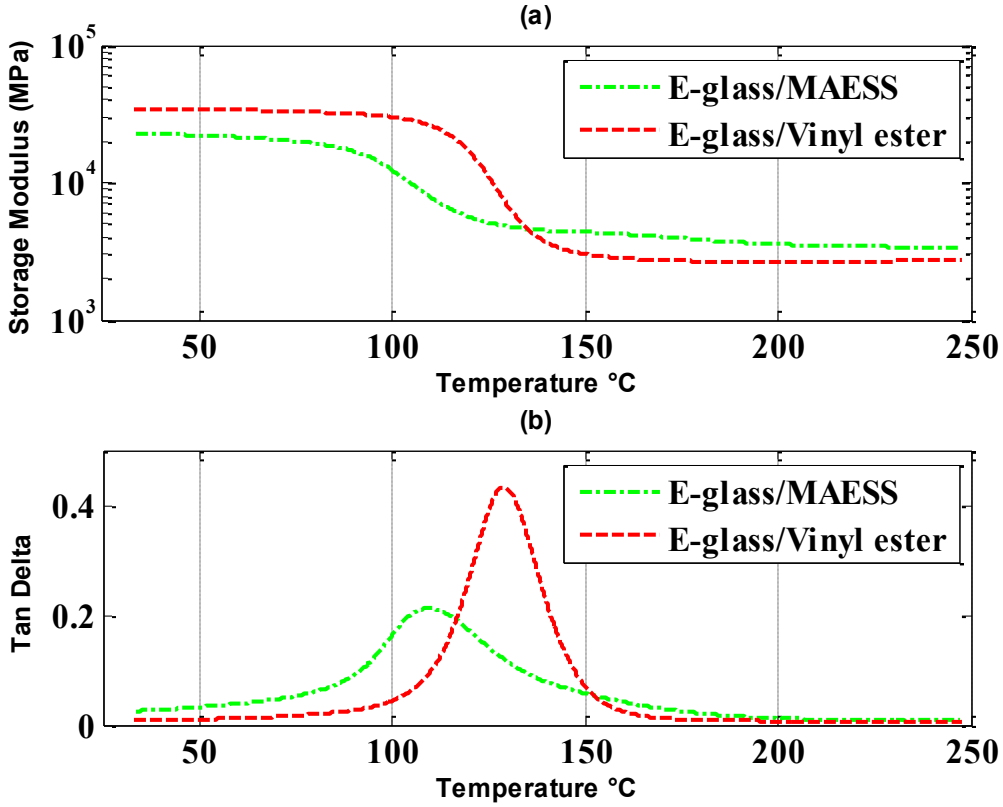

Figure 5-4. Temperature dependence of (a): storage modulus (E'), and (b): glass transition temperature (T_g) of E-glass/MAESS and E-glass/VE reinforced composites.

The HDT or softening point of polymer-based materials is another thermal properties for designing industrial products. Table 5-3 reports HDT for E-glass/MAESS, and E-glass/VE composite. The HDT value of pure MAESS rein is 51°C. It should be mentioned that a significant increase in the HDT by inserting fibers is due to high modulus of E-glass fibers as well as the high interfacial adhesion and crystallinity of the MAESS. HDT results for E-glass/MAESS, and E-glass/VE composite are 340 °C and 375 °C, respectively, confirming relatively comparable HDT results for both bio-based and petroleum based composites.

Table 5-3. Thermal Properties for 50 Vol. % E-Glass/MAESS and E-Glass/VE Composites.

Composite	DSC	DMA				HDT
	T_g(°C)	T_g (°C)	E' at 40°C (GPa)	$E'_{rubbery}$ plateau (GPa)	v_e (× 1000 mol/m^3)	(°C)
Neat MAESS	112.88	113 (1.50)	2.44	0.08 @ T_g+40°C	7.71	51.01 (3.82)
E-glass/VE	126.50	129.01 (0.59)	34.42	2.74 @ T_g+40°C	248.45	375.88 (3.71)
E-glass/MAESS	109.34	109.81 (0.25)	22.59	4.44 @ T_g+40°C	420.87	340.45 (3.90)

[a] Values in parentheses are standard deviations

In summary, as our goal in objective number 3, the composite made from MAESS and E-glass fiber showed improved mechanical properties. The composite using MAESS were hard and ductile with high modulus and exhibit excellent interface and mechanical properties due to high functionality, rigid and compact chemical structures of MAESS oligomers in thermoset resin.

CHAPTER 6. BIO-BASED COMPOSITES PREPARED BY COMPRESSION MOLDING WITH NOVEL THERMOSET RESINS FROM SUCROSE SOYATE AND FLAX-FIBER REINFORCEMENT

Natural fibers have an advantage over glass fibers in that they are less expensive and abundantly available from renewable resources and have a high specific strength. Using natural fibers with polymers based on renewable resources will allow many environmental issues to be solved. By embedding natural fibers with renewable resource–based polymers such as cellulosic plastics; and soy-based polymers, the so-called green bio-composites are continuously being developed. Highly functionalized bio-based monomers were investigated to take full advantage of the exceptional performance of both flax fibers and bio-based resins for bio-composite application. Two different novel high-functional bio-based resins from Methoxylated Sucrose Soyate Polyol (MSSP) and methacrylated epoxidized sucrose soyate (MAESS) were synthesized by ring-opening of ESS through methanol and metacrilated acid, respectively. The main objective of this Chapter is to study the mechanical properties of composites based on the new high functionalized sucrose soyate resins from renewable origins as matrices and with flax fibers as reinforcements. Composites based on a conventional chemical-based resin matrix and E-glass fibers were also produced, and investigated comparatively as the references.

Therefore, the motivation in this Chapter was drawn from comparing the mechanical and thermo-mechanical properties of the new bio-based resins reinforced with flax fiber with those reinforced with glass fibers. Composite plates were manufactured in the 100 mm x 200 mm closed mold compression with the pressure of 110 kN. All composites were cured at the same conditions in order to be comparable. The composites cured at room temperature for 12 hours and postcured at 150 °C temperature for 1 hour.

6.1. Physical Properties of Composites

The density of the cured VE and the flax fibers have been measured to be 1.10 g/cm^3 and 1.44 ± 0.02 g/cm^3, respectively [102]. The densities of the composites with flax fibers and glass fibers were observed to be between 1.21 g/cm^3 to 1.26 g/cm^3 and 1.74 g/cm^3 to 1.76 g/cm^3, respectively. The fiber volume fraction of composites were either the same or normalized with respect to 50 vol % in order to be compared. The physical properties of composites are reported in Table 6-1.

Table 6-1. Physical Properties of Glass and Flax Reinforced Composites after Normalized with Respect to 50 vol%.

Composite	Composite dencity(g/cm3)	Fiber Vol Fraction	Weight Fraction	Fiber Density	Void Percent
Flax/MSSP	1.26	50	57.23	1.44	1.1
Flax/MAESS	1.21	50	58.85	1.44	4.23
Flax/VE	1.23	50	57.76	1.44	2.14
E-glass/MSSP	1.74	50	72.25	2.56	5.3
E-glass/MAESS	1.76	50	71.10	2.56	2.7
E-glass/VE	1.74	50	71.71	2.56	4.11

6.2. Curing Analysis

Figure 6-1 shows typical curves in MDSC method for cured MAESS reinforced flax fiber. This method cleanly separates the glass transition (reversing heat flow) and enthalpy recovery (non-reversing heat flow) events in the amorphous sample. As discussed earlier in Chapter 4 for E-glass/MAESS and E-glass/MSSP, the non-reversing signals are those kinetic events such as crystallization, decomposition, cure, etc. Additionally, as indicated at Figure 6-1, the, flax/MAESS sample shows an enthalpic recovery peak in the non-reversing signal nonreversing curves (red line) which indicate either the composite are not fully cured or furthere

crystalization occures in composite by increasing temperature. Curing conversion is diminished in flax composites compared to glass composites due to lack of chemical treatment and higher moisture uptake in flax fiber mats compared to E-glass fibers. On the other hand, the glass transition temperature (T_g) are noted by the sudden decrease in the heat flow of the cured sample at around 102 °C in flax/MAESS composite as was shown in reversing curve (green line). Glass transition by DSC method are compared for all composites in this study in Table 6-2.

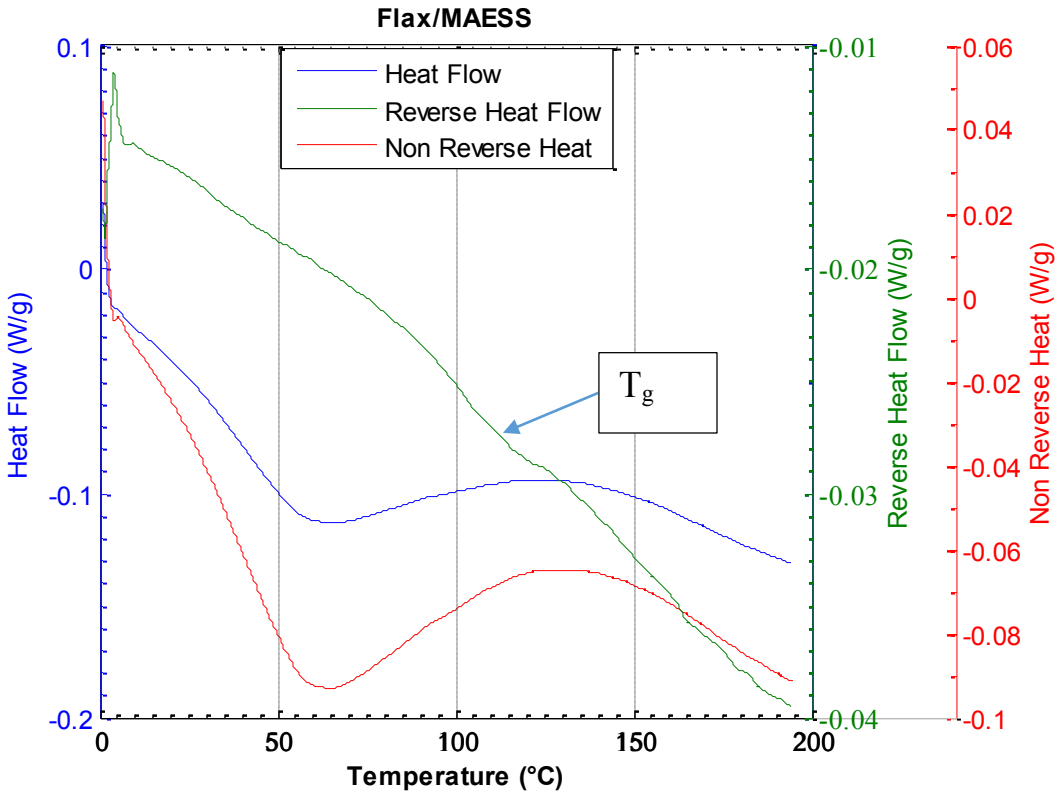

Figure 6-1. Typical scan of MDSC of the "cured flax fiber reinforced MAESS composite".

6.3. Dynamic Mechanical Properties

Temperature-dependent mechanical properties were characterized by DMA. Typical DMA curves are shown in Figure 6-2 and tabulated in Table 6-2. The storage modulus plots for composites containing MAESS and MSSP matrices reinforced with E-glass and flax fibers are compared with each other and against E-glass/VE and flax/VE composites in Figure 6-2a. The

storage modulus indicates the amount of energy stored in the composite as elastic energy, which is highly affected by the reinforcement mechanical properties and, the interfacial bonding strength between reinforcement and matrix [103]. The storage modulus in the composites with E-glass fibers are higher due to higher mechanical properties of E-glass fiber compared to flax fibers. The storage modulus of flax/MSSP, flax/MAESS and flax/VE at 40°C were 9.01, 10.2, and 17.44 GPa respectively, and that of E-glass/MSSP, E-glass /MAESS and E-glass /VE at 40°C is 20.69, 22.59, and 34.42 GPa, respectively. This indicates about 56% and 59% and 49% decrease in storage modulus of flax composites, respectively, compared to their counterparts. The storage modulus in composites with the same fiber type highly influenced by the interfacial modulus between the reinforcement fiber and resin matrix. The lower storage modulus could be contribute to the softer interphase. The storage modulus of flax/MSSP and flax/MAESS at 40°C decreased by 48% and 40 % respectively, compared to flax/VE. On the other hand, by increasing temperature, storage modulus of composites contains VE drop rapidly, while composites contains bio resins keep the storage modulus for higher range of temperature. This indicate that adhesion between fiber and bio resins are higher at high temperature compared VE composites. Cross link density in E-glass/MSSP and E-glass /MAESS showed 133 % and 62% increase, respectively, compared to E-glass/VE. Cross-link density was determined at 40 °C above glass transition at rubbery plateau region.

Moreover, the glass transition temperature of the composite has changed, as reported in Table 6-2 and is shown in Figure 6-2b. For flax/MSSP and E-glass/MSSP the glass transition temperature (T_g) is about 101 °C and 132 °C respectively. The decrease in T_g for the flax composites originates from the reduced cross-linkage for the composite. The dampening, or tan δ gives also information about the internal friction of the material. A decreased peak of the tan δ in

composite contains bio resins compared with VE composite is due to the fact that freely motion of molecular chains in interphase affect glass transition temperature and storage modulus.

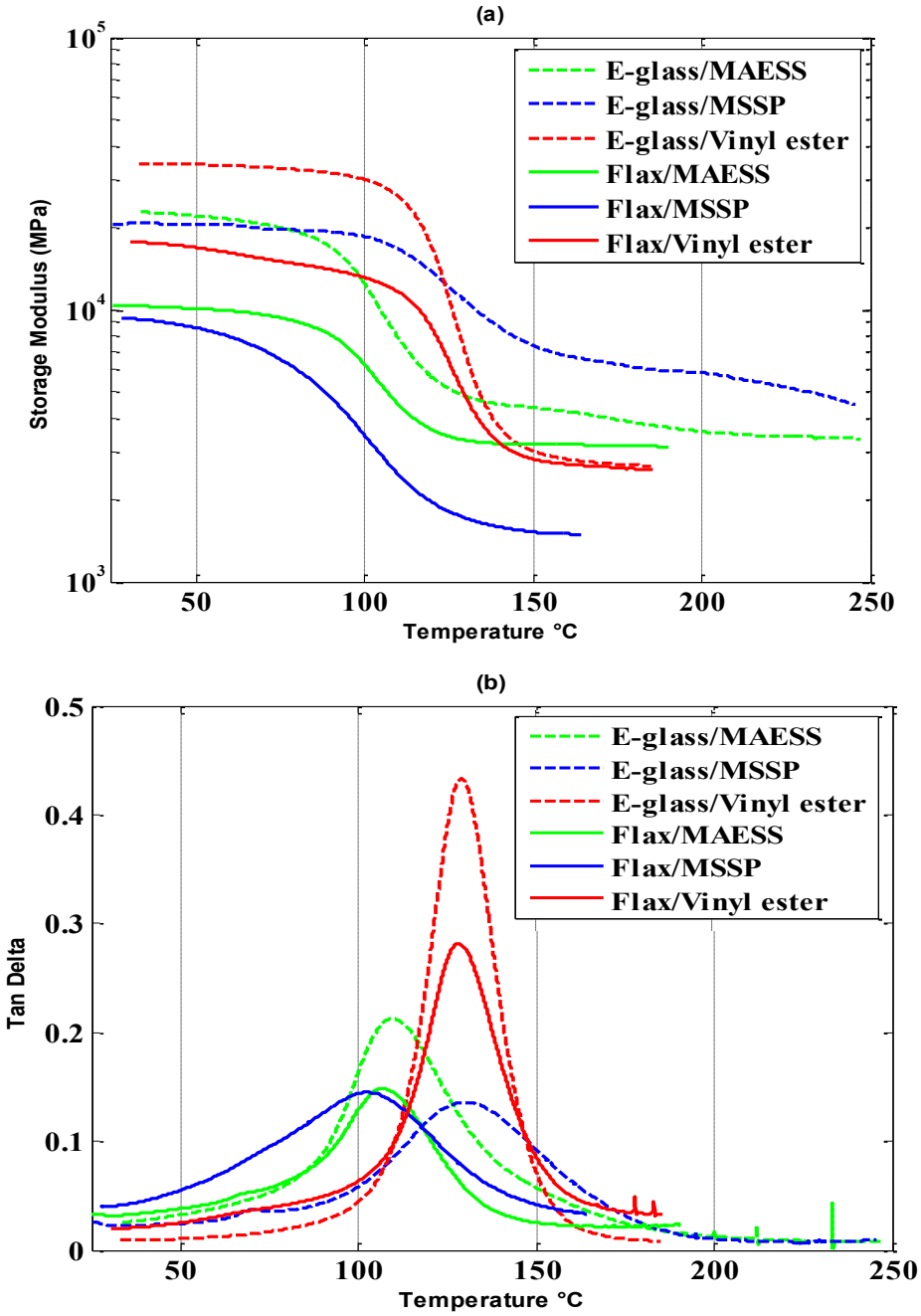

Figure 6-2. Effect of fiber reinforcements and bio resins on (a) storage modulus, (b) tan δ.

Lower glass transition in flax/MAESS and flax/MSSP compared to flax/VE could be attributed to some possible dangling molecular chains in bio resins structure. It is also possible

that some oil moleculrs on the surface of flax fibers react with these dangling chains and make the interphase tougher. Overall, the effect of bio resins and flax fibers is to reduce the glass transition temperature and increase the effective crosslink density of system during its curing.

Table 6-2. Thermal Properties for Composite Materials Reinforced with E-Glass/Flax Fiber with Bio resins and VE Resin as a Reference.

Composite	DSC	DMA				HDT
	T_g (°C)	T_g (°C)	E' at 40°C (GPa)	E' *rubbery* plateau at T_g+40°C (GPa)	v_e (× 1000 mol/m^3)	(°C)
Flax/MSSP	100.01	101.45 (1.00)	9.01	1.58	152.79	249.50 (3.13)
Flax/MAESS	102.16	107.11 (0.11)	10.20	3.20	305.28	287.27 (2.31)
Flax/VE	127.1	128.88 (0.60)	17.44	2.65	240.36	257.84 (1.38)
E-glass/MSSP	125.3	132.22 (1.91)	20.69	6.41	578.33	302.35 (5.9)
E-glass/MAESS	109.34	109.81 (0.25)	22.59	4.44	420.87	340.45 (3.90)
E-glass/VE	126.50	129.01 (0.59)	34.42	2.74	248.45	375.88 (3.71)

[a] Values in parentheses are standard deviations

6.4. Tensile Testing

Results for specific tensile modulus and strength are tabulated in Table 6-3 and are shown in Figure 6-3. Using of bio resins with flax fiber increased tensile modulus compared with flax/VE, due to high stiffness of bio-resins. The specific tensile modulus of biocomposites flax/MSSP and flax/MAESS were increased by approximately 17% and 10%, respectively. Since the elastic modulus is mainly dependent on fiber reinforcement type and volume percentage, hence a major increase in tensile modulus in flax/MSSP and flax/MAESS was not expected. This increase in tensile modulus of the flax/MSSP and flax/MAESS composites is attributed to the

modifications at the molecular level of the fiber, which lead to fiber-matrix bonds, increased adhesion and more effective stress transfer behavior. Regarding strength, biocomposite flax/MSSP and flax/MAESS show comparable values to flax/VE composite. These comparable properties could be attributed to high performance of bio resins. Similarly, for E-glass/MSSP and E-glass/MAESS, tensile strengths and modulus are quite comparable. It can be seen from Figure 6-3 that there is larger variance in flax fiber reinforced composites. The variance could be due to many reasons, presence of voids and impurities, variation in fiber lengths, improper fiber and resin distribution, etc. The relative comparison discussed above does not take into account these variations. Overall, the use of bio-resins increased the tensile modulus of the composite. Compared to petroleum based composites (flax/VE and E-glass/VE), bio-resins with natural fibers shows higher modulus. This may be attributed to functional groups in bio-resins chemically reacted with functional groups in flax fibers and render more stiff composite.

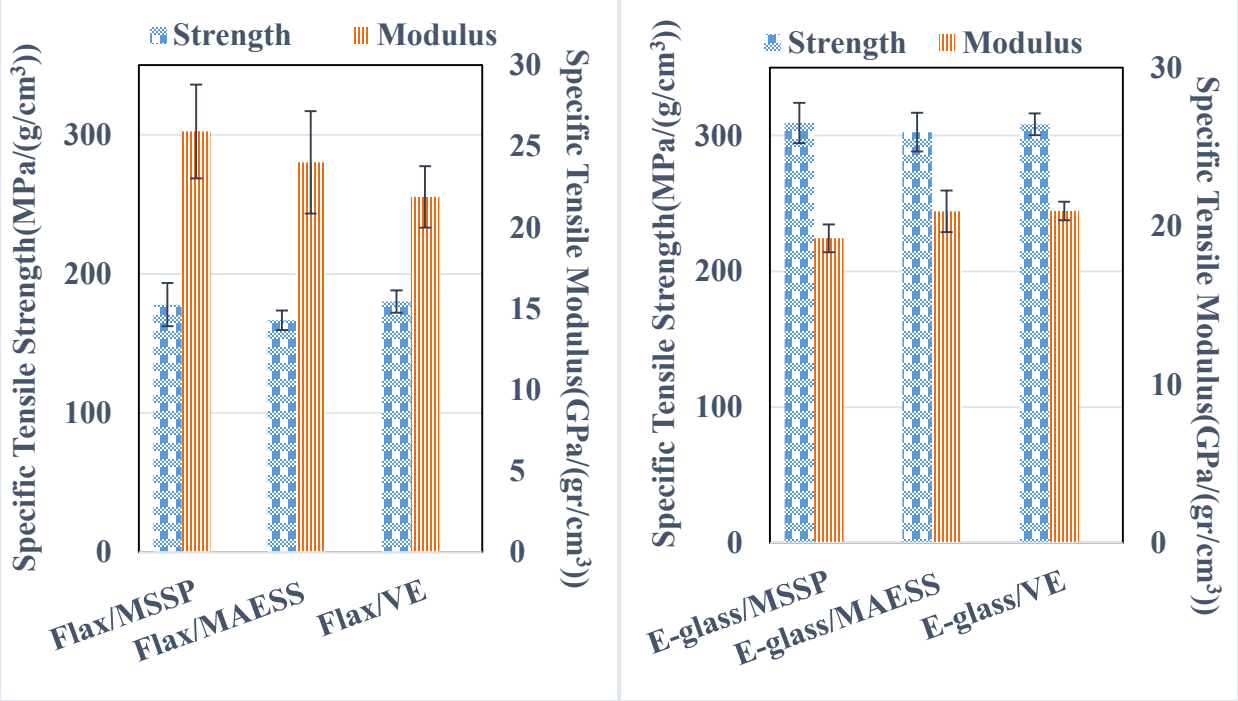

Figure 6-3. Specific Tensile Strength and Modulus of 50 vol.% Flax and E-glass reinforced MSSP, MAESS and VE resins.

6.5. Flexural Testing

Specific flexural properties are reported in Table 6-3 and are shown in Figure 6-4. The specific flexural modulus of biocomposites flax/MSSP and flax/MAESS were increased by approximately 3.5% and 13.9%, respectively, compared to flax/VE. On the contrary, their specific flexural strengths were decreased by approximately 15% and 10%, respectively. This decrease may be attributed to the embrittlement of the resin system, or delamination failure in specimens. On the other hand, using of MSSP and MAESS bio resins with E-glass fiber increased flexural strengths by 47% and 5% and decreased flexural modulus by 15% and 10%, respectively, when the results are compared with E-glass/VE. Similar to tensile properties, the increase in flexural strength of the E-glass/MSSP and flax/MAESS composites is attributed to the highly reacted functional groups in bio resins with E-glass sizing, which lead to fiber-matrix bonds, increased adhesion. On the other hand, the plasticizing effects of some possible dangling chains in interphase decrease the modulus and shows more effective stress transfer behavior. No specimen has failed by delamination during loading and the failure mode shows little or no fiber pull-out compared to E-glass/VE specimens.

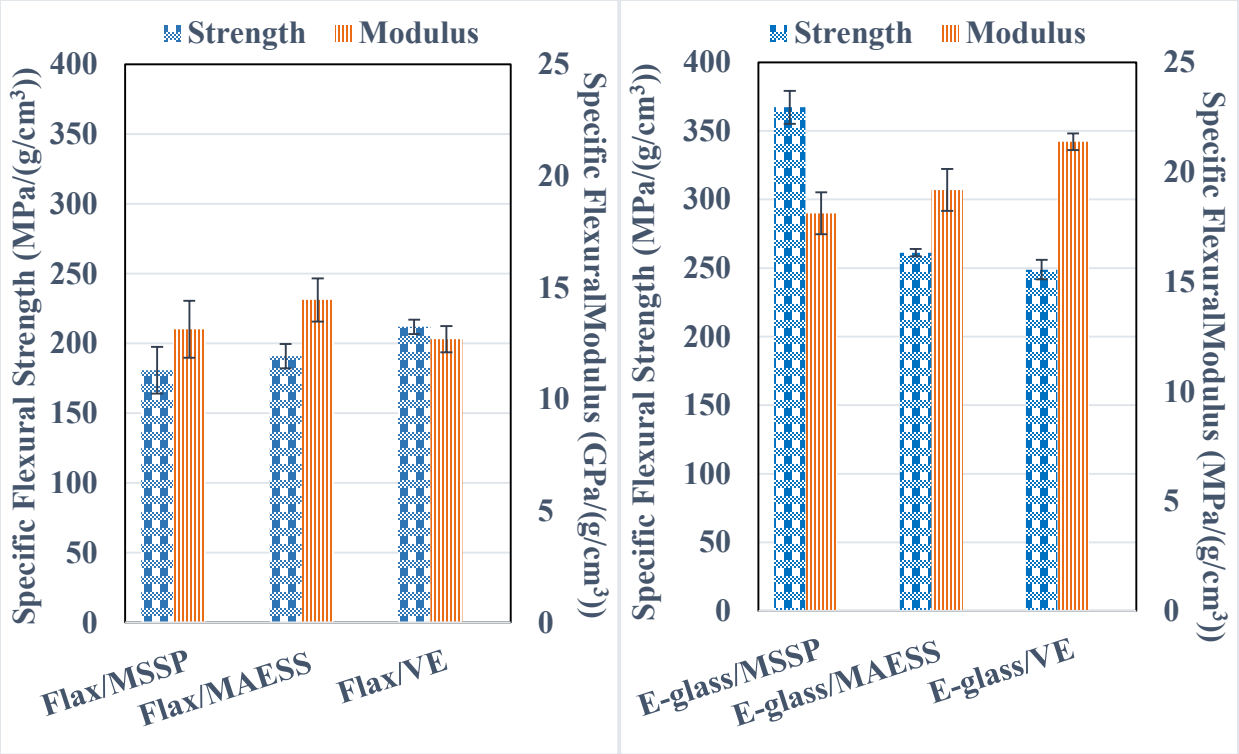

Figure 6-4. Specific Flexural Strength and Modulus of 50 vol.% Flax and E-glass reinforced MSSP, MAESS and VE resins.

Table 6-3. Comparison of Specific Mechanical Properties of 50 vol.% Flax and E-glass fiber reinforced with MSSP and MAESS Biocomposites against Those Reinforced with VE.

Composite	Specific Tensile Properties[a]		Specific Flexural Properties[a]		Specific ILSS[a]
	Strength MPa/(g/cm^3)	Modulus GPa/(g/cm^3)	Strength MPa/(g/cm^3)	Modulus GPa/(g/cm^3)	Strength MPa/(g/cm^3)
Flax/MSSP	176.50(15.31)	25.71 (2.86)	180.8(8.09)	13.13(1.27)	24.95 (1.72)
Flax/MAESS	166.72(7.06)	24.01 (3.16)	190.89(8.76)	14.45 (0.96)	21.43 (1.20)
Flax/VE	180.16(8.01)	21.88(1.88)	211.89(5.09)	12.68(0.58)	23.54(2.48)
E-glass/MSSP	309.19(14.88)	19.22(0.87)	367.24(12.4)	18.12(0.95)	27.70(0.42)
E-glass/MAESS	303.04(14.29)	20.97(1.32)	261.70(2.71)	19.18(0.96)	14.32(0.55)
E-glass/VE	308.02(8.74)	22.96(0.64)	248.86(7.12)	21.38(0.38)	14.17(1.56)

[a]Values in parentheses are standard deviations

6.6. Interfacial Properties and Impact Strength

Interfacial strength is an important properties in determining composite fracture toughness. The specific interlaminar shear strength (ILSS) and impact strength ($kJ/m^2/(g/cm^3)$) values for flax and E-glass fiber reinforced bio-based resins and VE specimens are compared in Figure 6-5 and Figure 6-6, respectively. Results of specific ILSS of flax/MSSP and flax/MAESS composites are reported in Table 6-3. Considering the error bar, interlaminar shear strength values in flax composites are almost the same. Considering the average values, ILSS in flax/MSSP was increased by 4.5 % and in flax/MAESS was decreased by 2.8 %, compared to flax/VE. E-glass/MSSP and E-glass/MAESS fiber-reinforced composites in the current studies show 114 % and 10 % increase in ILSS compared to E-glass/VE composites. The substantial increase in ILSS achieved in the MSSP and MAESS bio resin matrices reinforced with E-glass fiber were attributed to the high number of the hydroxyl functionality (10 epoxy group per molecule) and methacylate functionality (5.7), per molecule of the synthesized MSSP and MAESS, respectively. Which chemically reacted with functional groups in fibers.

It is a common observation that with most of the effective fiber surface treatments or modification in resin system, the flexural and tensile properties of the composite increase, but the impact strength decreases[5]. But in these novel resins in composite, not only do the flexural and tensile properties of the composite increase or were comparable with their counterpart petroleum based resin composite, but the impact strength increases as well. The fibers play a very important role in the impact resistance of the composite as they interact with the crack formation in the matrix and act as stress transferring medium. Therefore, fracture toughness of E-glass composites are substantially higher than untreated flax composites, due to role of E-glass fiber strength in fracture toughness. The specific notched impact strengths for E-glass/MSSP, E-

glass/MAESS, and E-glass/VE were increased by 267%, 317%, and 264% compared to flax/MSSP, flax/MAESS, and flax/VE, respectively. The MSSP and MAESS bio-resins reinforced with flax fiber showed 30% and 7% increase in impact strength compared with their counterpart flax/VE composite. Similarly, the MSSP and MAESS bio-resins reinforced with E-glass fiber showed 30% and 22% increase in impact strength compared with their counterpart E-glass/VE composite.

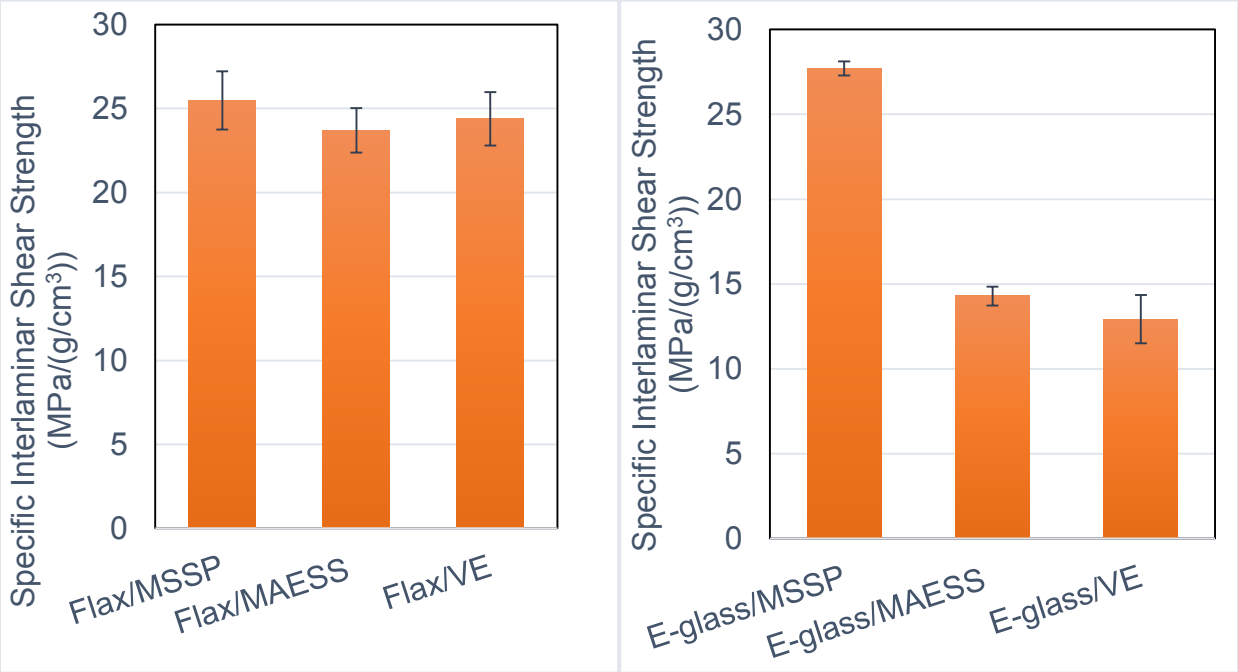

Figure 6-5. Specific interfacial strength of 50 vol.% Flax and E-glass reinforced MSSP, MAESS and VE resins.

There is greater energy absorption in the bio-composite containing MSSP and MAESS bio-resins. Energy absorbing capability of the composites during impact is therefore strongly depends on tensile strain capacity of resin, interface strength between fiber and resin and the flexibility of the interface molecular chains. When the cracks moves forward, the chain motions change due to their flexibility and create a barrier to the crack growth. Flexible resins derived from bio-based resins have higher strain-to failure properties compared to petroleum based

counterparts [104]. As mentioned before, improvement in the impact resistance of bio-based composites is due to resulting molecular structures contain a large concentration of dangling chains. Plasticizing effect of the dangling chains was also observed in other type of soy based resins.

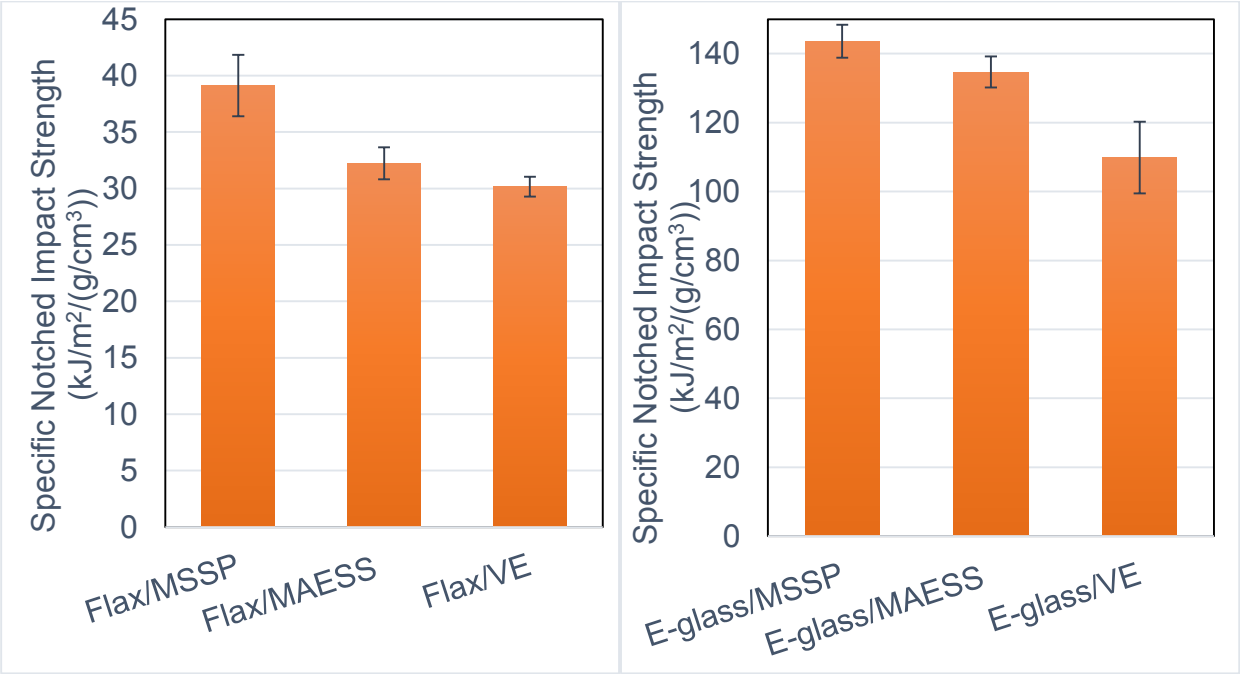

Figure 6-6. The specific notched impact strength of 50 vol.% Flax and E-glass reinforced MSSP, MAESS and VE resins.

6.7. Scanning Electron Microscopy

The SEM micrographs of tensile-fractured surface of bio-composites are shown in Figure 6-7(a-f). In general, flax and E-glass fibers with VE show poor interfacial bonding between the fiber and matrix, resulting in a relatively clean surface over the pulled out fibers due to greater extent of delamination. The failure in E-glass based composites results in a higher degree of pull out in comparison to flax based composites. Bio-resins based composites both with flax and E-glass fibers showed a smaller degree of fiber pull-out and good adhesion between fiber and matrix.

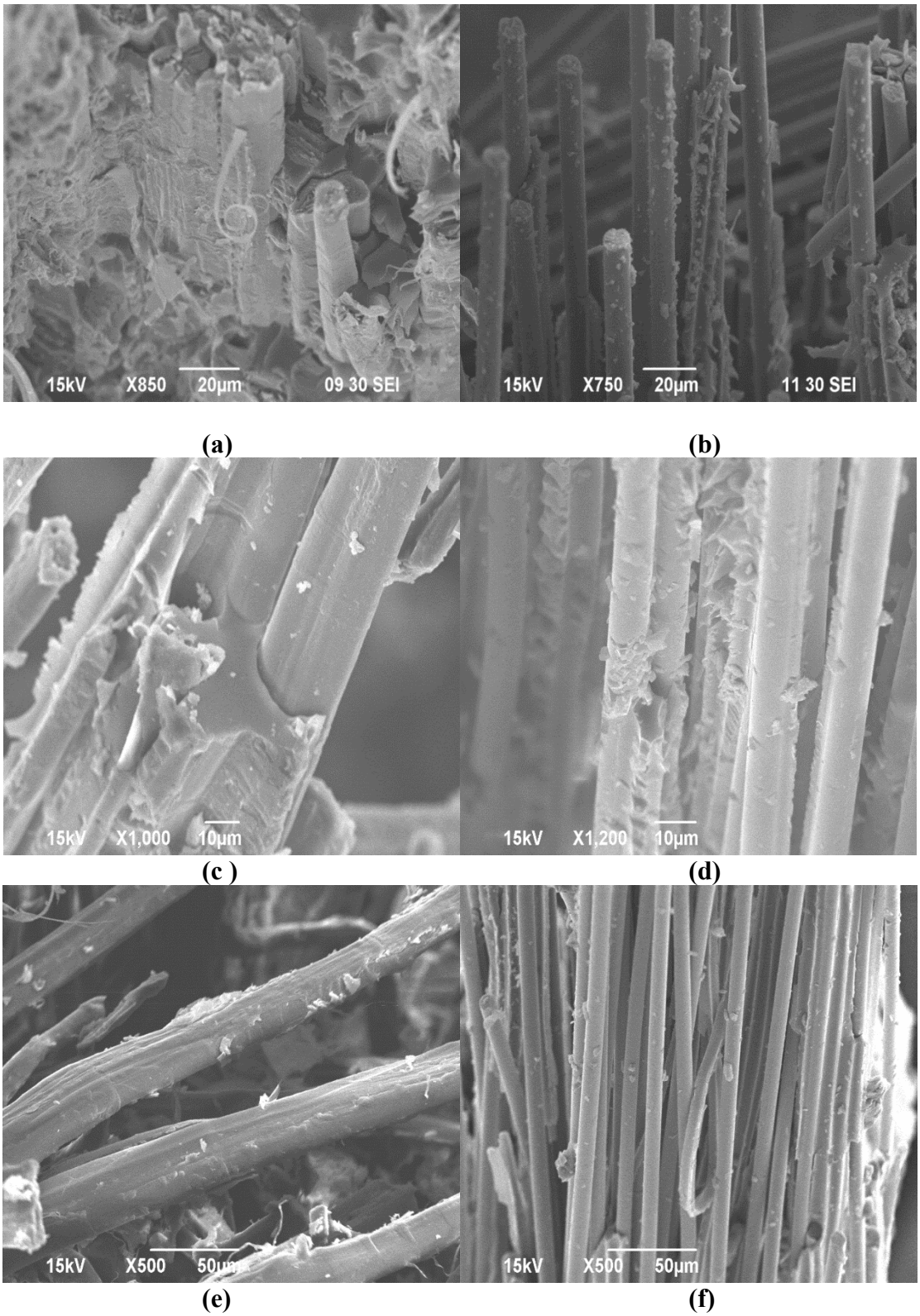

Figure 6-7. SEM scans of tensile fractured surfaces of: (a) flax/MSSP, (b) E-glass/MSSP, (c) flax/MAESS, (d) E-glass/MAESS, (e) flax/VE, and (f) E-glass/VE composites.

6.8. Nanoindentation Test

Figure 6-8 shows a distinct line of nano indents along a random path starting from the matrix and ending on the fiber in depth of 50 nm. The distinct properties of the transition zone were revealed by 5 to 7 µm in flax fiber reinforced MSSP-based composites (Figure 6-8(a)) and 1-2 µm in E-glass fiber reinforced MSSP-based composites (Figure 6-8 (b)). The initial gradient of the unloading curve is used to calculate the stiffness of the sample at that point. Table 6-4 shows the hardness, H, and reduced elastic modulus, E_r for the composites.

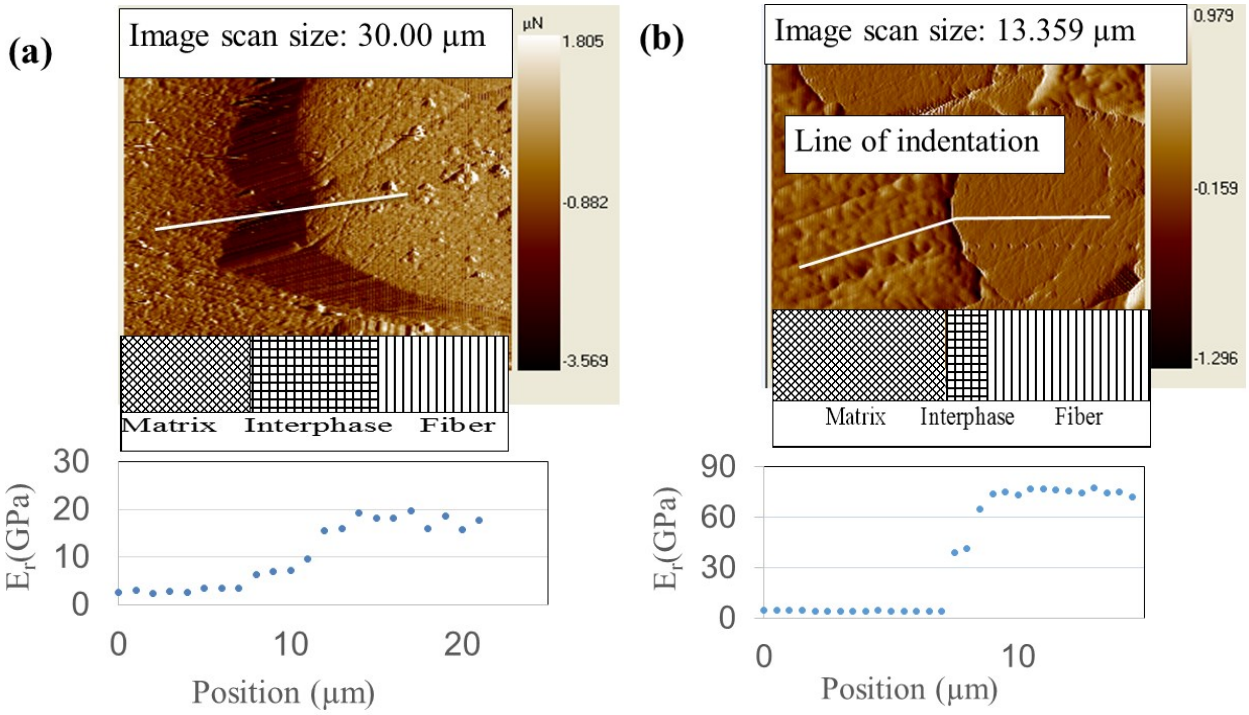

Figure 6-8. Reduced modulus of (a) flax fiber reinforced MSSP, (b) E-glass fiber reinforced MSSP, starting from the matrix and ending on the fiber.

Other than mechanical properties of interphase, the thickness of interphase has also significantly impacts on mechanical properties especially on interlaminar shear loading conditions and unnotched impact toughness. For instance, Jang- Kya Kim [89] used nanoindentation test and Atomic Force Microscopy (AFM) to investigate the mechanical

properties of glass–matrix interphase affected by silane agent based on novel experimental techniques, such as the nanoindentation and nanoscratch tests. The effective interphase thickness measured from the nanoscratch test in that study varies between 0.8 and 1.5 μm depending on the type and concentration of silane agent. The higher is the silane agent concentration, the larger is the interphase thickness. According to previous studies [89], depending on the ability of silane agent to interdiffuse into and to chemically react with the bulk matrix, the thickness of ensuing interphase also changes, which in turn has significant impact on the overall mechanical performance and fracture behavior of composites, especially under interlaminar loading conditions.

Table 6-4. Comparison of Hardness and Reduced Modulus in E-glass/MSSP and Flax/MSSP Composites based on Nanoindentation Test.

Sample		Hardness (GPa)	E_r (GPa)
E-glass/MSSP	Matrix	0.21	3.33
	Interphase	5.93	60.87
	Fiber	6.41	74.11
Flax/MSSP	Matrix	0.16	3.02
	Interphase	0.25	9.88
	Fiber	0.49	18.52

Furthermore, Ahlstrom and Gérard [87] and Daoust et al. [88], using an elastomer coating applied over glass fibers demonstrated a superior interfacial strength of an epoxy/glass fiber composite. Therefore, the improvement in adhesion between epoxy/glass fiber composite was attributed to the soft interphase being able to reduce the shear stress concentrations at the fragment ends. In the current study, nanoindentation tests demonstrated that the interphase in flax fiber reinforced MSSP are thicker and softer, therefore as the above studies showed, the high interlaminar shear strength in flax/MSSP can be attributed to the thick and though interphase

between fiber and matrix. Another reason for a good ILSS in flax/MSSP can be attributed to the fact that the strength values of interphase is close to those of flax and matrix.

In conclusion, the results of mechanical and thermal properties and SEM analysis confirmed the composites made from flax fiber with MSSP or MAESS resins achieve similar properties to E-glass/MSSP and E-glass/MAESS. Moreover, it was proved that flax/MSSP and flax/MAESS composites perform superior to previous bio-based and petroleum based composites studied.

CHAPTER 7. MICROMECHANICAL VISCOELASTIC ANALYSIS OF FLAX FIBER REINFORCED BIO-BASED POLYURETHANE COMPOSITES

In this study, a novel highly functional bio-based polyol, Methoxylated Sucrose Soyate Polyol (MSSP), was used as a new oligomer in formulation of polyurethane (PU) resin as the matrix for a composite material where flax fiber was used as the reinforcement. A micromechanical method was used to predict and define the viscoelastic behavior of the composite materials. As mentioned before, several micromechanical approaches have been developed for prediction of aligned fiber composite viscoelastic response using fiber and matrix properties [66-71, 105]. However, to the author's best knowledge, previous studies have not accurately addressed the viscoelastic behavior of flax fiber in these composites. This study, therefore, assessed material and viscoelastic properties of both flax fiber and bio-based polyurethane resin to obtain more accurate prediction of mechanical properties of the composite.

7.1. Viscoelastic Parameters

Figure 7-1 shows measured data and the Prony series fit for PU matrix. The averaged data obtained from stress-relaxation modulus were fitted in ABAQUS in the form of Prony series with three terms for matrix and two terms for flax fiber to determine the Prony parameters. The parameters of Prony series are summarized in Table 7-1. According to experimental stress relaxation data, the initial engineer constants are $E_0^f = 47.84\ GPa, v_0^f = 0.3$ and $E_0^m = 1.24\ GPa, v_0^m = 0.4$ for flax fiber and bio-based PU, respectively.

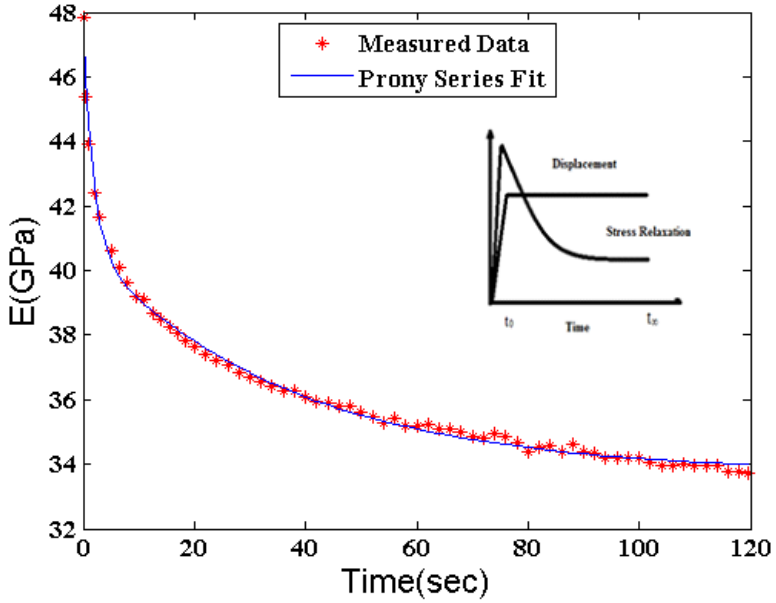

Figure 7-1. Measured and fitted relaxation of modulus for flax fiber under the strain 1.5 %.

Table 7-1. Prony Series Parameters for MSSP Matrix and Flax Fiber.

Material	i	g_i	τ_i	γ_i	ϑ_i
Matrix	1	0.026	0.074	2.563E-03	0.074
	2	0.094	41.28	9.102E-3	41.28
	3	0.013	628.13	1.112E-3	628.13
Fiber	1	0.148	1.74	3.091E-02	21.75
	2	0.147	36.63	2.964E-04	0.185

7.2. Local Stress Distribution in Flax Fiber Reinforced MSSP Composite

For flax/PU composite, the assumed RUC was analyzed under six types of loadings employing ABAQUS finite element package [106]. Three stress distributions for the composite RUC under load cases 1, 2, and 4 at two different times of 1 s and 100 s for 50% flax/PU composite are shown in Figure 7-2. A 0.2 % uniform stretch in the direction of fibers were applied on the RUC. The stress distribution varies over time due to response of viscoelastic behavior of flax fiber and PU composite. As the contours of stress distributions indicate, the elements located in the fibers have the same stress but higher than those elements of the matrix

domain. The stresses are distinctly uniform in each domain of the fibers and matrix. It is due to the uniform stretch of all elements in the longitudinal direction.

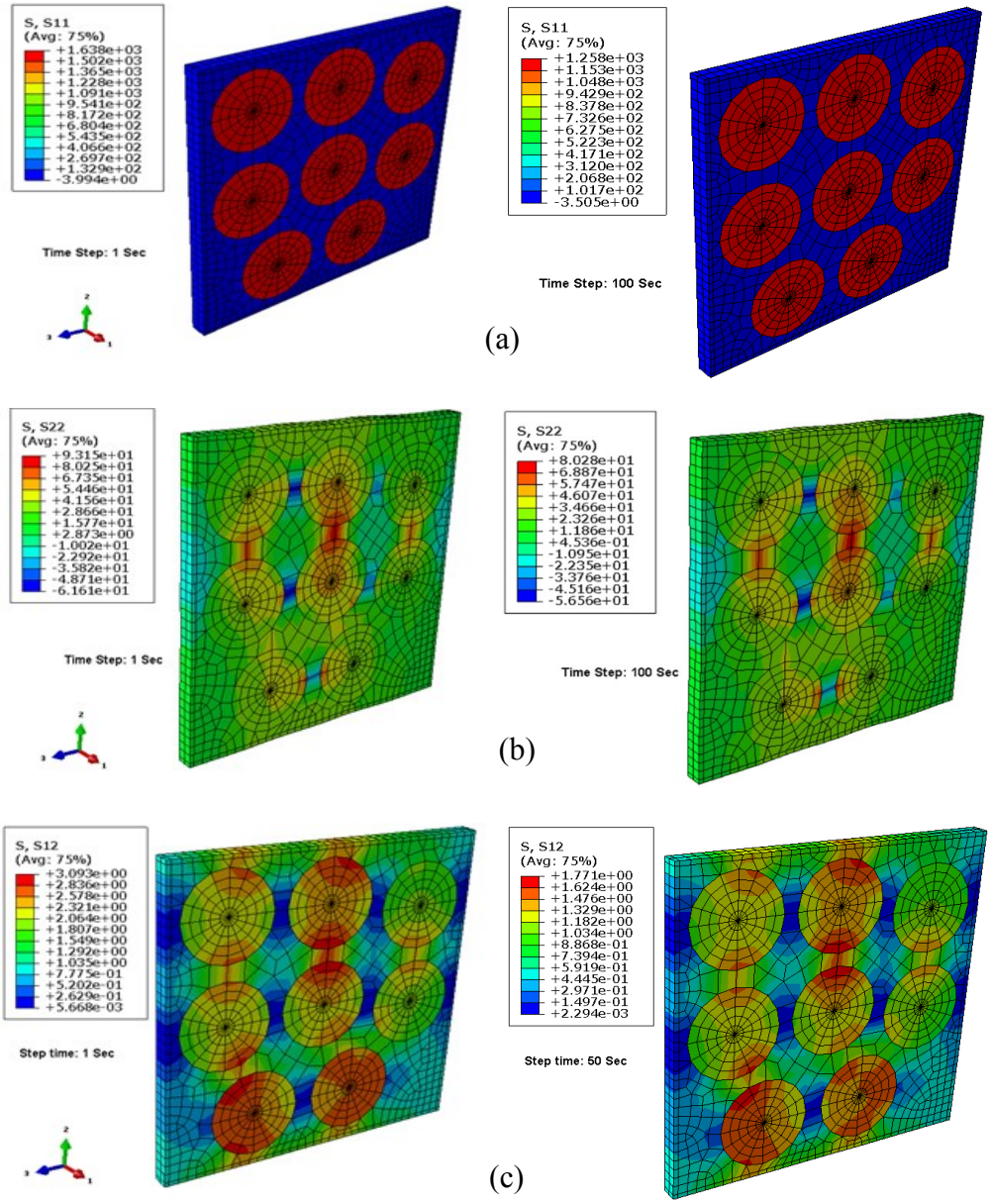

Figure 7-2. Stress distribution contours within the deformed shape of RUC of flax/PU composite with fiber volume of 50% under 0.2% strain at time of 1 and 100 s. for (a): load case 1 (S11), (b): load case 2 (S22) and (c): load case 4 (S12).

Using the volume average subroutine program interfaced with ABAQUS, resultant composite compliances are calculated and are plotted as they change with time in Figure 7-3. Due to symmetry and the fact that both fiber and matrix are isotropic, the number of compliance

coefficients is reduced from the total anisotropic case. The predicted compliance coefficients results from various volume elements showed thirteen distinct coefficients, an indication of a monoclinic isotropic material behavior for this case. Since some of these coefficients are close to each other and some are very small compared to others, transverse isotropic with five district compliance coefficients were assumed.

Mechanical properties for composites at different time steps were calculated and reported in Table 7-2. As it is reported in Table 7-3, at each fiber volume ratio of 40%, 50%, and 60%, E11, E22, E33, G12, G13, G23, v12, v13, v32 are reported for different time steps. These values are determined from the compliance coefficients.

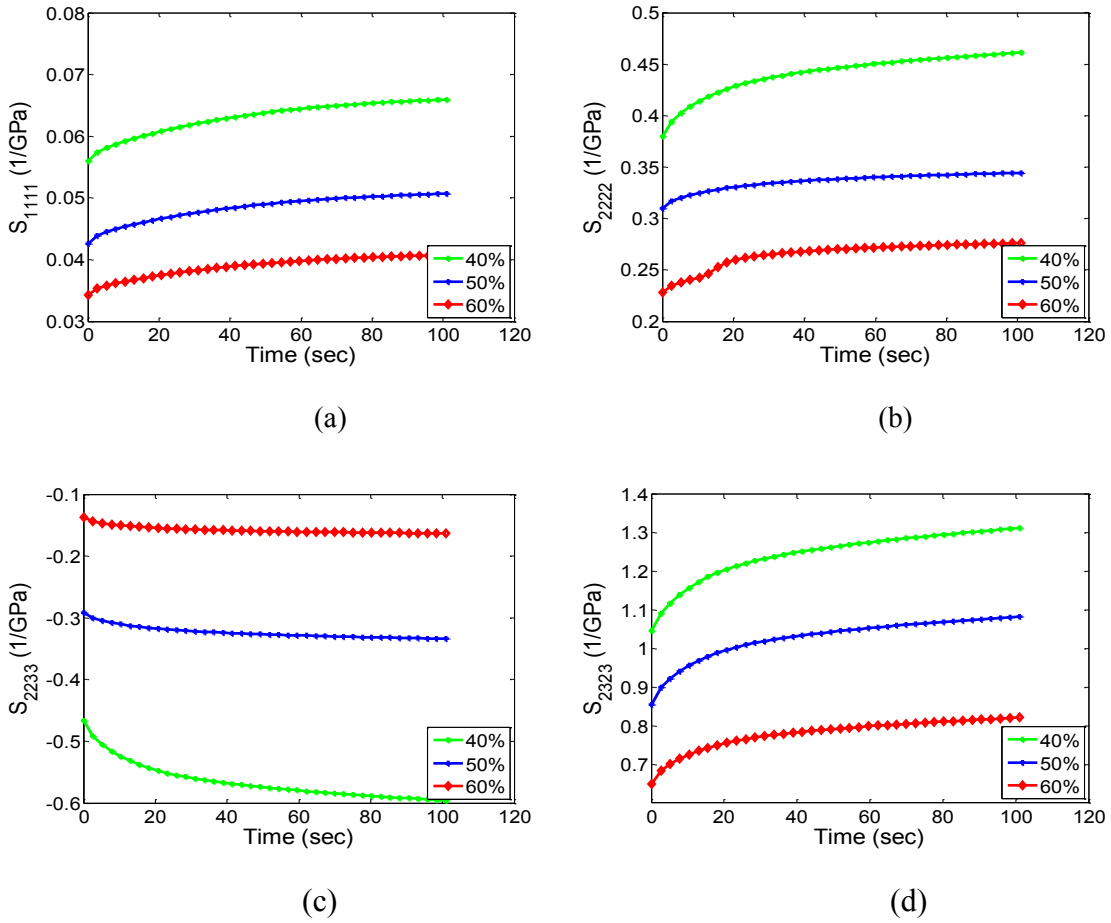

Figure 7-3. Compliance coefficients of Flax/PU composite for different fiber volume fraction (%): (a) S_{1111}, (b) S_{2222}, (c) S_{2233}, (d) S_{2323}.

Table 7-2. Compliance Coefficients, 1/GPa of Flax/PU Composite for Different Fiber Volume of 40%, 50%, and 60% at Three Different Time at 1 and 50 and 100 Sec.

t(s)	V_f (%)	S_{1111}	S_{2222}, S_{3333}	S_{1212}, S_{1313}	S_{2323}	S_{2233}	S_{3322}
1	40	0.06	0.39	0.99	1.07	-0.48	0.24
	50	0.04	0.31	0.85	0.88	-0.30	0.17
	60	0.03	0.23	0.45	0.67	-0.14	0.13
50	40	0.06	0.45	1.18	1.26	-0.57	0.25
	50	0.05	0.34	1.03	1.04	-0.33	0.18
	60	0.04	0.27	0.54	0.79	-0.16	0.14
100	40	0.07	0.46	1.23	1.31	-0.60	0.25
	50	0.05	0.34	1.07	1.08	-0.33	0.18
	60	0.04	0.28	0.56	0.82	-0.16	0.14

Table 7-3. The Predicted Mechanical Properties of Flax/PU Using Micromechanical Model.

		E_{11}	E_{22}	E_{33}	G_{12}	G_{13}	G_{23}			
t (s)	V_f(%)	(GPa)						ν_{12}	ν_{13}	ν_{32}
1	40	18.86	2.58	2.53	1.00	1.02	0.94	0.42	0.48	0.52
	50	23.12	3.18	3.15	1.17	1.15	1.14	0.40	0.39	0.50
	60	28.75	4.31	4.29	2.21	2.23	1.49	0.37	0.36	0.48
50	40	16.77	2.23	2.17	0.84	0.86	0.79	0.43	0.48	0.53
	50	20.36	2.96	2.92	0.97	0.96	0.96	0.41	0.40	0.51
	60	25.33	3.70	3.95	1.84	1.84	1.26	0.39	0.38	0.50
100	40	16.22	2.17	2.10	0.81	0.83	0.76	0.44	0.48	0.53
	50	19.73	2.90	2.87	0.93	0.93	0.92	0.41	0.41	0.52
	60	24.54	3.62	3.89	1.76	1.77	1.22	0.39	0.38	0.51

7.3. Experimental and Analytical Approach

In order to theoretically determine stress tensor in polymer materials, a function is needed to consider the effect of history dependent behavior in these materials. According to Lu H et al. [107], the Poisson's ratio of polymer is a time dependent variable. They showed if Poisson's ratio is assumed to be constant, theoretical values of stress tensor are poorly confirmed by

experimental results. The stress tensor for a linear viscoelastic polymer material can be defined as [108]:

$$\sigma_{ij(t)} = \frac{E_0}{3(1-2\nu_0)}\varepsilon_{kk(t)}\delta_{ij} + \frac{E_0}{1+\nu_0}(e_{ij(t)} - \int_0^t R_{(t-\tau)}\, e_{ij(t)}d\tau) \quad (7\text{-}1)$$

where $\sigma_{ij(t)}$ and $\varepsilon_{kk(t)}$ are stress and strain tensor respectively. $R_{(t-\tau)}$ is the relaxation kernel and $e_{ij(t)}$ is the deviatoric strain ($e_{ij(t)} = \varepsilon_{kk(t)} - \delta_{ij}/3$), ν_0 and E_0 are the instantaneous Poisson's ratio and elastic modulus, respectively. Relaxation function can be described by Prony series as defined in Eq. (2-3).

By applying a constant value of ε_0 at time t=0 in Eq. (6-1), along to fiber direction, the axial stress relaxation behavior of polymer material along to the direction of extension and the Poisson's ratio for linear isotropic materials can be determined as:

$$\sigma_{11(t)} = \frac{E_0\varepsilon_0}{3}[\frac{1-2\nu_{(t)}}{1-2\nu_0} + \frac{2(1+\nu_{(t)})}{1+\nu_0} - \frac{2}{1+\nu_0}\int_0^t R_{(t-\tau)}\left(1+\nu_{(\tau)}\right)d\tau] \quad (7\text{-}2)$$

$$\nu_t = \nu_0 + \frac{1-2\nu_0}{3}\int_0^t R_{(t-\tau)}\left(1+\nu_{(\tau)}\right)d\tau \quad (7\text{-}3)$$

$\nu_{(\tau)}$ is the time-dependent Poisson's ratio which depends on time. By substituting Eq. (6-3) in Eq. (6-1), the axial stress along to the extension direction will be determined as:

$$\sigma_{11(t)} = E_0\varepsilon_0\frac{1-2\nu_{(t)}}{1-2\nu_0} \quad (7\text{-}4)$$

A constant axial strain ε₀ in the direction of 1 is applied on the unit cell. Both fiber and matrix are stretched by the same amount in fiber direction, because a perfect bond between the flax fiber and matrix is assumed. Therefore, the total stress in the flax/PU composite material is obtained by summation of forces in the fiber and matrix:

$$\sigma_{11(t)} = (E_0^f V^f\frac{1-2\nu_{(t)}^f}{1-2\nu_0^f} + E_0^m V^m\frac{1-2\nu_{(t)}^m}{1-2\nu_0^m})\varepsilon_0 \quad (7\text{-}5)$$

where V^f and V^m are the volume fractions of fiber and matrix, respectively. Using the Laplace transformation, the Poisson's ratio in Eq. (6-4) becomes:

$$\nu_{(t)} = \nu_0 + \sum_{i=1}^{n} \gamma_i (1 - e^{\frac{-t}{\vartheta_i}}) \quad (7\text{-}6)$$

where γ_i and ϑ_i, depend on g_i and τ_i and ν_0. These values are calculated and reported in Table 7-1. By substituting Eq (6-6) in Eq. (6-5), axial stress in the composite material will be determined as follow:

$$\frac{\sigma_{11(t)}}{\varepsilon_0} = (E_0^f V^f [1 - \frac{2}{1-2\nu_0^f} \sum_{i=1}^{n} \gamma_i \left(1 - e^{\frac{-t}{\vartheta_i}}\right) + E_0^m V^m \left[1 - \frac{2}{1-2\nu_0^m} \sum_{i=1}^{n} \gamma_i \left(1 - e^{\frac{-t}{\vartheta_i}}\right)\right] \quad (7\text{-}7)$$

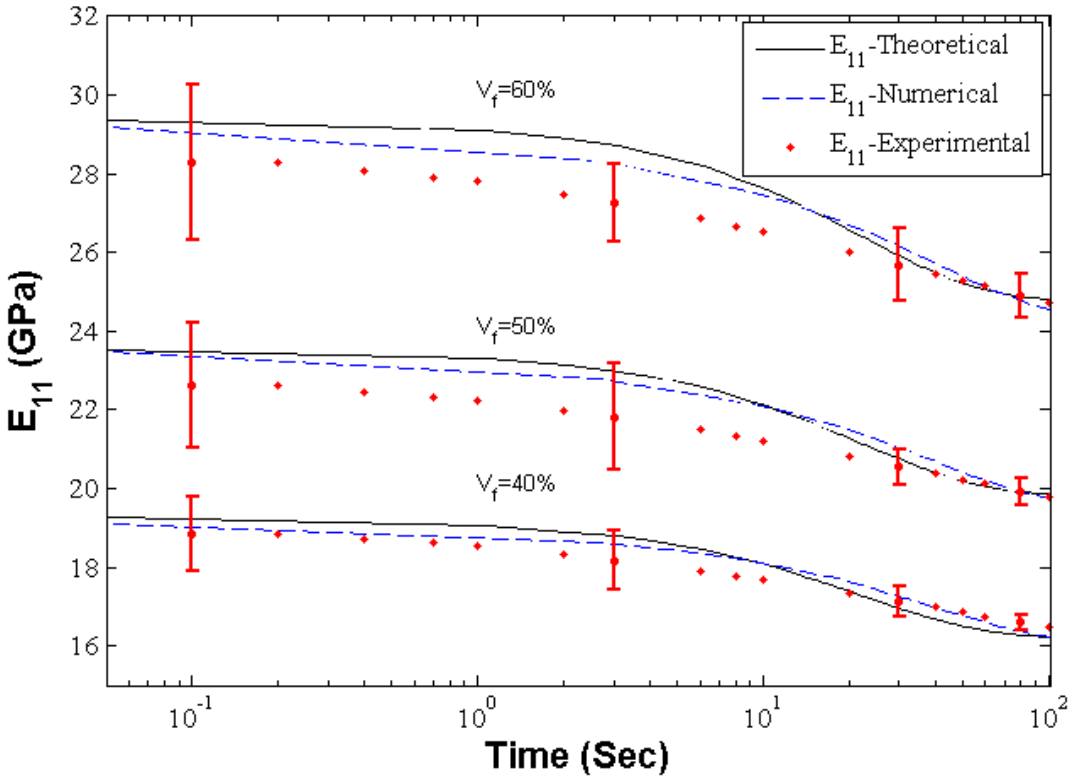

Figure 7-4 shows the modulus relaxation predictions of the finite element model with random packing of fiber and the theoretical expression as a function of time and fiber volume fraction in the flax/PU composite under 0.2 % strain. Considering the standard deviation of less than 10% in experimental data, the analytical expression as well as the numerical results are

quite accurate for the prediction of the relaxation stress in the 40 and 50 % flax fiber-reinforced material as it is shown in Figure 7-4. In analytical and numerical results, it is assumed there are no voids or misalignment of fibers in composite and perfect adhesion between fibers and matrix exists, therefore as Figure 7-4 shows, the accuracy of micromechanical models decreases as the fiber volume fraction increases.

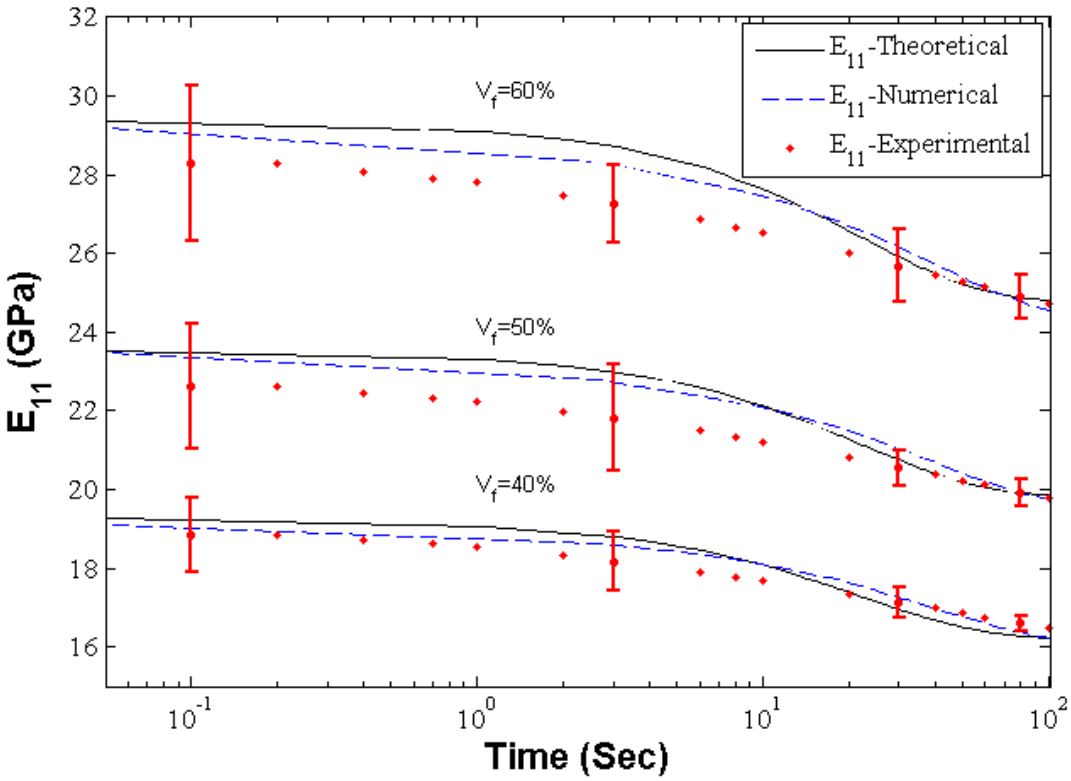

Figure 7-4. The drop of modulus versus time and fiber volume fraction for the flax/PU composite.

Due to Poisson's effect, the composite material does not contract in two directions at the same amount. The transverse axial strain of composite material can be determined as:

$$\varepsilon_{22(t)} = V^f \varepsilon^f_{22(t)} + V^m \varepsilon^m_{22(t)} = -(V^f \nu^f_{(t)} + V^m \nu^m_{(t)})\varepsilon_0 \qquad (7\text{-}8)$$

For flax fiber Poisson's ratio constants leads to two terms (i=1, 2) and for matrix they make three parameters (i=1, 2, 3). Figure 7-5 illustrates the Poisson's ratio values over the time

for flax/PU in different fiber volume fractions measured by analytical expression. The finite element results of ν_{12} were also used for comparisons. Similar to the accuracy of the analytical predictions for E_{11}, the accuracy of analytical methods for ν_{12} is also quite clear.

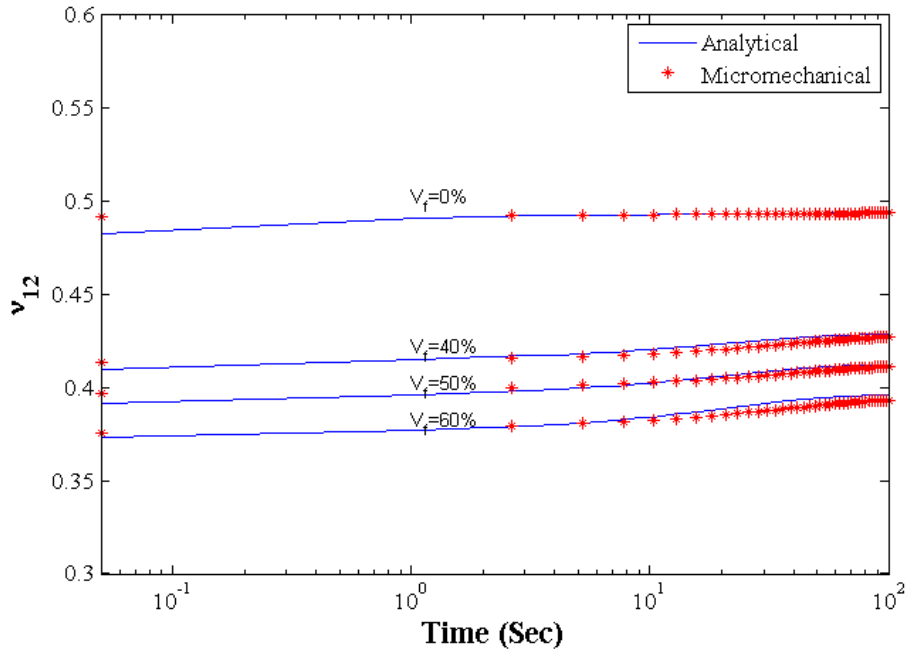

Figure 7-5. The variation of Poisson's ratio as a function of time and fiber volume fraction for flax/PU composite.

The viscoelastic behavior of flax/MSSP composite consisting of linearly viscoelastic matrix and fiber was determined by micromechanical and analytical models. Using a simplified unit cell subjected to the prescribed axial loading and expanding the stress tensor for linear viscoelastic polymer and matrix results in the analytical expressions that accurately predict the relaxation response of composite materials. A good agreement between the micromechanical and analytical modeling data and experimental results were observed for the linear viscoelastic response of the bio-based composite. Indeed, in the absence of a robust predictive model for biocomposite materials, researches apply model that composite constituents are elastic materials. However, the measured linear viscoelastic parameters of bio-based PU resin and flax fiber and

the proposed micromechanical model in this study, can be extended for different loading conditions to model the long-term behavior of different biocomposites. As discussed before and was also shown in

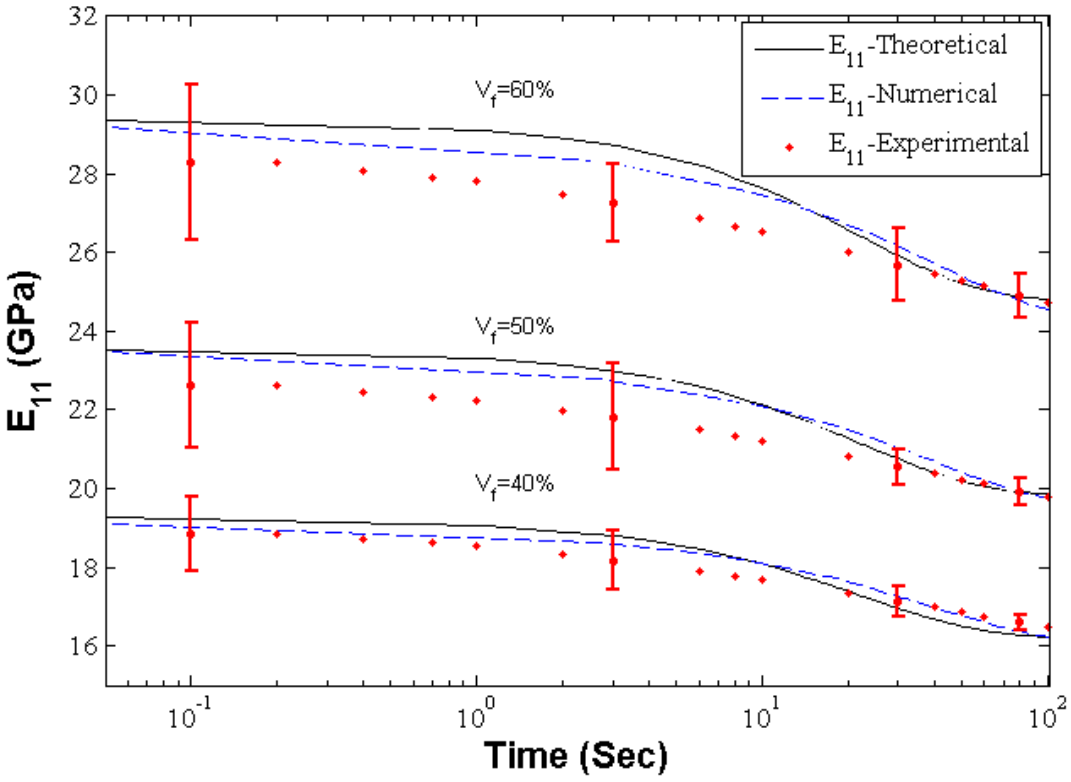

Figure 7-4, for flax/MSSP composite, stress relaxation at room temperature is normal and must be considered in design of structural sections. Therefore, assuming elastic material properties for flax and PU resin which mostly contain polymer material cannot predict the initial relaxation response of the composite. However, for stress relaxation of biocomposites, such as E-glass/MSSP or E-glass/MAESS composites, the assumption of linearly viscoelastic matrices and transversely isotropic elastic synthetic fibers, are valid assumptions as verified with Abadi et. al in [105]. In stress relaxation, there is a tendency for the fibers to carry a larger portion of the stress, therefore for the case of elastic fibers in a short time, it is very smaller decay in stress relaxation compared to natural fiber reinforced composites. Stress relaxation analysis for

biocomposites could have a broad applications in which a biocomposite specimen is deformed a given amount and decrease in stress occurs over prolonged period of exposure at constant elevated temperature.

CHAPTER 8. GENERAL SUMMARY CONCLUSIONS AND FUTURE WORKS

8.1. Conclusion

Recent advances in composite science, green chemistry and green engineering offer significant opportunities for developing new, improved materials from renewable resources for a wide range of materials using plant oils. By applying natural fibers with bio–based polymers such as soy-based polymers, the so-called green bio-composites are continuously being developed. However, the big challenge is obtaining rigid new bio-based polymers with high modulus, strength, durability, and improving the knowledge based on use of flax fibers and bio resins and their compatibility as reinforcement and matrices for composite applications. The present study investigated the possibility of replacing the petroleum based resins and E-glass fiber with novel bio resins reinforced with flax in composite application. The following sections summarize the main contributions from this work.

1. **Compression molding process:**

   The optimal processing conditions for MSSP and MAESS resins were established using compression molding to fabricate high quality fiber volume content composites. Experimental results showed that optimum compression pressure, control of resin viscosity by temperature of the mold and curing temperature are significant parameters for improvements in the mechanical properties of the composite. The optimum pressure was determined as 110 kN and 50 kN, when composites were fabricated at room temperature and at 150 °C, respectively. The room temperature is the optimum temperature for mold. Preheating the mold resulted in high fiber volume fraction and dry spots on fiber surface, even under the low pressure. Moreover, curing at room temperature resulted in higher strength and modulus, but lower impact

results. Whereas, curing at 150 °C resulted in composites with lower modulus, but higher impact resistance.

2. **Use of MSSP with E-glass fiber:**

   Compared to existing soybean oil based composites [41, 79-82], the mechanical properties of E-glass reinforced MSSP-based PU composites were significantly improved. Tensile strength and modulus were higher up to 40% and 75%, respectively. For flexural strength and modulus 130% and 110% improvements were observed compared to existing studies. Results of SEM images of failed samples along with interlaminar shear strength and impact tests revealed better wetting of fibers by matrix, stronger adhesion between fiber and matrix and greater interfacial bonding compared to other bio-based composites. Great rigidity of the molecular structure and higher functionality of sucrose ring has led to higher glass transition temperature both in neat resin and resulting E-glass reinforced composite.

3. **Use of MAESS with E-glass fiber:**

   The tensile strength and modules of MAESS and vinyl ester resins reinforced with E-glass fibers are 532 MPa, 36.79 GPa and 536 MPa, 36.40 GPa, respectively. The flexural strength and modules of MAESS and vinyl ester resins reinforced with E-glass fibers are 459 MPa, 432 GPa and 34 MPa, 37 GPa, respectively. The impact strength of the composites with MAESS resin reinforced with E-glass fibers was 237 kJ/m^2, whereas that of the vinyl ester resin reinforced with same E-glass fiber was 191 kJ/m^2. Compared to bio-based composites used in previous studies [10, 25, 43], 115% and 270% higher tensile strength and modulus, respectively and 20% and 95% greater flexural strength and modulus was measured respectively. Results of SEM

images along with flexural strength, interlaminar shear strength and impact tests revealed better wetting of fibers by matrix, stronger adhesion between fiber and matrix and greater interfacial bonding compared to corresponding E-glass/vinyl ester composites. The composite using MAESS were hard and ductile with high modulus and exhibit excellent interface and mechanical properties due to high functionality, rigid and compact chemical structures of MAESS oligomers in thermoset resin. Whereas, thermosets using modified bio-based resins used in previous studies are highly flexible and rubbery with low modulus and exhibit poor mechanical performance.

4. **Bio-based composites prepared with novel thermoset resins and flax-fiber reinforcement:**

   Interphase properties is a predominant parameter in determining the impact strength and interfacial strength of composites. Functional groups in the chemical structure of bio-based matrices chemically reacted with functional groups on the fiber surfaces and changed the interphase thickness of ensuing interphase, which in turn has significant effects on the mechanical performance and fracture behavior of composites. On the other hand, the possible presence of dangling chains in the chemical structure of bio-based matrices especially MSSP resin plasticized the inherently brittle high cross-linked interphase between fiber and the resins, causing the interphase material to become tough. These factors render high interfacial bonding and high impact strength in the current bio-composite materials. In conclusion, an increase in the mechanical and thermal properties was observed for both flax and E-glass fiber based bio-resins composites. Use of bio-based resins in

composite applications can be effective and economic way in improving the fiber-matrix adhesion. The SEM and nanoindentation tests proves the claims that adhesion and interfacial bonding between fiber and matrix is substantially higher by using these novel bio-resins especially by using MSSP. For most of properties including, glass transition, HDT, storage modulus, tensile modules in flax/MSSP, tensile strength in E-glass/MSSP, ILSS, and impact tests, MSSP showed superior properties compared its counterparts MAESS. Higher epoxy functionality and possible presence of dangling chains in MSSP makes this resins high modulus and strength while keeping the impact strength high. The composites prepared with bio resins showed improved modulus and interlaminar shear strength of the fibers with the resin, producing a stronger bond at the interface and higher mechanical strength. In general, the improvement in all mechanical of the bio-composite based on bio-resins are because of the high functional compact structure of these resins which reacted with functional groups in fibers and giving rise to a highly cross-linked molecule during the curing reaction. However, the storage modulus in bio resins does not track the trend in flexural and tensile moduli due to the fact that freely motion of molecular chains in interphase affect glass transition temperature and storage modulus.

5. **Bio-based content of biocomposites**

   Almost 86% (wt %) of flax/MSSP and flax/MAESS composites and 18% (wt %) of E-glass/MSSP and E-glass/MAESS composites contains renewable resources.

6. **Micromechanical and analytical analysis:**

A micromechanical model was applied to determine the viscoelastic properties of flax/MSSP using the properties of the constituents. A linear viscoelastic behavior was assumed for both flax fiber and PU resin under small deformation. Six independent loading cases were applied on a unit cell with randomly distributed cylindrical fiber in matrix under periodic boundary condition. In this inverse characterization analysis, time-dependent stresses and strains were measured by volume-averaged over the RUC. An analytical approach was also developed to predict the stress relaxation response of the composite material consisting linear viscoelastic flax fiber and bio-based PU matrix. A good agreement between the micromechanical modeling data and experimental results was observed for the linear viscoelastic response of the bio-based composite. The measured viscoelastic parameters of bio-based PU resin and flax fiber and the proposed micromechanical model in this study have a broad application in housing and automotive industries. As mentioned before, in this study, perfect bonding between fiber and matrix and cylindrical cross sectional area for fibers were assumed, which is different than reality. Applying an intermediate phase between fiber and matrix may change the predicted results.

8.2. Future Work

This study has shown the improvement in all mechanical properties of the bio-composite based on bio-resins. These improvements is due to the high functional compact structure of these resins which reacted with functional groups in fibers and giving rise to a highly cross-linked molecule during the curing reaction. However, there are still more elements of the technology which could be investigated. First, the storage modulus in the bio resins does not follow the trend

seen in the flexural and tensile moduli due to the fact that free motion of molecular chains in interphase affect glass transition temperature and storage modulus. Improvement the thermo-mechanical properties of these novel biocomposites, in a way that other mechanical properties would not be sacrificed, could be an interesting study for future. In addition, interphase and interfacial properties in this study were investigated based on nanoindentation and ILSS. However, in future, a better understanding of the nature of adhesion between fiber and matrix could be achieved using FTIR analysis.

To improve the micromechanical and analytical model, further investigation on the effect of different fiber gage length and various strain rate along with an appropriate statistical model is necessary. For instance, distribution of imperfections for longer gauge length is bigger, therefore, in this study, the 4mm gauge length was applied. However, considering different fiber gauge lengths gives more accurate real data. Moreover, the initial Young's modulus and strength of fibers increase with increasing strain rate. However, based on the current study, it is not clear what the effect of the fiber gauge lengths and strain rates are on the viscoelastic properties. Furthermore, it is highly recommended that analytical or numerical models be based on an appropriate statistical model, e.g.Weibull. The advantage of using this approach is that the random behavior associated with the material including can be readily quantified. Therefore, investigating the effect of different fiber gauge length and various strain rate along with an appropriate statistical model could give more deep insights on viscoelastic behavior of flax fibers.

In addition, conducting stress relaxation for longer time and using of strain-cycling procedure to reduce the time necessary for stress relaxation will be extremely useful in improvement of the micromechanical models of natural fiber based composites. Moreover,

conducting more replicate tests of the stress relaxation of flax fibers along with statistical analysis (i.e. more than 90 fiber) could provide more accurate viscoelastic properties and as a result, more accurate model could be established.

Moreover, in this study, perfect bonding between fiber and matrix and cylindrical cross sectional area for fibers were assumed, which is different than reality. Applying an intermediate phase between fiber and matrix may change the predicted results. Therefore, the average properties of interphase which were measured by nanoindentation could be used for future FEA. As it was shown in cross sectional area of flax/MSSP in, the assumption of circular cross section for flax fiber is not valid. Future studies could also focus on the effect of irregular cross-sectional shape of flax fiber on the micromechanical model for the viscoelastic natural fiber reinforcement composites.

Finally, the analysis of price and availability of biocomposites versus those of commercial composites could be studied in order to prove their technical applications.

REFERENCES

1. Yan, J. and D.C. Webster *Thermosets from highly functional methacrylated epoxidized sucrose soyate*. Green Materials, 2014. **2**, 132-143.
2. Wool, R. and X.S. Sun, *Bio-based polymers and composites*. 2011: Academic Press.
3. John, M.J. and S. Thomas, *Biofibres and biocomposites.* 2008. **71**(3): p. 343-364.
4. Mohanty, A.K., M. Misra, and L.T. Drzal, *Natural fibers, biopolymers, and biocomposites*. 2005: CRC Press.
5. Adekunle, K., D. Akesson, and M. Skrifvars, *Biobased Composites Prepared by Compression Molding with a Novel Thermoset Resin from Soybean Oil and a Natural-Fiber Reinforcement.* Journal of Applied Polymer Science, 2010. **116**(3): p. 1759-1765.
6. Adekunle, K., et al., *Impact and flexural properties of flax fabrics and Lyocell fiber-reinforced bio-based thermoset.* Journal of Reinforced Plastics and Composites, 2011. **30**(8): p. 685-697.
7. Bouchareb, B. and M.T. Benaniba, *Effects of epoxidized sunflower oil on the mechanical and dynamical analysis of the plasticized poly (vinyl chloride).* Journal of applied polymer science, 2008. **107**(6): p. 3442-3450.
8. Can, E., R. Wool, and S. Küsefoğlu, *Soybean-and castor-oil-based thermosetting polymers: Mechanical properties.* Journal of applied polymer science, 2006. **102**(2): p. 1497-1504.
9. Zhu, J., et al., *Manufacturing and mechanical properties of soy-based composites using pultrusion.* Composites Part A: Applied Science and Manufacturing, 2004. **35**(1): p. 95-101.

10. Khot, S.N., et al., *Development and application of triglyceride-based polymers and composites.* 2001. **82**(3): p. 703-723.

11. Czub, P. *Application of modified natural oils as reactive diluents for epoxy resins*. Wiley Online Library.

12. Dweib, M.A., et al., *All natural composite sandwich beams for structural applications.* Composite structures, 2004. **63**(2): p. 147-157.

13. Pérez, J.D.E., et al., *Production and characterization of epoxidized canola oil.* Transactions of the ASAE (American Society of Agricultural Engineers), 2009. **52**(4): p. 1289.

14. Espinoza Perez, J., et al. *Study of the process parameters of the canola oil epoxidation*.

15. Hong, C.K. and R.P. Wool, *Development of a bio-based composite material from soybean oil and keratin fibers.* Journal of Applied Polymer Science, 2005. **95**(6): p. 1524-1538.

16. Meyer, P.P., et al., *Epoxidation of soybean oil and Jatropha oil.* Thammasat Int J Sci Technol, 2008. **13**: p. 1-5.

17. O'Donnell, A., M.A. Dweib, and R.P. Wool, *Natural fiber composites with plant oil-based resin.* Composites Science and Technology, 2004. **64**(9): p. 1135-1145.

18. Ma, Q., et al., *Synthesis and properties of full bio-based thermosetting resins from rosin acid and soybean oil: the role of rosin acid derivatives.* Green Chemistry, 2013.

19. Jin, F.L. and S.J. Park, *Thermomechanical behavior of epoxy resins modified with epoxidized vegetable oils.* Polymer International, 2008. **57**(4): p. 577-583.

20. Takahashi, T., et al., *Biocomposites composed of epoxidized soybean oil cured with terpene-based acid anhydride and cellulose fibers.* Journal of applied polymer science, 2008. **108**(3): p. 1596-1602.

21. Pan, X. and D.C. Webster, *New Biobased High Functionality Polyols and Their Use in Polyurethane Coatings.* ChemSusChem, 2012. **5**(2): p. 419-429.

22. Nelson, T.J., et al., *Bio-Based High Functionality Polyols and Their Use in 1K Polyurethane Coatings.* Journal of Renewable Materials, 2013. **1**(2): p. 141-153.

23. Pan, X., P. Sengupta, and D.C. Webster, *Novel biobased epoxy compounds: epoxidized sucrose esters of fatty acids.* Green Chemistry, 2011. **13**(4): p. 965-975.

24. Bunsell, A.R. and J. Renard, *Fundamentals of fibre reinforced composite materials*. 2005: CRC Press.

25. Morye, S.S. and R.P. Wool, *Mechanical properties of glass/flax hybrid composites based on a novel modified soybean oil matrix material.* 2005. **26**(4): p. 407-416.

26. Nagieb, Z.A., M.A. Nassar, and M.G. El-Meligy, *Effect of addition of boric acid and borax on fire-retardant and mechanical properties of urea formaldehyde saw dust composites.* International Journal of Carbohydrate Chemistry, 2011. **2011**.

27. Li, X., L.G. Tabil, and S. Panigrahi, *Chemical treatments of natural fiber for use in natural fiber-reinforced composites: a review.* Journal of Polymers and the Environment, 2007. **15**(1): p. 25-33.

28. Van de Velde, K. and E. Baetens, *Thermal and mechanical properties of flax fibres as potential composite reinforcement.* Macromolecular Materials and Engineering, 2001. **286**(6): p. 342-349.

29. Davies, G.C. and D.M. Bruce, *Effect of environmental relative humidity and damage on the tensile properties of flax and nettle fibers.* Textile Research Journal, 1998. **68**(9): p. 623-629.

30. Santulli, C., *Impact properties of glass/plant fibre hybrid laminates.* Journal of Materials Science, 2007. **42**(11): p. 3699-3707.

31. Faruk, O., et al., *Biocomposites reinforced with natural fibers: 2000–2010.* 2012. **37**(11): p. 1552-1596.

32. Bledzki, A.K., et al. *Natural and wood fibre reinforcement in polymers*. 2002; Available from: http://public.eblib.com/EBLPublic/PublicView.do?ptiID=485258.

33. Joshi, S.V., et al., *Are natural fiber composites environmentally superior to glass fiber reinforced composites?* Composites Part a-Applied Science and Manufacturing, 2004. **35**(3): p. 371-376.

34. Pascault JP, S.H., Verdu J, Williams RJJ., *Thermosetting Polymers:*. 2002: Taylor & Francis Books, Inc.

35. Holbery, J. and D. Houston, *Natural-fiber-reinforced polymer composites in automotive applications.* Jom, 2006. **58**(11): p. 80-86.

36. Malkapuram, R., V. Kumar, and Y.S. Negi, *Recent development in natural fiber reinforced polypropylene composites.* Journal of Reinforced Plastics and Composites, 2008.

37. Sharmin, E. and F. Zafar, *Polyurethane: An Introduction.* 2012.

38. Li, H., *Synthesis, characterization and properties of vinyl ester matrix resins.* 1998.

39. Belgacem, M.N. and A. Gandini, *Monomers, polymers and composites from renewable resources*. 2011: Access Online via Elsevier.

40. Raquez, J.M., et al., *Thermosetting (bio)materials derived from renewable resources: A critical review.* Progress in Polymer Science, 2010. **35**(4): p. 487-509.

41. Husić, S., I. Javni, and Z.S. Petrović, *Thermal and mechanical properties of glass reinforced soy-based polyurethane composites.* Composites Science and Technology, 2005. **65**(1): p. 19-25.

42. Lu, Y. and R.C. Larock, *Fabrication, Morphology and Properties of Soybean Oil-Based Composites Reinforced with Continuous Glass Fibers.* Macromolecular Materials and Engineering, 2007. **292**(10-11): p. 1085-1094.

43. Henna, P.H., M.R. Kessler, and R.C. Larock, *Fabrication and Properties of Vegetable-Oil-Based Glass Fiber Composites by Ring-Opening Metathesis Polymerization.* Macromolecular Materials and Engineering, 2008. **293**(12): p. 979-990.

44. Wan Rosli, W.D., et al., *UV radiation curing of epoxidized palm oil–cycloaliphatic diepoxide system induced by cationic photoinitiators for surface coatings.* 2003. **39**(3): p. 593-600.

45. Pan, X., P. Sengupta, and D.C. Webster, *High Biobased Content Epoxy–Anhydride Thermosets from Epoxidized Sucrose Esters of Fatty Acids.* Biomacromolecules, 2011. **12**(6): p. 2416-2428.

46. Mosiewicki, M.A., et al., *Polyurethane Foams Obtained from Castor Oil-based Polyol and Filled with Wood Flour.* Journal of Composite Materials, 2009. **43**(25): p. 3057-3072.

47. Wik, V.M., M.I. Aranguren, and M.A. Mosiewicki, *Castor Oil-based Polyurethanes Containing Cellulose Nanocrystals.* Polymer Engineering and Science, 2011. **51**(7): p. 1389-1396.

48. Petrović, Z.S., et al., *Polyurethane networks from polyols obtained by hydroformylation of soybean oil.* Polymer International, 2008. **57**(2): p. 275-281.

49. Desroches, M., et al., *From Vegetable Oils to Polyurethanes: Synthetic Routes to Polyols and Main Industrial Products.* Polymer Reviews, 2012. **52**(1): p. 38-79.

50. Hu, Y.H., et al., *Rigid polyurethane foam prepared from a rape seed oil based polyol.* Journal of Applied Polymer Science, 2002. **84**(3): p. 591-597.

51. Adekunle, K., D. Åkesson, and M. Skrifvars, *Synthesis of reactive soybean oils for use as a biobased thermoset resins in structural natural fiber composites.* Journal of applied polymer science, 2010. **115**(6): p. 3137-3145.

52. Cheung, H.-y., et al., *Natural fibre-reinforced composites for bioengineering and environmental engineering applications.* Composites Part B: Engineering, 2009. **40**(7): p. 655-663.

53. Gadam, S.U.K., et al., *The impact of pultrusion processing parameters on resin pressure rise inside a tapered cylindrical die for glass-fibre/epoxy composites.* Composites Science and Technology, 2000. **60**(6): p. 945-958.

54. Van de Velde, K. and P. Kiekens, *Thermoplastic pultrusion of natural fibre reinforced composites.* Composite Structures, 2001. **54**(2-3): p. 355-360.

55. Akil, H.M., et al., *Water absorption study on pultruded jute fibre reinforced unsaturated polyester composites.* Composites Science and Technology, 2009. **69**(11-12): p. 1942-1948.

56. W., J. *Is NF always the best material choice for a product? Example: an automotive doorpanel.* in *the 6th global wood and natural fibre composites symposium*. 2006.

57. Idicula, M., et al., *Dynamic mechanical analysis of randomly oriented intimately mixed short banana/sisal hybrid fibre reinforced polyester composites.* Composites Science and Technology, 2005. **65**(7-8): p. 1077-1087.

58. Idicula, M., et al., *Thermophysical properties of natural fibre reinforced polyester composites.* Composites Science and Technology, 2006. **66**(15): p. 2719-2725.

59. Williamson, M.A., *US biobased products market potential and projections through 2025.* 2010.

60. Liu, Z., et al., *"Green" composites from renewable resources: preparation of epoxidized soybean oil and flax fiber composites.* Journal of agricultural and food chemistry, 2006. **54**(6): p. 2134-2137.

61. Bourmaud, A., C. Morvan, and C. Baley, *Importance of fiber preparation to optimize the surface and mechanical properties of unitary flax fiber.* Industrial Crops and Products, 2010. **32**(3): p. 662-667.

62. Zhang, Y., Z. Xia, and F. Ellyin, *Nonlinear viscoelastic micromechanical analysis of fibre-reinforced polymer laminates with damage evolution.* International journal of solids and structures, 2005. **42**(2): p. 591-604.

63. Javid, S., et al., *Micromechanics of Unidirectional Viscoelastic Fibrous Composites-Homogenized vs Local Characterization.* Journal of Multifunctional Composites, 2013. **1**(1).

64. Sridharan, S., *Nonlinear viscoelastic analysis of composites using competing micromechanical models.* Journal of composite materials, 2006. **40**(3): p. 257-282.

65. Hsu, S.Y., T.J. Vogler, and S. Kyriakides, *Inelastic behavior of an AS4/PEEK composite under combined transverse compressionand shear. Part II: modeling.* International Journal of Plasticity, 1999. **15**(8): p. 807-836.

66. Huang, Z.-M., *On a general constitutive description for the inelastic and failure behavior of fibrous laminates—Part I: Lamina theory.* Computers & Structures, 2002. **80**(13): p. 1159-1176.

67. Raimondo, L., et al., *Modelling of strain rate effects on matrix dominated elastic and failure properties of unidirectional fibre-reinforced polymer–matrix composites.* Composites Science and Technology, 2012. **72**(7): p. 819-827.

68. Tahaye Abadi, M., *Characterization of heterogeneous materials under shear loading at finite strain.* Composite Structures, 2010. **92**(2): p. 578-584.

69. Li, S., *General unit cells for micromechanical analyses of unidirectional composites.* Composites Part A: applied science and manufacturing, 2001. **32**(6): p. 815-826.

70. Huang, Z.M., *Micromechanical strength formulae of unidirectional composites.* Materials Letters, 1999. **40**(4): p. 164-169.

71. Mishnaevsky Jr, L. and P. Brøndsted, *Micromechanical modeling of damage and fracture of unidirectional fiber reinforced composites: A review.* Computational Materials Science, 2009. **44**(4): p. 1351-1359.

72. Odegard, G.M., et al., *Constitutive modeling of nanotube–reinforced polymer composites.* Composites science and technology, 2003. **63**(11): p. 1671-1687.

73. Naik, A., et al., *Micromechanical viscoelastic characterization of fibrous composites.* Journal of composite materials, 2008. **42**(12): p. 1179-1204.

74. Ahci, E. and R. Talreja, *Characterization of viscoelasticity and damage in high temperature polymer matrix composites.* Composites science and technology, 2006. **66**(14): p. 2506-2519.

75. Abolfathi, N., et al., *A micromechanical characterization of angular bidirectional fibrous composites.* Computational Materials Science, 2008. **43**(4): p. 1193-1206.

76. Riley, M.B. and J.M. Whitney, *Elastic properties of fiber reinforced composite materials.* Aiaa Journal, 1966. **4**(9): p. 1537-1542.

77. Nemat-Nasser, S. and M. Hori, *Micromechanics: overall properties of heterogeneous materials*. Vol. 2. 1999: Elsevier Amsterdam.

78. Foreman, J., S. Sauerbrunn, and C. Marcozzi, *Exploring the sensitivity of thermal analysis techniques to the glass transition.* TA Instruments: Thermal Analysis & Rheology, 2006.

79. Mourad, A.-H.I., et al., *Effect of seawater and warm environment on glass/epoxy and glass/polyurethane composites.* Applied Composite Materials, 2010. **17**(5): p. 557-573.

80. Bledzki, A.K., W. Zhang, and A. Chate, *Natural-fibre-reinforced polyurethane microfoams.* Composites Science and Technology, 2001. **61**(16): p. 2405-2411.

81. Dwan'isa, J.-P.L., et al., *Biobased polyurethane and its composite with glass fiber.* Journal of materials science, 2004. **39**(6): p. 2081-2087.

82. kumar Konga, S., *Low Cost Manufacturing and Performance Evaluation of Soy-based Polyurethane/E-glass Composites*. 2008, Texas State University-San Marcos.

83. Fuqua, M.A., S. Huo, and C.A. Ulven, *Natural fiber reinforced composites.* Polymer Reviews, 2012. **52**(3): p. 259-320.

84. Agrawal, R. and L. Drzal, *Adhesion mechanisms of polyurethanes to glass surfaces. III. Investigation of possible physico-chemical interactions at the interphase.* The Journal of Adhesion, 1996. **55**(3-4): p. 221-243.

85. Gerard, J.-F., *Characterization and role of an elastomeric interphase on carbon fibers reinforcing an epoxy matrix.* 1988. **28**(9): p. 568-577.

86. Mosiewicki, M.A. and M.I. Aranguren, *A short review on novel biocomposites based on plant oil precursors.* European Polymer Journal, 2013. **49**(6): p. 1243-1256.

87. Ahlstrom, C. and J.F. Gerard, *The adhesion of elastomer-coated glass fibers to an epoxy matrix. Part I: The effect of the surface treatments on the tensile strength of the glass fibers.* 1995. **16**(4): p. 305-312.

88. Daoust, J., et al., *A finite element model of the fragmentation test for the case of a coated fiber.* Special Issue Microphenomena in Advanced Composites, 1993. **48**(1–4): p. 143-149.

89. Kim, J.-K., M.-L. Sham, and J. Wu, *Nanoscale characterisation of interphase in silane treated glass fibre composites.* Composites Part A: applied science and manufacturing, 2001. **32**(5): p. 607-618.

90. Kim, J.-K. and A. Hodzic, *Nanoscale characterisation of thickness and properties of interphase in polymer matrix composites.* The Journal of Adhesion, 2003. **79**(4): p. 383-414.

91. Seyler, R.J., *Assignment of the glass transition*. Vol. 1249. 1994: ASTM International.

92. Akay, M., *Aspects of dynamic mechanical analysis in polymeric composites.* Composites science and technology, 1993. **47**(4): p. 419-423.

93. Marcovich, N.E., M.M. Reboredo, and M.I. Aranguren, *Mechanical properties of woodflour unsaturated polyester composites.* Journal of Applied Polymer Science, 1998. **70**(11): p. 2121-2131.

94. Dwan'isa, J.P.L., et al., *Novel soy oil based polyurethane composites: Fabrication and dynamic mechanical properties evaluation.* Journal of Materials Science, 2004. **39**(5): p. 1887-1890.

95. Miao, S., et al., *A novel vegetable oil–lactate hybrid monomer for synthesis of high-Tg polyurethanes.* 2010. **48**(1): p. 243-250.

96. Xie, W. and T. Instruments, *APPLICATIONS OF THERMAL ANALYSIS IN POLYMER AND COMPOSITES CHARACTERIZATION.*

97. Zhu, J., et al., *Processing a glass fiber reinforced vinyl ester composite with nanotube enhancement of interlaminar shear strength.* Composites Science and Technology, 2007. **67**(7–8): p. 1509-1517.

98. Thulasiraman, V., S. Rakesh, and M. Sarojadevi, *Synthesis and characterization of chlorinated soy oil based epoxy resin/glass fiber composites.* Polymer Composites, 2009. **30**(1): p. 49-58.

99. Petrović, Z.S., *Polyurethanes from Vegetable Oils.* Polymer Reviews, 2008. **48**(1): p. 109-155.

100. Miyagawa, H., et al., *Novel biobased nanocomposites from functionalized vegetable oil and organically-modified layered silicate clay.* Polymer, 2005. **46**(2): p. 445-453.

101. Pan, X. and D.C. Webster, *Impact of Structure and Functionality of Core Polyol in Highly Functional Biobased Epoxy Resins.* 2011. **32**(17): p. 1324-1330.

102. Huo, S., V.S. Chevali, and C.A. Ulven, *Study on interfacial properties of unidirectional flax/vinyl ester composites: resin manipulation on vinyl ester system.* Journal of Applied Polymer Science, 2013. **128**(5): p. 3490-3500.

103. Shiren Wang and Zhiyong Liang and Tina Liu and Ben Wang and Chuck, Z., *Effective amino-functionalization of carbon nanotubes for reinforcing epoxy polymer composites.* Nanotechnology, 2006. **17**(6): p. 1551.

104. Richardson, M.O.W. and M.J. Wisheart, *Review of low-velocity impact properties of composite materials.* Composites Part A: Applied Science and Manufacturing, 1996. **27**(12): p. 1123-1131.

105. Abadi, M.T., *Micromechanical analysis of stress relaxation response of fiber-reinforced polymers.* Composites Science and Technology, 2009. **69**(7): p. 1286-1292.

106. ABAQUS, *Standard Finite Element Software*. 2011, Dassault Systemes Simulia Corp.

107. Lu, H., X. Zhang, and W.G. Knauss, *Uniaxial, shear, and poisson relaxation and their conversion to bulk relaxation: Studies on poly(methyl methacrylate).* Polymer Engineering & Science, 1997. **37**(6): p. 1053-1064.

108. Drozdov, A.D., *Mechanics of viscoelastic solids*. 1998: Wiley Chicheater etc.